

FURTHER INVESTIGATION OF FLUOBORIC ACID IN SANDSTONE ACIDIZING  
USING  $^{11}\text{B}$  AND  $^{19}\text{F}$  NMR

A Thesis

by

ARPAJIT PITUCKCHON

Submitted to the Office of Graduate and Professional Studies of  
Texas A&M University  
in partial fulfillment of the requirements for the degree of

MASTER OF SCIENCE

Chair of Committee,	Hisham A. Nasr-El-Din
Committee Members,	Maria A. Barrufet
	Mahmoud El-Halwagi
Head of Department,	A. Daniel Hill

May 2014

Major Subject: Petroleum Engineering

Copyright 2014 Arpajit Pituckchon

## ABSTRACT

Although fluoboric acid ( $\text{HBF}_4$ ) has long been known as one of the low-damaging acid treatments for clayey sandstone formations, little is known of its chemistry which could explain the mixed results of fluoboric acid in actual field application. A better understanding of its limitations would contribute to an improved success rate in  $\text{HBF}_4$  stimulation application.

The unique advantages of this acid system are the ability to reach deeper into formation to address damage at extended radius before spending, owing to its slow hydrolytic reaction to produce HF, as well as the stabilization and desensitization of undissolved fines with borosilicate.

A more comprehensive understanding of how the chemistry of fluoboric acid and its reaction products affect silica and aluminosilicates is crucial to the design and optimization of fluoboric acidizing treatment. Through a novel application of  $^{11}\text{B}$  and  $^{19}\text{F}$  Solution State High Field Nuclear Magnetic Resonance (NMR) spectroscopy, chemical complexes involved in the reaction were defined.

Various other experimental techniques were also employed in studies on the ability of hydrolyzed fluoboric acid to react with common clays found in sandstone at room and elevated temperatures, as well as coreflooding to investigate clay migration development. Analyzing fresh and spent acid with inductively coupled plasma (ICP) and  $^{11}\text{B}$  and  $^{19}\text{F}$  NMR helps identify reaction products and their distribution. A set of 12-3

mud acid experiments was done in parallel to serve as a reference to 3%- equivalent-HF fluoboric acid in aqueous-HCl solution.

NMR results show complex mixtures of fluoborate species from  $\text{HBF}_4$  hydrolysis and products from HF-aluminosilicates reaction. The fresh  $\text{HBF}_4$  hydrolysis study at room temperature has confirmed retarded HF generation with presence of  $\text{BF}_4^-$  and  $\text{BF}_3(\text{OH})^-$  and absence of  $\text{BF}_2(\text{OH})_2^-$  or  $\text{BF}(\text{OH})_3^-$  species . The effect of temperature on  $\text{HBF}_4$  reaction has also been studied to validate functionality of acid at 75°F and 200°F. A series of lab dynamic flow testing in Berea sandstone corroborates conclusions from lab experiments by showing decrease in permeability when treating Berea sandstone cores with  $\text{HBF}_4$  at 200°F. Fluoboric acid treatment is therefore not suitable for formations with approximate temperature of 200°F.

## ACKNOWLEDGEMENTS

I would like to thank my committee chair, Dr. Nasr-El-Din, and my committee members, Dr. Barrufet, and Dr. El-Halwagi, for their guidance and support throughout the course of this research.

Thanks also goes to lab technicians, Don Conlee and Joevan Beladi, and administrative officer, Kristina Hansen for fulfilling all requests made throughout the extended period of laboratory work. I also want to extend my gratitude to my friends and colleagues and the department faculty and staff for making my time at Texas A&M University a great experience.

Finally, I give thanks to my family and Napon H. for their encouragement, patience and love.

## NOMENCLATURE

DIW	Deionized water
HF	Hydrofluoric Acid
HCl	Hydrochloric Acid
HF <sub>4</sub>	Fluoboric Acid
PV	Core Pore Volume
ACS	American Chemical Society
ASTM	American Society for Testing and Materials
md	Millidarcy
CEC	Cation Exchange Capacity
wt%	Weight Percent
rpm	Revolutions per Minute

## TABLE OF CONTENTS

	Page
ABSTRACT .....	ii
ACKNOWLEDGEMENTS .....	iv
NOMENCLATURE .....	v
TABLE OF CONTENTS .....	vi
LIST OF FIGURES .....	viii
LIST OF TABLES .....	xii
CHAPTER I INTRODUCTION AND LITERATURE REVIEW .....	1
Background .....	1
Fluoboric Acid.....	4
Literature Review .....	7
CHAPTER II EXPERIMENTAL STUDIES .....	14
Acid Used .....	15
Clay Particle Size Selection .....	16
HBF <sub>4</sub> Hydrolysis Investigation with <sup>11</sup> B and <sup>19</sup> F NMR .....	19
Clay Dissolution Test at 75°F .....	20
Clay Dissolution Test at 200°F .....	20
Berea Sandstone Coreflood at 200°F .....	22
CHAPTER III RESULTS AND DISCUSSION .....	25
HBF <sub>4</sub> Hydrolysis Investigation with <sup>11</sup> B and <sup>19</sup> F NMR .....	25
Clay Dissolution Test at 75°F .....	27
Clay Dissolution Test at 200°F .....	42
Berea Sandstone Coreflood at 200°F .....	57
CHAPTER IV FUTURE WORK.....	77
CHAPTER V CONCLUSIONS .....	78

REFERENCES.....	80
APPENDIX A .....	84

## LIST OF FIGURES

	Page
Figure 1: Kaolinite particle size distribution histogram. ....	17
Figure 2: Bentonite particle size distribution histogram. ....	18
Figure 3: Illite particle size distribution histogram. ....	18
Figure 4: A sample spectrum of a different $\text{HBF}_4$ acid concentration. ....	19
Figure 5: OFITE aging cell. ....	22
Figure 6: $^{11}\text{B}$ NMR spectra of fluoboric acid at different times after preparation. ....	26
Figure 7: $^{19}\text{F}$ NMR spectra of fluoboric acid immediately after preparation. ....	27
Figure 8: Clay weight loss % for mud acid dissolution test at 75°F. ....	28
Figure 9: Clay weight loss % for 3% $\text{HBF}_4$ dissolution test at 75°F. ....	28
Figure 10: EDS spectra of fresh clays (top row) vs 3% $\text{HBF}_4$ dissolved clays at 75°F for 4 hours (bottom row). ....	29
Figure 11: Boron concentration in supernatant of 3% $\text{HBF}_4$ reacted with kaolinite at 75°F for 4 hours. ....	30
Figure 12: Boron concentration in supernatant of 3% $\text{HBF}_4$ reacted with illite at 75°F for 4 hours. ....	31
Figure 13: Boron concentration in supernatant of 3% $\text{HBF}_4$ reacted with bentonite at 75°F for 4 hours. ....	31
Figure 14: Key elements in solution of illite + 12-3 mud acid and 3% $\text{HBF}_4$ at 75°F. ....	33
Figure 15: $^{19}\text{F}$ NMR spectrum of 12-3 mud acid solution reacted with kaolinite at 75°F for 4 hours. ....	34
Figure 16: $^{19}\text{F}$ NMR spectrum of 3% $\text{HBF}_4$ solution reacted with kaolinite at 75°F for 4 hours. ....	35
Figure 17: $^{19}\text{F}$ NMR spectrum of 3% $\text{HBF}_4$ solution reacted with illite at 75°F for 4 hours. ....	36



Figure 18: Al concentration available when reacting with different clay with 3% HBF <sub>4</sub> at 75°F.....	37
Figure 19: <sup>19</sup> F NMR spectrum of 3% HBF <sub>4</sub> solution reacted with bentonite at 75°F for 4 hours. ....	38
Figure 20: <sup>11</sup> B NMR spectrum of 3% HBF <sub>4</sub> solution reacted with kaolinite at 75°F for 4 hours. ....	39
Figure 21: <sup>11</sup> B NMR spectrum of 3% HBF <sub>4</sub> solution reacted with illite at 75°F for 4 hours. ....	40
Figure 22: <sup>11</sup> B NMR spectrum of 3% HBF <sub>4</sub> solution reacted with bentonite at 75°F for 4 hours.....	41
Figure 23: Kaolinite weight loss percent by 12-3 mud acid and 3% HBF <sub>4</sub> at 200°F.....	42
Figure 24: Clay weight loss percent by 3% HBF <sub>4</sub> at 200°F.....	43
Figure 25: Precipitate from illite + HBF <sub>4</sub> dissolution at 200°F for 6 hours.....	43
Figure 26: XRD spectrum matched with KBF <sub>4</sub> using EVA database.....	44
Figure 27: Potassium concentration leached from illite by 3% HBF <sub>4</sub> at different temperatures.....	45
Figure 28: Key elements concentration in supernatant of kaolinite reacted with HBF <sub>4</sub> at 200°F.....	45
Figure 29: Key elements concentration in supernatant of illite reacted with HBF <sub>4</sub> at 200°F.....	46
Figure 30: Key elements concentration in supernatant of bentonite reacted with HBF <sub>4</sub> at 200°F.....	47
Figure 31: EDS spectra of 3% HBF <sub>4</sub> dissolved clays at 75°F for 4 hours (top row) vs 3% HBF <sub>4</sub> dissolved clays at 200°F for 6 hours.....	48
Figure 32: Effect of temperature on Si and Al concentrations in 3% HBF <sub>4</sub> supernatant with kaolinite. ....	49
Figure 33: Effect of temperature on Si and Al concentrations in 3% HBF <sub>4</sub> supernatant with illite.....	50

Figure 34: Effect of temperature on Si and Al concentrations in 3% HBF <sub>4</sub> supernatant with bentonite. ....	50
Figure 35: <sup>19</sup> F NMR spectrum of 3% HBF <sub>4</sub> solution reacted with kaolinite at 200°F for 6 hours. ....	51
Figure 36: <sup>19</sup> F NMR spectrum of 3% HBF <sub>4</sub> solution reacted with illite at 200°F for 6 hours. ....	52
Figure 37: <sup>19</sup> F NMR spectrum of 3% HBF <sub>4</sub> solution reacted with bentonite at 200°F for 6 hours. ....	53
Figure 38: <sup>11</sup> B NMR spectrum of 3% HBF <sub>4</sub> solution reacted with kaolinite at 200°F for 6 hours. ....	54
Figure 39: <sup>11</sup> B NMR spectrum of 3% HBF <sub>4</sub> solution reacted with illite at 200°F for 6 hours. ....	55
Figure 40: <sup>11</sup> B NMR spectrum of 3% HBF <sub>4</sub> solution reacted with bentonite at 200°F for 6 hours. ....	56
Figure 41: Pressure drop across the core during injection in Berea sandstone with 3% HBF <sub>4</sub> main acid at 200°F. ....	58
Figure 42: Si and Al concentrations in Berea coreflood effluent samples at 200°F with 3% HBF <sub>4</sub> main acid. ....	59
Figure 43: Ca and Mg concentrations in Berea coreflood effluent samples at 200°F with 3% HBF <sub>4</sub> main acid. ....	60
Figure 44: K and Na concentrations in Berea coreflood effluent samples at 200°F with 3% HBF <sub>4</sub> main acid. ....	61
Figure 45: Fe and B concentrations in Berea coreflood effluent samples at 200°F with 3% HBF <sub>4</sub> main acid. ....	62
Figure 46: Pressure drop across the core during injection in Berea sandstone with 8% HBF <sub>4</sub> main acid at 200°F. ....	63
Figure 47: Si and Al concentrations in Berea coreflood effluent samples at 200°F with 8% HBF <sub>4</sub> main acid. ....	64
Figure 48: Ca and Mg concentrations in Berea coreflood effluent samples at 200°F with 8% HBF <sub>4</sub> main acid. ....	65

Figure 49: K and Na concentrations in Berea coreflood effluent samples at 200°F with 8% HBF <sub>4</sub> main acid.....	66
Figure 50: Fe and B concentrations in Berea coreflood effluent samples at 200°F with 8% HBF <sub>4</sub> main acid.....	67
Figure 51: Pressure drop across the core during injection in Berea sandstone with 3% HBF <sub>4</sub> main acid at 200°F. ....	68
Figure 52: Si and Al concentrations in Berea coreflood effluent samples at 200°F with 12-3 mud acid as main acid.....	69
Figure 53: Ca and Mg concentrations in Berea coreflood effluent samples at 200°F with 12-3 mud acid as main acid. ....	70
Figure 54: K and Na concentrations in Berea coreflood effluent samples at 200°F with 12-3 mud acid as main acid.....	71
Figure 55: Fe concentration in Berea coreflood effluent samples at 200°F with 12-3 mud acid as main acid. ....	72
Figure 56: <sup>19</sup> F NMR spectrum of effluent sample 25 from Berea coreflood at 200°F with 3% HBF <sub>4</sub> main acid. ....	73
Figure 57: <sup>11</sup> B NMR spectrum of effluent sample 25 from Berea coreflood at 200°F with 3% HBF <sub>4</sub> main acid. ....	74
Figure 58: <sup>19</sup> F NMR spectrum of effluent sample 29 from Berea coreflood at 200°F with 8% HBF <sub>4</sub> main acid. ....	75
Figure 59: <sup>11</sup> B NMR spectrum of effluent sample 29 from Berea coreflood at 200°F with 8% HBF <sub>4</sub> main acid. ....	76

## LIST OF TABLES

	Page
Table 1: NMR acquisition parameters. ....	15
Table 2: Content of 3% $\text{HBF}_4$ acid.....	16
Table 3: Content of 8% $\text{HBF}_4$ acid.....	16
Table 4: Content of 12-3 mud acid.....	16
Table 5: Coreflood pumping sequences in Berea sandstone.....	24

# CHAPTER I

## INTRODUCTION AND LITERATURE REVIEW

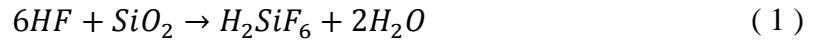
### **Background**

Hydrofluoric acid (HF)-hydrochloric (HCl) acid mixtures, or mud acid, have been used to stimulate sandstone reservoirs since the 1930s. Use of mud acid treatment can include fracturing operations, acidizing operations, scale removal, drilling operations or even sand control operations.

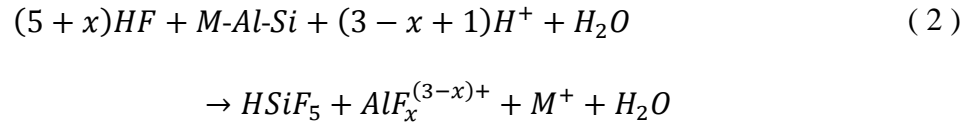
Most sandstone formations consist primarily of quartz or sand particles bonded together by cementing materials which are typically calcite ( $\text{CaCO}_3$ ), silicates and aluminosilicates (clay and feldspar). While most carbonate formations can be effectively treated with various mineral acids or organic acids relying on the acidity of treatment fluid, siliceous formations are not noticeably reacted by the same mechanism. The most common method of treating sandstone formations is to introduce an acid system comprised of HF into the target formation. The HF component is recognized specifically for its first order reaction with aluminosilicates (Smith and Hendrickson 1965) as a function of mineral surface area, removing aluminosilicates from the conductive flow path. HF can dissolve clays, feldspar, quartz, micas and chert, but the primary objective is to remove clays. Reactions of HF with indigenous clay and siliceous matrix in sandstone are complex and vary from one formation to another, depending on which types of clay it contains. Reactivity of different clays with HF has been investigated by Gdanski (Gdanski 1999, Gdanski 1998) and Hartman et al (Hartman et al. 2006). The

use of low pH fluid can cause higher mineral dissolution which further induces adverse effects in certain instances, especially the precipitation of dissolved fluoride with group 1 metal ions ( $\text{Na}^+$  and  $\text{K}^+$ ), group 2 metal ions ( $\text{Mg}^{2+}$ ,  $\text{Ca}^{2+}$ , and  $\text{Ba}^{2+}$ ), and  $\text{Al}^{3+}$  (Reyes 2012). An HCl preflush sequence can be applied to dissolve carbonate minerals as much as possible before HF will be pumped to treat clay at a later stage.

The reaction of HF with quartz is expressed in eq. 1



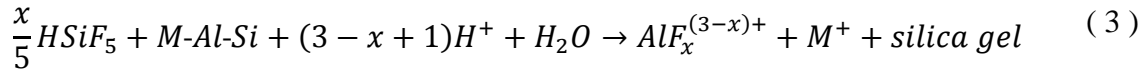
The primary reaction of HF and aluminosilicates according to Gdanski is:



Where x is F/Al ratio and  $\text{M}^+$  is all other cations, such as Na or K. This reaction will completely dissolve aluminosilicates and generate only soluble products. This is the only reaction that removes clay damage hence greatly improving permeability.

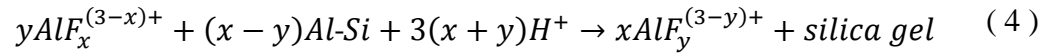
Fluorosilicates can be especially problematic because redissolution can be difficult. Fluoroaluminates are thought to be soluble as long as the pH is below about 2 and the F/Al ratio is maintained below about 2.5 (Shuchart and Gdanski 1996). If precipitated, their dissolution typically requires strong hydroxide concentration of more than 5%.

$\text{HSiF}_5$  or fluosilicic acid is capable of reacting further with aluminosilicates, therefore being referred to as the secondary reaction (eq. 3).



The secondary reaction dissolves all other portions of clays except for Si from the structure of aluminosilicates, leaving amorphous silica gel film in place. This process is found to be significantly fast and go to completion at temperature above 125°F (Gdanski 1999). The reaction rate is much slower at any temperature below that.

The tertiary reaction occurs when aluminum fluoride complexes react with clays, continuing to reduce the F/Al ratio in the spent HF until all remaining  $H^+$  is consumed (eq. 4).



The fluoride number coordinated with aluminum before tertiary reaction (x) is more than that after reaction (y). The tertiary reaction rate was found to be very slow below 200°F (Gdanski 1998).

A literature review has indicated at least two distinct drawbacks of traditional mud acid in stimulating sandstone formations. Firstly, at certain reservoir temperatures, the rapid reaction of HF with siliceous materials, specifically clay, deter the penetration capacity of acid into the formation. It is generally believed that mud acid removes skin damage from only the first few inches around the wellbore (McBride et al. 1979).

Another reason is early production decline soon after the formation has been stimulated, resulting from pore throat plugging by migratory clays and other fines (Thomas and Crowe 1978), exacerbating formation deliverability to even lower than pre-treatment level. Severe loss of permeability in sandstones due to authigenic clay

migration in response to mechanical forces or water salinity changes was found to induce total pore plugging even in sandstone of 500 milli-darcy initial permeability (Gray and Rex 1990).

### **Fluoboric Acid**

Fluoboric acid ( $HBF_4$ ) is a water unstable compound of which extent of hydrolysis is markedly dependent on temperature and acid concentration. The slow hydrolytic reaction gradually releases hydrofluoric acid to its environment. The hydrolysis reaction of fluoboric acid at room temperature has been investigated in detail (Wamser 1948, 1951).

By nature, aqueous solutions of fluoboric acid will be hydrolyzed at a degree which depends on acid concentration, temperature, and standing time after preparation (Ryss 1956) as well as HF/  $H_3BO_3$  molar ratio in the starting mixture (Radosavljević et al. 1979). The hydrolysis constant of  $BF_4^-$  at various conditions had been determined from pH data by Ryss and Bakina according to the equilibrium hydrolysis of the  $BF_4^-$  ion corresponding to the following reactions, with the assumption that  $BF_3OH^-$  and  $BF_4^-$  are completely dissociated and no  $HF_2^-$  formed:



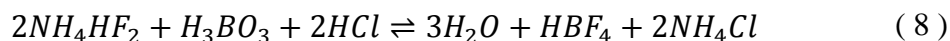
$$\text{Degree of hydrolysis, } k = \frac{[BF_3OH^-][HF]}{[BF_4^-]} \quad (7)$$



The degree of hydrolysis of  $HBF_4$  increases with an increase in temperature or an excess amount of boric acid present but decreases with increasing acid concentration or an excess amount of HF present (Wamser 1948). At room temperature, only around 8-10% of  $HBF_4$  will hydrolyze and yield available HF to react with clay. When HF is consumed, the equilibrium will shift to the right causing more  $BF_4^-$  to hydrolyze and produce a substitute amount of HF to maintain its constant level. The limited HF availability at any given time has made  $HBF_4$  hydrolysis the control process when comparing to the mud acid spending rate on aluminosilicates. This is usually called a retarded HF acid system.

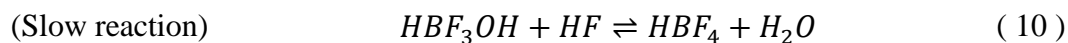
In 1978, Thomas and Crowe introduced the use of fluoboric acid in treating sandstone reservoirs. It was found to be very effective in increasing live acid penetration and stabilizing undissolved clays to the sand grain with borosilicate (Thomas and Crowe 1978, Thomas et al. 1978). During the fixing process, aluminum will be extracted from clays and exchanged with boron to produce borosilicate material. Due to its retarding feature,  $HBF_4$  could dissolve clays as effectively as mud acid but at a much slower rate. Therefore, to adequately address the damage,  $HBF_4$  acid is usually designed as a postflush to mud acid.

The aqueous fluoboric acid used in this experiment was prepared by treating ammonium bifluoride with stoichiometric amounts of boric acid and hydrochloric acid.



Fluoboric acid will not form in the mixture immediately after preparation (Wamser 1948). At this stage, the total titratable acidity corresponds to 5 equivalent of

acid and leaves  $F^-$  and  $BO_2^-$  anions at the end point of titration. Fluoboric acid content will gradually increase in solution over time to equilibrium levels while total acidity decreases to a certain value. At titration end point, the solution will contain additional  $BF_4^-$  ions compared to those mentioned above. These phenomena are represented by a 2-step chemical reaction (Travers 1930):



Hydrogen ions catalyze the formation of  $HBF_4$ . The rate of reaction of  $HBF_3OH$  with HF depends essentially on the acidity of the solution. Hydrolysis of  $HBF_4$  is also catalyzed by  $Ca^+$  ions (Ryss 1956).

Alkali salts of  $BF_4^-$  are much less soluble than those of  $BF_3OH^-$  (Ryss 1956), and are likely to precipitate out of solution. This is due to the fact that the replacement of the  $F^-$  ions by the  $OH^-$  ions leaves the lattice energy unchanged but increases the hydration of the anion.  $KBF_4$  is one of the least soluble fluoborate compounds.

$BF_3OH^-$  is an acid anion of considerably greater strength than HF. Thus only in very dilute solutions (0.002M at 20°C) will further hydrolysis of  $HBF_3OH$  to  $HBF_2(OH)_2$  occur (Ryss 1956). The assumption that this hydrolytic equilibrium is very rapidly established (in contrast to the slow hydrolysis of  $HBF_4$ ) is further supported by the result of  $KBF_4$  and  $KBF_3OH$  aqueous solution titration with thorium nitrate in the presence of alizarin red S, which suggested that none of the fluoride in  $BF_4^-$  is available but the fluorine in  $BF_3OH^-$  is rapidly and quantitatively available (Wamser 1951).

The observed decrease in acid strength in the order  $HBF_4 > HBF_3OH > HBF_2(OH)_2 > HBF(OH)_3 > H_3BO_3$  may be explained by the changes in the electrostatic inductive effect of the anion on the proton as fluorine atoms are successively replaced by hydroxyl groups. The highly electronegative fluorine atoms attract electrons more strongly than oxygen atoms, so that the tendency for the proton is to be held more firmly by a B-linked OH group than by B-F unit (Wamser 1951).

The  $HBF_4$  acid system used in this study is similar to that used in a study by Al-Dahlan et al (Al-Dahlan et al. 2001).

NMR analysis is the main research technique used in this study. This technique exploits the magnetic properties of certain atomic nuclei in a magnetic field which absorb and re-emit electromagnetic radiation that resonates with the intramolecular magnetic fields around an atom. The spectrum obtained can then provide detailed information about the structure, dynamics, reaction state, and chemical environment of molecules, which can be used to confirm the identity of a substance.  $^{11}\text{B}$  and  $^{19}\text{F}$  NMR have never before been used to study the  $HBF_4$  acid reaction with clay and sandstone.

### **Literature Review**

In 1948, Wamser studied the hydrolysis of fluoboric acid in aqueous solution and found that when mixing 4 moles of HF acid with 1 mole of boric acid in aqueous medium, 3 moles of HF will react immediately to form  $HBF_3OH$ . Then, the remaining HF will react slowly with  $HBF_3OH$  to gradually form  $HBF_4$  until equilibrium is reached (Wamser 1948). The equilibrium constant of 0.1105 M fluoboric acid at 25°C has been

determined to be  $2.3 \times 10^{-3}$ . It was noted that the prepared solution contains no  $HB\dot{F}_4$  immediately after preparation and that hydrolyzed aqueous fluoboric acid solutions do not contain any free boric acid. From conductivity titration, it was believed that an appreciable amounts of  $HB\dot{F}_2(OH)_2$  and  $HB\dot{F}(OH)_3$  also exist at their reversible equilibrium with  $HB\dot{F}_3OH$  (Wamser 1948).

Fluoboric acid or clay acid, had later been employed in field application to stimulate and control clay in a sandstone formation by Thomas and Crowe in 1978 (Thomas and Crowe 1978, Thomas et al. 1978). Clay acid was proven to be effective in providing deeper live acid penetration and minimizing clay swelling and migration through chemical fusion of clay platelets from the borosilicate formation when  $HB\dot{F}_3OH$  reacts with siliceous material. Tests showed that  $HB\dot{F}_4$  has an ability to reduce the CEC of bentonite up to 93%. In order to achieve these features of clay acid, a shut-in period following acid injection is required as the decrease in clay swelling is a function of time. The shut-in period varies from 30 minutes at 300°F to 96 hours at 100°F for the cores used in this study. Mud acid generally precedes clay acid to remove surface plugging, then a postflush with clay acid is used to attain deep penetration. A reaction rate comparison test between 12-3 mud acid and the equivalent HF generating capacity 12%  $HB\dot{F}_4$  on glass slides at 150°F reveals a 10 fold difference in rate. Another test performed on sandstone with kaolinite showed an identical dissolution effect between the  $HB\dot{F}_4$  system at 150°F after 2 hours and 12-3 mud acid at 75°F after 20 minutes.

In 1979, McBride et al. used fluoboric acid to treat clay and quartz fines in gas wells with gravel pack completions in offshore Louisiana (McBride et al. 1979). They

observed that there was no increased precipitation of hexafluorosilicates and other reaction products after long term  $HB\text{F}_4$  exposure. All wells treated by  $HB\text{F}_4$  showed removal of damage in both gravel pack, perforations, and effective wellbore area with a slower production decline after treatment.

In 1983, Kunze and Shaughnessy pointed out that at typical formation temperatures (150-200°F), a supposedly retarded  $HB\text{F}_4$  system will spend at the same rate as mud acid (Kunze and Shaughnessy 1983). Furthermore, the effect of the added HCl on the solution acidity has catalyzed the reaction and caused more  $\text{BF}_4^-$  to hydrolyze at equilibrium. Experimental results indicated similar acid penetration in both Berea and actual formation corefloods across 2 acid systems. The stirred reaction experiments likewise confirmed no difference in acid-clay dissolution. No fresh water sensitivity existed in cores treated with conventional HF acid and cores treated with  $HB\text{F}_4$ . It was found that  $\text{BF}_4^-$  hydrolysis will increase with soluble aluminum concentration. Shutting in  $\text{BF}_4^-$  will lead to silica precipitation and possible pore plugging as much as if conventional HF were shut-in.

Laboratory work by Boyer and Wu in 1983 concluded that  $HB\text{F}_4$  is suitable for clay bearing sandstones (Boyer and Wu 1983). Less silica precipitation was observed with  $HB\text{F}_4$  than mud acid.

Bertaux adopted 8%  $HB\text{F}_4$  acidizing in potassic mineral sandstone (containing K-feldspar and illite) in 1989 (Bertaux 1989) and concluded it enhanced permeability. Also the  $\text{KBF}_4$  that was generated was non damaging. Meanwhile, the HF acid-mineral reaction led to  $\text{K}_2\text{SiF}_6$  precipitation, resulting in a significant permeability reduction.

Moreover, silica and borosilicates formed during the shut-in period fused non-dissolved particles and provided permanent stabilization.

Ayorinde et al. (1992) applied  $HB\dot{F}_4$  in high rate oil and gas wells (cased or gravel packs) to prevent post treatment fines migration and to sustain production as an alternative to conventional clay control agents (cationic polymers) used in the overflush (Ayorinde 1992).

Paccaloni and Tambini used  $HB\dot{F}_4$  to treat a well with silt and clay damage resulting from mud acid treatment in 1993 (Paccaloni and Tambini 1993). Production was reported to plateau for 5 years following treatment.

Previous work by Shuchart (1995) used  $^{19}\text{F}$  NMR spectroscopy to study aluminum and silicon fluorides equilibria and the reactions of HF acid and  $H_2SiF_6$  on aluminosilicates (Shuchart and Buster 1995). During the secondary reaction of silicon fluorides with aluminosilicates, a constant F/Al ratio was maintained until the silicon fluorides had reacted completely. The distribution of fluoride species depends on the HCl concentration. When the silicon fluorides have reacted completely to give silica gel, the aluminum fluoride complexes continue to react on fresh aluminosilicates (tertiary reaction) and cause the aluminum content to increase (leaching more Al) and the F/Al ratio and acid concentration to decrease below 1. The final F/Al ratio is dependent upon acid strength and temperature. In wells with temperatures of 150 to 200°F, the reaction of  $H_2SiF_6$  continued to completion. Silicon content was low and pH levels were 2 to 3. The F/Al ratios of the returns were 0.5 to 1.3, depending on the concentration of HCl and HF in the treatment.

In 1999, Kume et al. reported that the use of fluoboric acid to treat wells in Niger Delta returned mixed results, including some with unimproved or damaged permeability (Kume et al. 1999).

Al-Dahlan et al. (2001) studied retarded acid systems, one of which was  $HB\text{F}_4$ , against mud acid (Al-Dahlan et al. 2001). Observations from lab experiments are that  $HB\text{F}_4$  does not react with quartz and was retarded only in the first 30 minutes when reacted with kaolinite and chlorite and 1 hour when reacted with illite and bentonite.  $HB\text{F}_4$  had the weakest dissolving power for silicon. This system precipitated hydrated silica with increasing reaction time.  $HB\text{F}_4$  precipitates  $KB\text{F}_4$  when reacted with illite.

Jaramillo et al. introduced a blend of organic/fluoboric acid system in 2010 (Jaramillo et al. 2010). Organic acid acted as chelant to minimize precipitations. This acid was used as the main treatment acid, eliminating the HF preflush stage. Productivity improvement was evident after treatment and remained stable, indicating efficient fines control. It claimed to be effective in fines stabilization at all temperatures.

In 2011, Feng et al. has developed a new sandstone acid formulation (HTDP, a chemically modified organo-phosphonic acid) that has proven better in enhancing permeability in lab formation coreflood than  $HB\text{F}_4$  (Feng et al. 2011).

Field study in 2012 by Restrepo et al. used a system of organic acids -  $HB\text{F}_4$  to obtain deep live acid penetration and to minimize secondary/tertiary reactions associated with the formation of scales, HCl sensitive asphaltenes, and oil wet fines problems (Restrepo et al. 2012). Organic acids chelate  $\text{Al}^{3+}$  ions, keeping silica from precipitating

as hydrated silica inside solution. Consequently, this leads to more aluminosilicates dissolving.

Reyes (2012) patented a treatment fluid that contained boron trifluoride complexes with chelating agents for use in formations with temperatures of at least 200°F (Reyes 2012). The boron trifluoride complex serves as a precursor of HF acid with an advantage of having higher pH ( $>2$ ) than  $\text{HBF}_4$ , which lessens the risk of unwanted precipitation. Another advantage claimed by this system is that a number of different boron trifluoride complexes, having differential stabilities, may advantageously be utilized to control the release of HF acid at a desired time or location within the formation.  $\text{HBF}_4$  solution is rapid in generating HF and other BF species, while the hydrolysis rate of boron trifluoride complexes is not as rapid. Furthermore, the ligands that complex with boron trifluoride and are released into treating fluid when boron trifluoride decomposes may enhance treatment in certain applications, e.g., solvents (alcohols and ethers), acids (phosphorus and acetic acid), or amines (methylamine and ethylamine).

In 2013, Gomaa et al. devised a one-step sandstone acid system that eliminates the HCl preflush/postflush stage (Gomaa et al. 2013). This acid system was composed of  $\text{HBF}_4$ , HCl, organic acid, acid retarder and clay control additives. Lab stimulation on Bandera sandstone cores at 180°F yielded permeability enhancement. It was discovered that increasing the HCl/HF ratio increased the permeability enhancement and reduced the acid volume needed. There is a minimum acid volume needed to achieve



permeability enhancement. This minimum PV depends on the HCl:HF ratio of the acid system and sandstone composition.

## CHAPTER II

### EXPERIMENTAL STUDIES

NMR analysis is the main research technique used in this study. This technique exploits the magnetic properties of certain atomic nuclei in a magnetic field which absorb and re-emit electromagnetic radiation that resonates with intramolecular magnetic field around an atom. The spectrum obtained can then provide detailed information about the structure, dynamics, reaction state, and chemical environment of molecules, which can be used to confirm the identity of a substance.

All  $^{11}\text{B}$  and  $^{19}\text{F}$  NMR spectra were recorded in  $\text{CDCl}_3$  using a Varian Inova 400 MHz spectrometer. Chemical shifts for fluorine were recorded in parts per million (ppm,  $\delta$ ) relative to  $\text{CFCl}_3$  using trifluorotoluene ( $\text{C}_6\text{H}_5\text{CF}_3$ ,  $\delta -63.72$  ppm) as an internal standard.  $^{11}\text{B}$  NMR shifts are reported in ppm relative to boron trifluoride etherate ( $\text{BF}_3\cdot\text{OEt}_2$ ) as the external reference. Samples are contained in 5 mm OD borosilicate tubes lined with FEP NMR tube liners to prevent contamination from borosilicate glass.  $^{11}\text{B}$  and  $^{19}\text{F}$  NMR acquisition parameters are as shown in table 1.

<sup>19</sup> F NMR Acquisition Parameters	<sup>11</sup> B NMR Acquisition Parameters
<ul style="list-style-type: none"> <li>○ Inova400 Brand, turned to 375.9 MHz</li> <li>○ Run sample w/o internal lock signal in 5 mm OD tubes</li> <li>○ Acquisition parameters <ul style="list-style-type: none"> <li>▪ Spectral width of 50,000 Hz</li> <li>▪ 45 degree pulse angle</li> <li>▪ 2 second relaxation delay</li> <li>▪ 44 to 128 scans per data set,- depending on fluorine-concentration</li> </ul> </li> </ul>	<ul style="list-style-type: none"> <li>○ Inova400 Brand, turned to 128.2 MHz</li> <li>○ Run sample w/o internal lock signal in 5 mm OD tubes</li> <li>○ Acquisition parameters <ul style="list-style-type: none"> <li>▪ Spectral width of 38,461.5 Hz</li> <li>▪ 45 degree pulse angle</li> <li>▪ 0.001 second relaxation delay</li> <li>▪ 200 to 620 scans per data set,- depending on Boron-concentration</li> </ul> </li> </ul>

**Table 1: NMR acquisition parameters.**

### Acid Used

Three different acid formulations are used in this research: 3% HBF<sub>4</sub>, 8% HBF<sub>4</sub>, and 12-3 mud acid. Both 3% and 8% HBF<sub>4</sub> are prepared according to eq (8). Due to the limited solubility of boric acid in high HCl content, the 8% HBF<sub>4</sub> solution contains no excess HCl.

The solutions were prepared using 18.2 MΩ•cm DIW, concentrated ACS grade HCl acid 36.5 wt% concentration, crystalized ammonium bifluoride, and powdered boric acid. Acids content are shown in table 2, 3, and 4.

	wt %
HF	3.3%
HCl	12.0%
NH <sub>4</sub> Cl	4.0%
H <sub>2</sub> O	80.7%
	100.0%

**Table 2: Content of 3% HBF<sub>4</sub> acid.**

	wt %
HF	8.0%
NH <sub>4</sub> Cl	9.7%
H <sub>2</sub> O	82.3%
	100.0%

**Table 3: Content of 8% HBF<sub>4</sub> acid.**

	wt %
HF	3.0%
HCl	12.0%
NH <sub>4</sub> Cl	4.0%
H <sub>2</sub> O	81.0%
	100.0%

**Table 4: Content of 12-3 mud acid.**

### **Clay Particle Size Selection**

A sonic sifter with a series of sieves complying with ASTM E 11 standard, from top to bottom: 212 μm, 150 μm, 106 μm, 90 μm, 75 μm, and 45 μm were used to separate dry powdered clay as received from Ward's Science. Kaolinite and bentonite have a non-normal distribution for available sieve size ranges (Fig. 1 and 2). Particles

with diameters between 32-45  $\mu\text{m}$  were selected to represent kaolinite and bentonite samples in this study, as this range is likely the mode of the size variation.

Illite samples were received in cobble sizes. They were broken down to final sizes using a rock grinder and a shatter box. Its particle distribution histogram appeared to be a normal-right skewed pattern, and is shown in Fig. 3. The particle diameters ranging from 90-106  $\mu\text{m}$  were selected to represent illite.

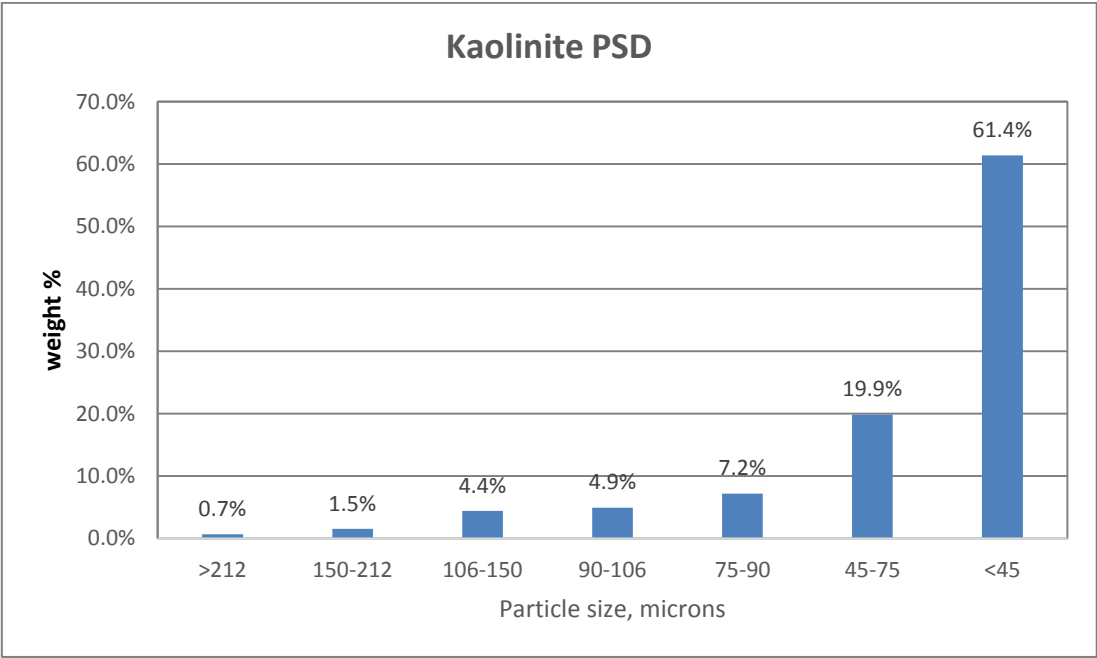


**Figure 1: Kaolinite particle size distribution histogram.**

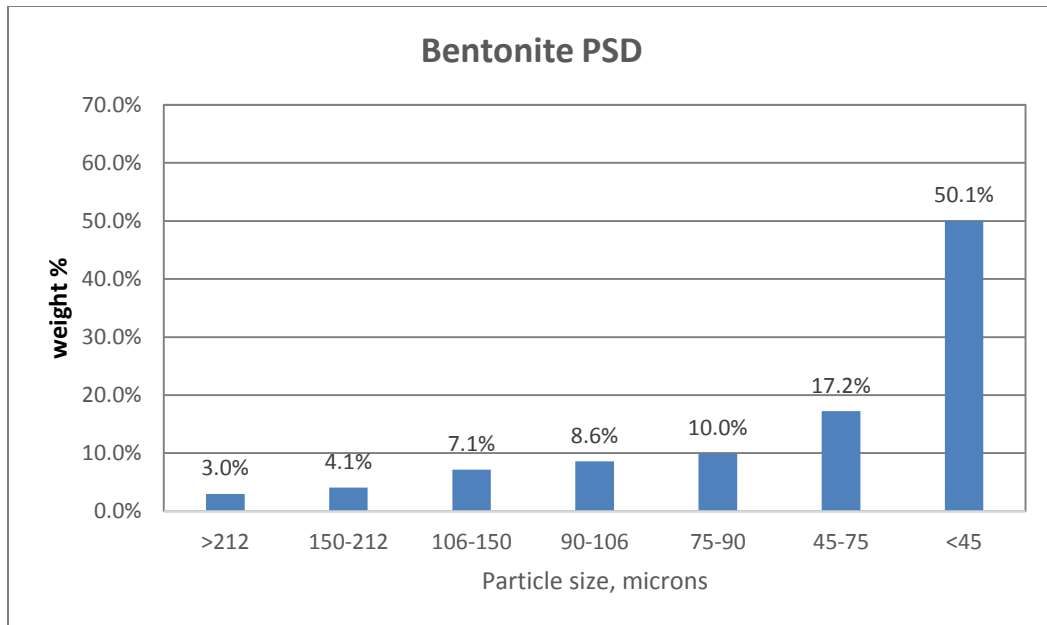


**Figure 2: Bentonite particle size distribution histogram.**

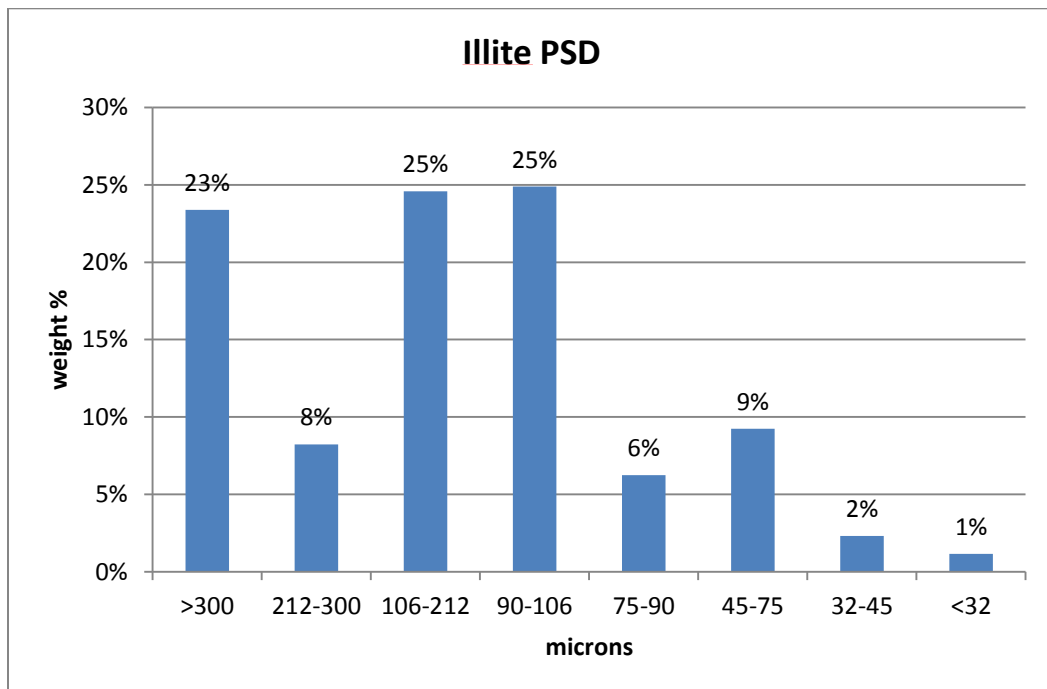


**Figure 3: Illite particle size distribution histogram.**

### **HF<sub>4</sub> Hydrolysis Investigation with <sup>11</sup>B and <sup>19</sup>F NMR**

To understand the extent of the hydrolysis process of HF<sub>4</sub> and the fluoride distribution, a sample of 12% HCl-3% HF<sub>4</sub> at 75°F was analyzed by <sup>11</sup>B and <sup>19</sup>F NMR at different times after acid preparation and the results will be compared to determine HF development in the system. Fig. 4 below is a sample spectrum of a different HF<sub>4</sub> acid concentration showing the fluoborate ion as the predominant species present (Reyes 2012).

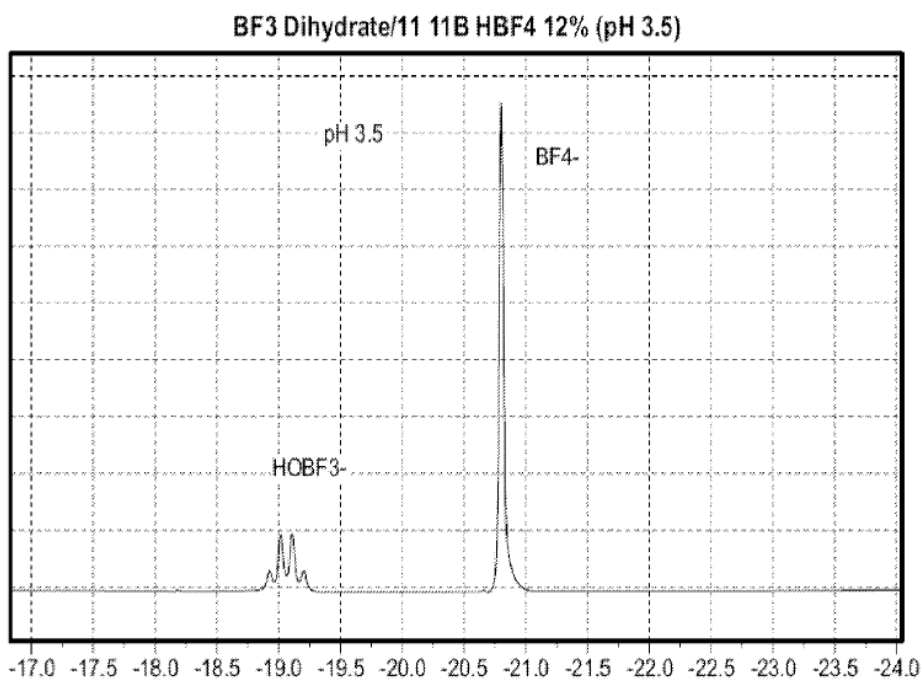


**Figure 4: A sample spectrum of a different HF<sub>4</sub> acid concentration.**

### **Clay Dissolution Test at 75°F**

This experiment is conducted to investigate the mechanisms which affect the dissolution behavior of kaolinite, bentonite and illite in aqueous fluoboric acid compared to aqueous hydrofluoric acid at 75°F. Four grams of each clay, sieved to control particle sizes and dried in an oven to remove excess water, is mixed with 40 g of 12% HCl-3% HBF<sub>4</sub> or 12% HCl-3% HF and allowed to react for 0.5, 1, 1.5, 2, 3 and 4 hours on a magnetic stirrer plate. When reaction time had elapsed, the mixture was centrifuged at 6000 rpm for 2 minutes to separate free acid from clay, preventing further reaction. Quantitative grade filter paper was then used to separate the supernatant from the undissolved clay.

Clay weight loss percentages were recorded along with solution pH and free fluoride ion levels using a Cole-Parmer Fluoride Ion Electrode. The concentrations of key ions in these acids, aluminum, boron, phosphorus, silicon, calcium, magnesium, sodium, potassium, and total iron concentrations, were measured by Inductively Coupled Plasma Spectroscopy (ICP-OES). Dry clays and any precipitates were analyzed with an Evex Mini-SEM/EDS NanoAnalysis. Finally, the supernatant acid solution corresponding to 4 hours reaction time was analyzed by <sup>11</sup>B and <sup>19</sup>F NMR.

### **Clay Dissolution Test at 200°F**

This experiment was conducted to investigate the mechanisms which affect the dissolution behavior of kaolinite, bentonite, and illite in aqueous fluoboric acid compared to aqueous hydrofluoric acid at 200°F, which could be considered normal



formation temperature. The experiment design was such that the secondary reaction of HF goes to completion.

Using the same clay as the 75°F test, 10 g of each clay is mixed with 100g of 12% HCl-3% HBF<sub>4</sub> or 12% HCl-3% HF and 1% vol corrosion inhibitor. The mixture was then contained in an OFITE aging cell (shown in Fig. 5), pressurized with nitrogen to 300 psi, and placed in rolling oven that was heated up to 200°F. The reactions were allowed to continue for 1,3 and 6 hours. When the reaction time has elapsed and the cell had cooled, the mixture was centrifuged at 6000 rpm for 2 minutes to separate live acid from clay, preventing further reaction. Quantitative grade filter paper was then used to separate the supernatant from the undissolved clay.

Clay weight loss percentages were recorded along with solution pH and free fluoride ion levels using a Cole-Parmer Fluoride Ion Electrode. The concentrations of key ions in these acids, aluminum, boron, phosphorus, silicon, calcium, magnesium, sodium, potassium, and total iron concentrations were measured by Inductively Coupled Plasma Spectroscopy (ICP-OES). Dry clays and any precipitates were analyzed with Evex Mini-SEM/EDS NanoAnalysis. Finally the supernatant acid solution corresponding with 6 hours reaction time was analyzed by <sup>11</sup>B and <sup>19</sup>F NMR.



**Figure 5: OFITE aging cell.**

### **Berea Sandstone Coreflood at 200°F**

Berea sandstone is the most commonly used media in studying core flow test due to its homogeneity, which is favorable in control experiments, as well as its high permeability and porosity, resembling a good reservoir. The samples used had permeabilities ranging from 100-200 md.

Core flow tests were conducted using Berea sandstone cores of 1" diameter and 6" length saturated with 5 wt%  $\text{NH}_4\text{Cl}$  before use. A confining pressure of 2000 psi and a back pressure of 1000 psi were applied. The core temperature was stabilized at 200°F. Flow rates of 3-5 ml/min were employed. Effluent samples were collected at regular intervals and were later analyzed with Inductively Coupled Plasma Spectroscopy (ICP-OES) for key elements concentration and  $^{11}\text{B}$  and  $^{19}\text{F}$  NMR. A shut-in period of 1 hour

was incorporated in each test to allow for in situ HF generation and reaction from  $\text{HBF}_4$ .

Coreflood pumping sequences are as shown in table 5.

Pressure drop across the core was recorded and plotted against pump schedule to track permeability change in the core when different fluids were pumped through. Initial and final permeability were calculated and compared.

Coreflood Pumping Sequences in Berea Sandstone	
	<p>Pump 5 wt% <math>\text{NH}_4\text{Cl}</math> at 3 and 5 ml/min. Allow for pressure stabilization then measure initial permeability.</p> <p>Heat up the core to 200°F while pumping 5 wt% <math>\text{NH}_4\text{Cl}</math> at 1 ml/min.</p>
Preflush	5 wt% $\text{HCl}$ + 1 vol% corrosion inhibitor, 5 PV at 3 ml/min
Main acid	<p>a) 3% <math>\text{HBF}_4</math>, 2 PV at 3 ml/min then shut-in for 1 hour.</p> <p>b) 8% <math>\text{HBF}_4</math>, 2 PV at 3 ml/min then shut-in for 1 hour.</p> <p>c) 12-3 mud acid + 1 vol% corrosion inhibitor, 2 PV at 3 ml/min</p>
Postflush	5 wt% $\text{NH}_4\text{Cl}$ , 5 PV at 3 ml/min
	<p>Cool down the system to room temperature while pumping 5 wt% <math>\text{NH}_4\text{Cl}</math> at 1 ml/min</p> <p>Pump 5 wt% <math>\text{NH}_4\text{Cl}</math> at 3 and 5 ml/min. Allow for pressure stabilization then measure final permeability.</p>

**Table 5: Coreflood pumping sequences in Berea sandstone.**

## CHAPTER III

### RESULTS AND DISCUSSION

#### **HF<sub>4</sub> Hydrolysis Investigation with <sup>11</sup>B and <sup>19</sup>F NMR**

Fig. 6 shows the <sup>11</sup>B NMR spectra of fresh HF<sub>4</sub> acid at t = 0, t = 30 minutes, t = 24 hours after preparation at 75°F. It appeared that only 2 species existed at all times. The sharp singlet at  $\delta = -1.8$  ppm is tetrafluoroborate ( $BF_4^-$ ) and a quartet at around  $\delta = -1.4$  ppm is hydroxyfluoborate  $BF_3(OH)^-$  (Prakash et al. 2011). The fluoborate ion is the predominant species present. Both species reach equilibrium very fast and maintain their levels past 24 hours.

The plot reveals that  $BF_4^-$  is formed instantly after HF<sub>4</sub> acid was prepared at this H<sup>+</sup> concentration and that HF was readily available in the system at equilibrium. The plots also demonstrated that further acid decomposition to HF<sub>2</sub>(OH)<sub>2</sub> would not noticeably progress in the absence of material to react with.

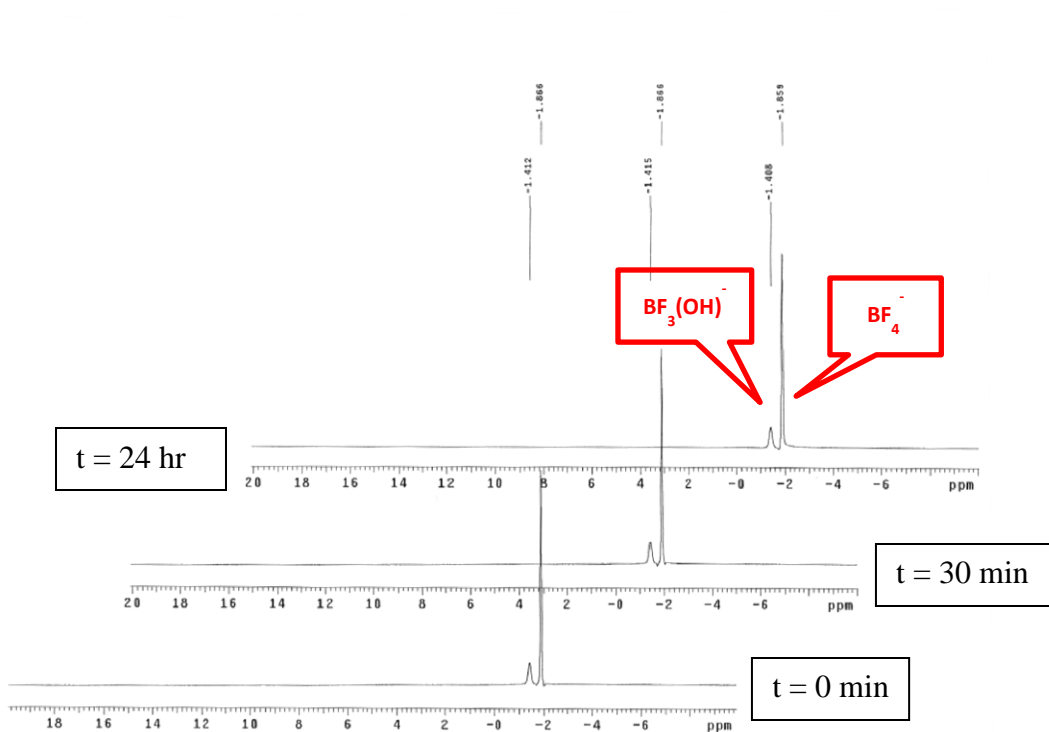


**Figure 6:  $^{11}\text{B}$  NMR spectra of fluoboric acid at different times after preparation.**

Fig. 7 shows the  $^{19}\text{F}$  NMR spectrum of fresh  $\text{HBF}_4$  acid at  $t = 0$  at  $75^\circ\text{F}$ . Two distinct species are  $\text{BF}_4^-$  at  $\delta = -150$  ppm and  $\text{BF}_3(\text{OH})^-$  at around  $\delta = -147$  ppm (Prakash et al. 2011). A third minor amount of fluoride containing species was also formed. Based on the chemical shift  $\delta = -162$  ppm, this is believed to be HF (Dungan and Van Wazer 1970). This reveals that HF is readily available in the acid solution once prepared but at a very limited quantity.

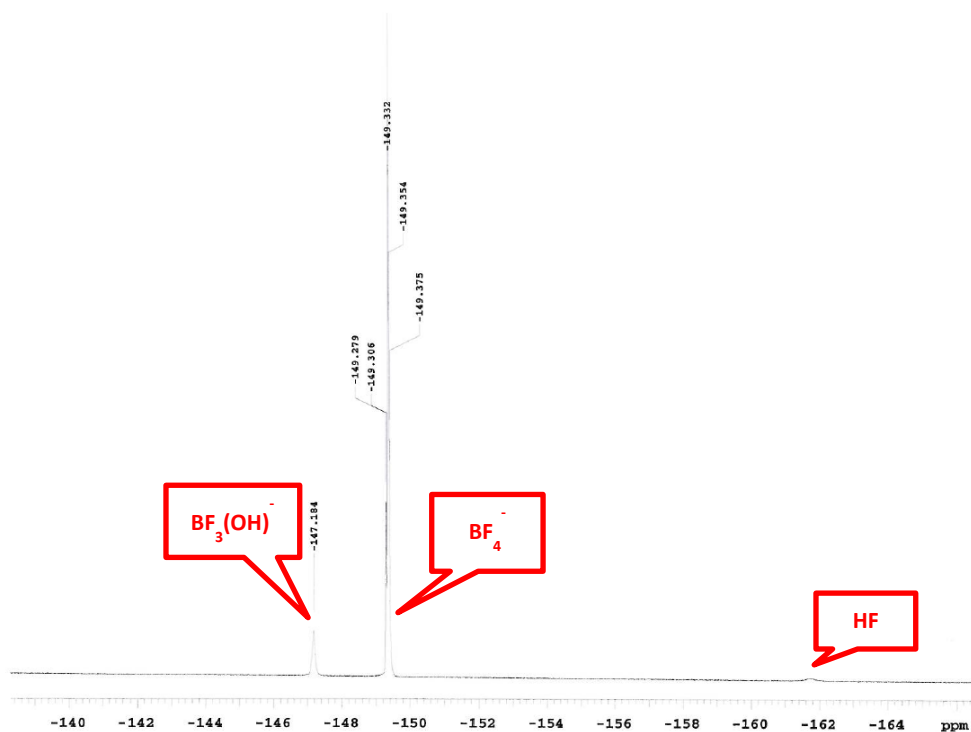


**Figure 7:  $^{19}\text{F}$  NMR spectra of fluoboric acid immediately after preparation.**

### **Clay Dissolution Test at 75°F**

Comparing Fig. 8 and Fig. 9, the retardation effect of 3%  $\text{HBF}_4$  at room temperature is up to 60% of the conventional mud acid reaction rate for kaolinite and illite. For bentonite, the retardation of  $\text{HBF}_4$  went up as high as 80-90%.

Fresh clays and clays which were dissolved by  $\text{HBF}_4$  for 4 hours at 75°F were analyzed by SEM-EDS and compared side by side in Fig. 10. Each clay's Al/Si ratio before and after  $\text{HBF}_4$  dissolution remains almost constant, maintaining their structural properties of 1:1 (kaolinite) clay or 2:1 (illite and bentonite) clay.  $\text{HBF}_4$  can then be

assumed to attack the tetrahedral silicate sheet and octahedral aluminate sheet equivalently.

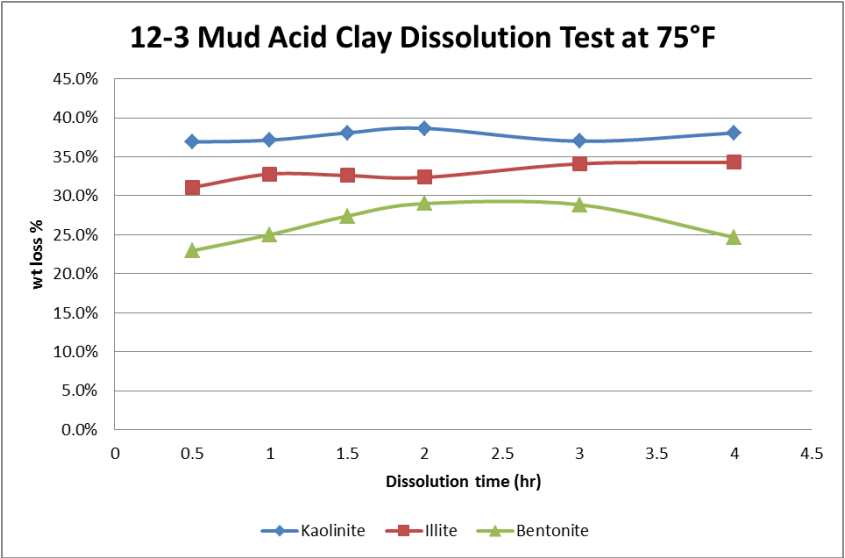


Figure 8: Clay weight loss % for mud acid dissolution test at 75°F.

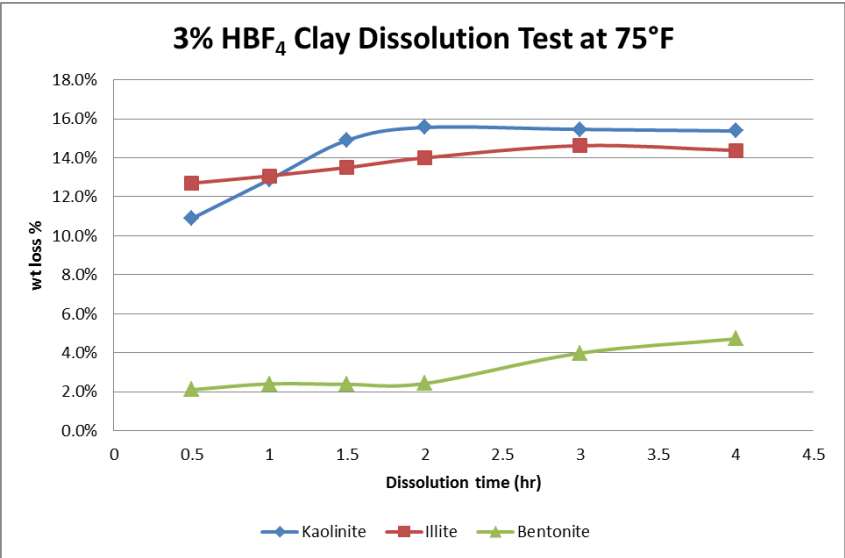
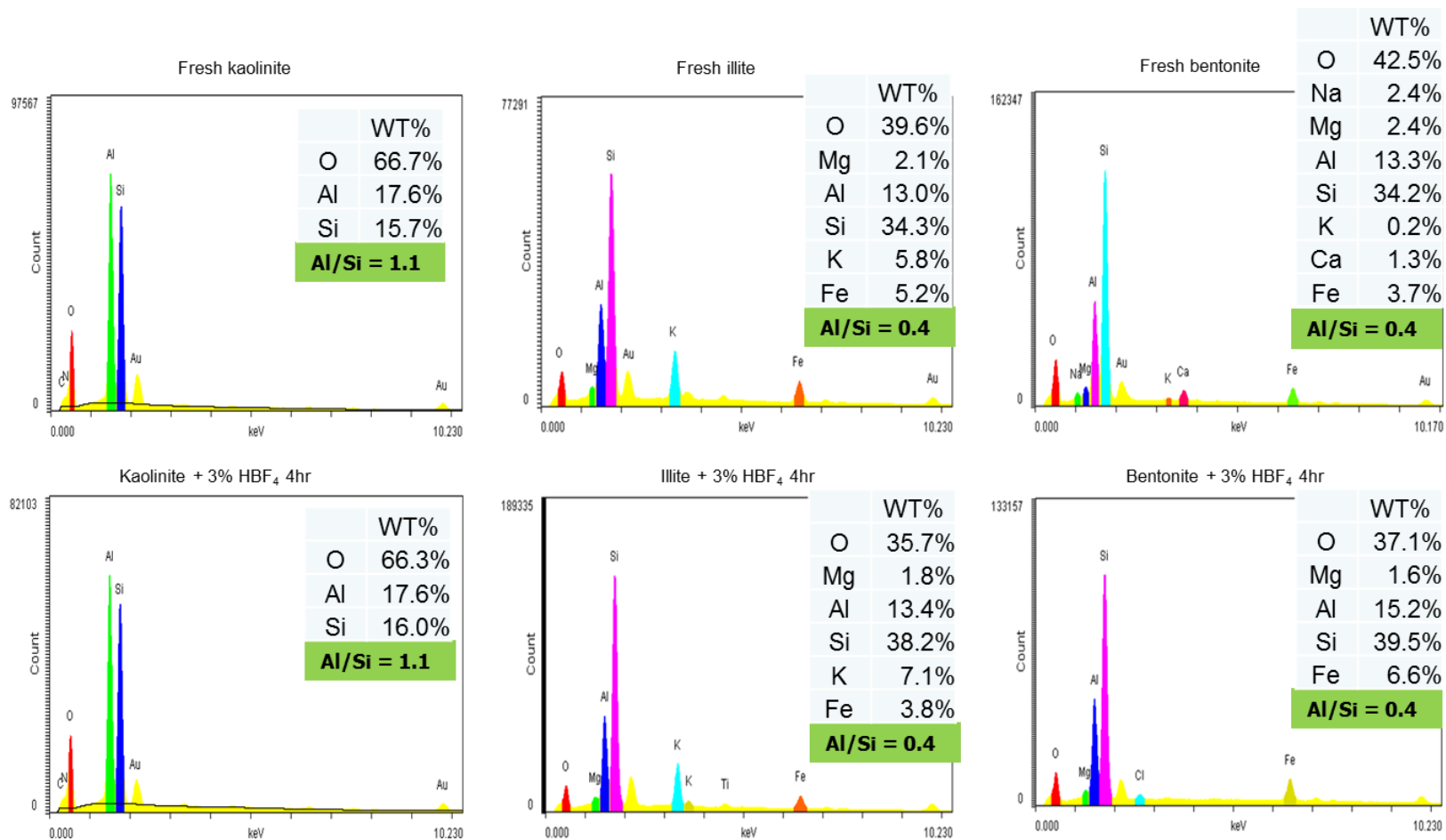


Figure 9: Clay weight loss % for 3% HBF<sub>4</sub> dissolution test at 75°F.





**Figure 10: EDS spectra of fresh clays (top row) vs 3% HBF<sub>4</sub> dissolved clays at 75°F for 4 hours (bottom row).**

Fig. 11-13 show boron concentration in the supernatant of 3%  $\text{HBF}_4$  reacted with clays at 75°F for 4 hours. Among all 3 clays, only illite shows a decreasing level of boron in solution. Traces of white precipitate were also observed lying on bottom of the test tubes. This precipitate was filtered out of solution, washed with DIW, dried, and sent for X-Ray diffraction (XRD) analysis. Result confirms existence of  $\text{KBF}_4$ . No precipitate was observed with kaolinite or bentonite.

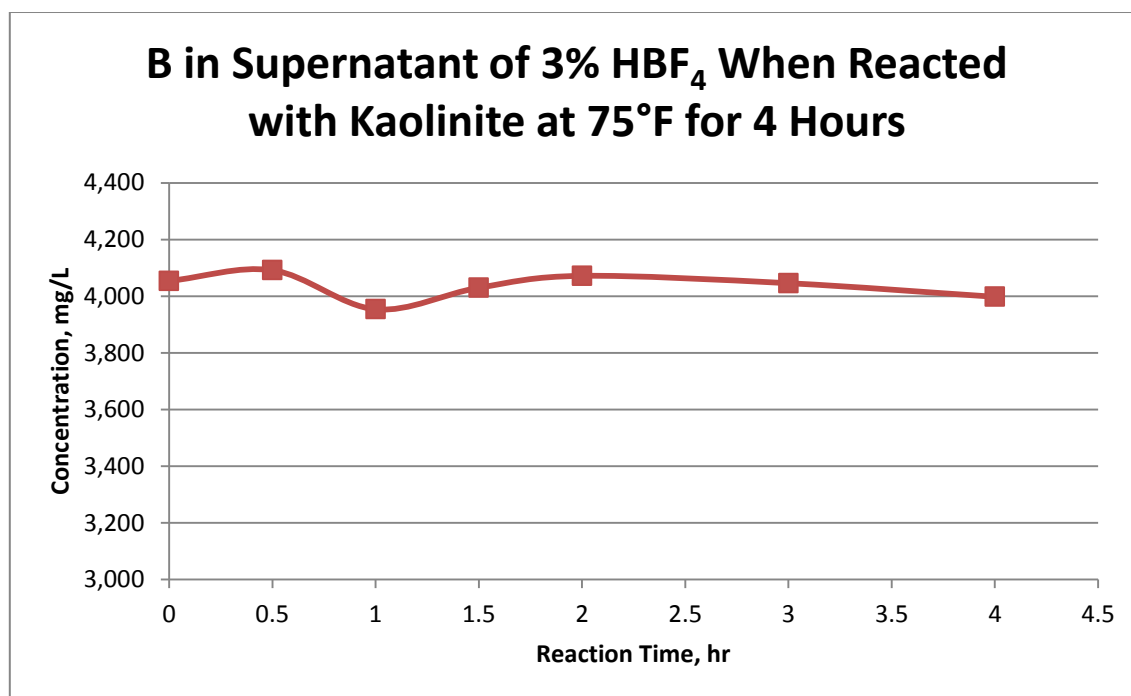


**Figure 11: Boron concentration in supernatant of 3%  $\text{HBF}_4$  reacted with kaolinite at 75°F for 4 hours.**

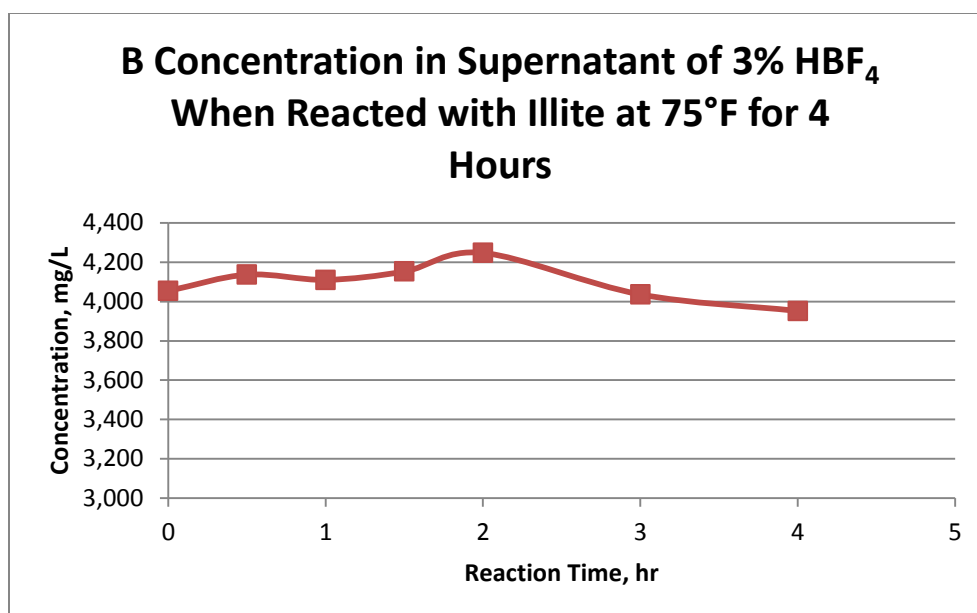


**Figure 12: Boron concentration in supernatant of 3% HBF<sub>4</sub> reacted with illite at 75°F for 4 hours.**

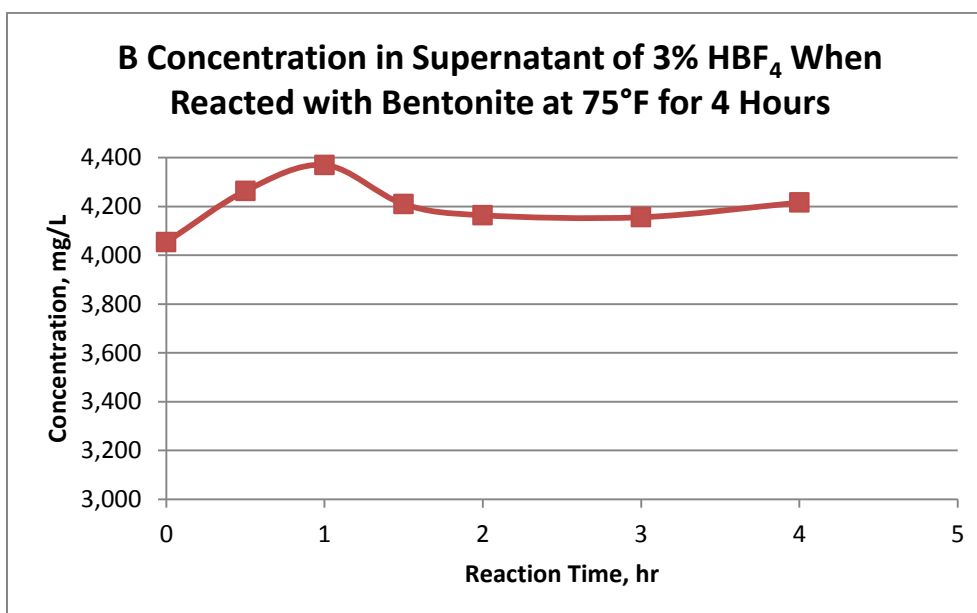


**Figure 13: Boron concentration in supernatant of 3% HBF<sub>4</sub> reacted with bentonite at 75°F for 4 hours.**

In Fig. 14, while all other key elements except Ca are reflecting the retarded reaction of  $\text{HBF}_4$ , potassium concentration extracted by  $\text{HBF}_4$  is at around five times of that extracted by mud acid. Fig. 15 shows the  $^{19}\text{F}$  NMR spectrum of 12-3 mud acid reacted with kaolinite for 4 hours at  $75^\circ\text{F}$ . Two species can be identified as silicon fluoride ( $\text{SiF}_y$ ) at  $\delta=-129$  ppm and aluminum fluoride ( $\text{AlF}_x^{(3-x)}$ ) at  $\delta=-155$ - $156$  ppm. Comparing this spectrum with Fig. 16, two expected additional species appeared at  $\delta=-145$  ppm, which was assigned as  $\text{BF}_3\text{OH}^-$  and  $\delta=-150$  ppm, which was assigned as  $\text{BF}_4^-$ . A spectrum in Fig. 16 has smaller intensity at both the  $\text{SiF}_y$  peak and the  $\text{AlF}_x^{(3-x)}$  peak when compared to Fig. 15. This reflects the retardation effect of  $\text{HBF}_4$ . The  $\text{AlF}_x^{(3-x)}$  peak in Fig. 17 has diminished to a very low level comparing to kaolinite due to less Al available to complex with  $\text{F}^-$  (see Fig. 18). The reason that a  $^{19}\text{F}$  NMR spectrum in Fig. 19 only shows  $\text{BF}_3\text{OH}^-$  at  $\delta=-147$  ppm and  $\text{BF}_4^-$  at  $\delta=-149$  ppm is probably because the very low dissolution rate provided a limited amount of Si and Al from bentonite to complex with  $\text{F}^-$ . The peaks then become unnoticeable.

Three species of boron containing compounds were found in  $^{11}\text{B}$  NMR spectra of reacted 3%  $\text{HBF}_4$  with clays (Fig. 20-22). A peak at  $\delta=19$  is assigned as  $\text{H}_3\text{BO}_3$  (Dewar and Jones 1967), a peak at  $\delta=0$  is assigned as  $\text{BF}_3\text{OH}^-$  and the last peak at  $\delta=-2$  is assigned as  $\text{BF}_4^-$ . None of the spectra show the  $\text{BF}_2(\text{OH})_2^-$  or  $\text{BF}(\text{OH})_3^-$  species since  $\text{BF}_3\text{OH}^-$  is rapidly converted to a less fluorinated borate in water to its final form ( $\text{H}_3\text{BO}_3$ ). In Fig. 21-22, the spectra got cut off before the range of boric acid. This is probably due to a very a low boric intensity since these systems are retarded more than kaolinite.

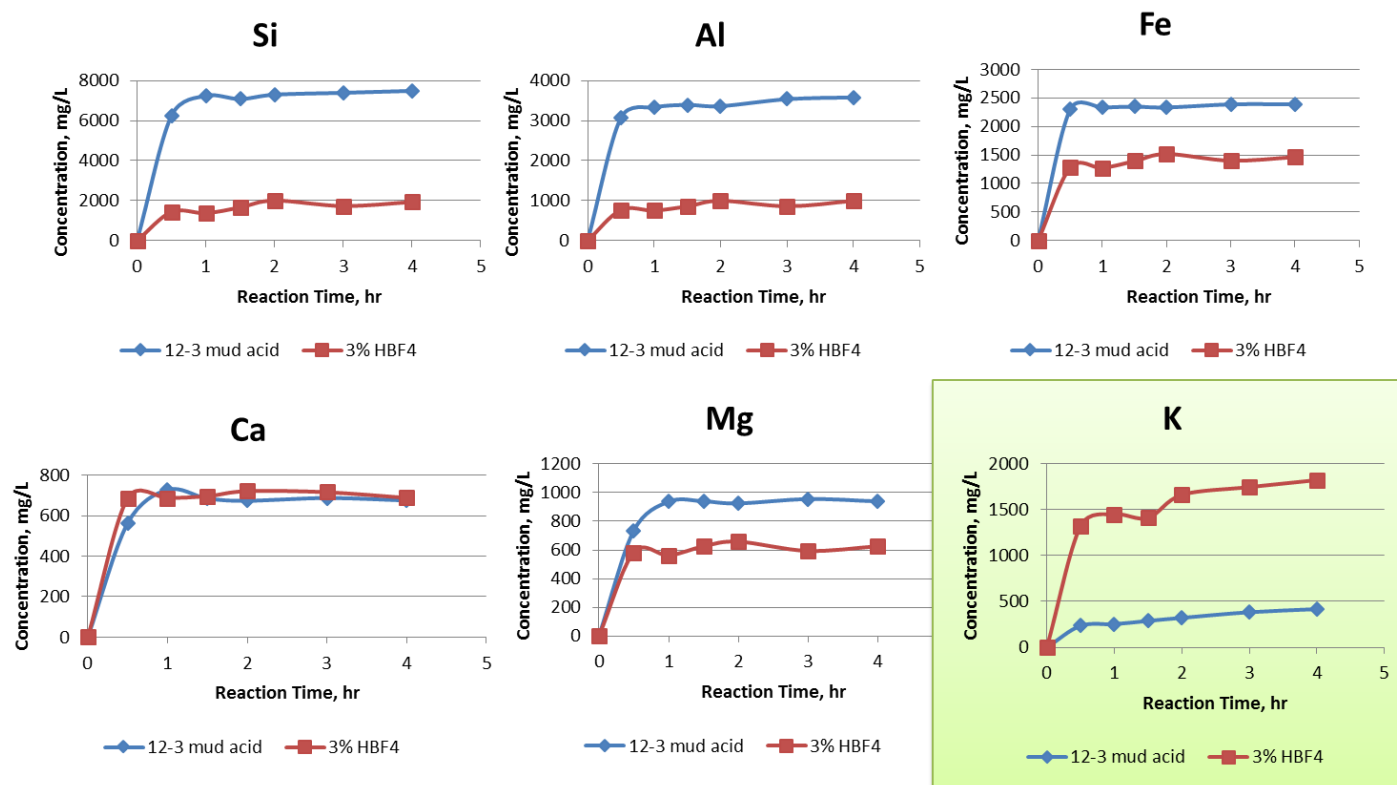


**Figure 14: Key elements in solution of illite + 12-3 mud acid and 3% HBF<sub>4</sub> at 75°F.**

Sample 2 D2O ArpaJit  
Inova400 asw5mm  
z0 at D2O 19F  
June 2013

File: xp

Pulse Sequence: s2pu1

Solvent: d2o

Ambient temperature

Operator: vnmr1

INOVA-400 "inova400"

Relax. delay 2.000 sec

Pulse 45.0 degrees

Acq. time 2.000 sec

Width 50000.0 Hz

128 repetitions

OBSERVE F19, 375.9242465 MHz

DATA PROCESSING

Line broadening 0.3 Hz

FT size 262144

Total time 8 min, 33 sec

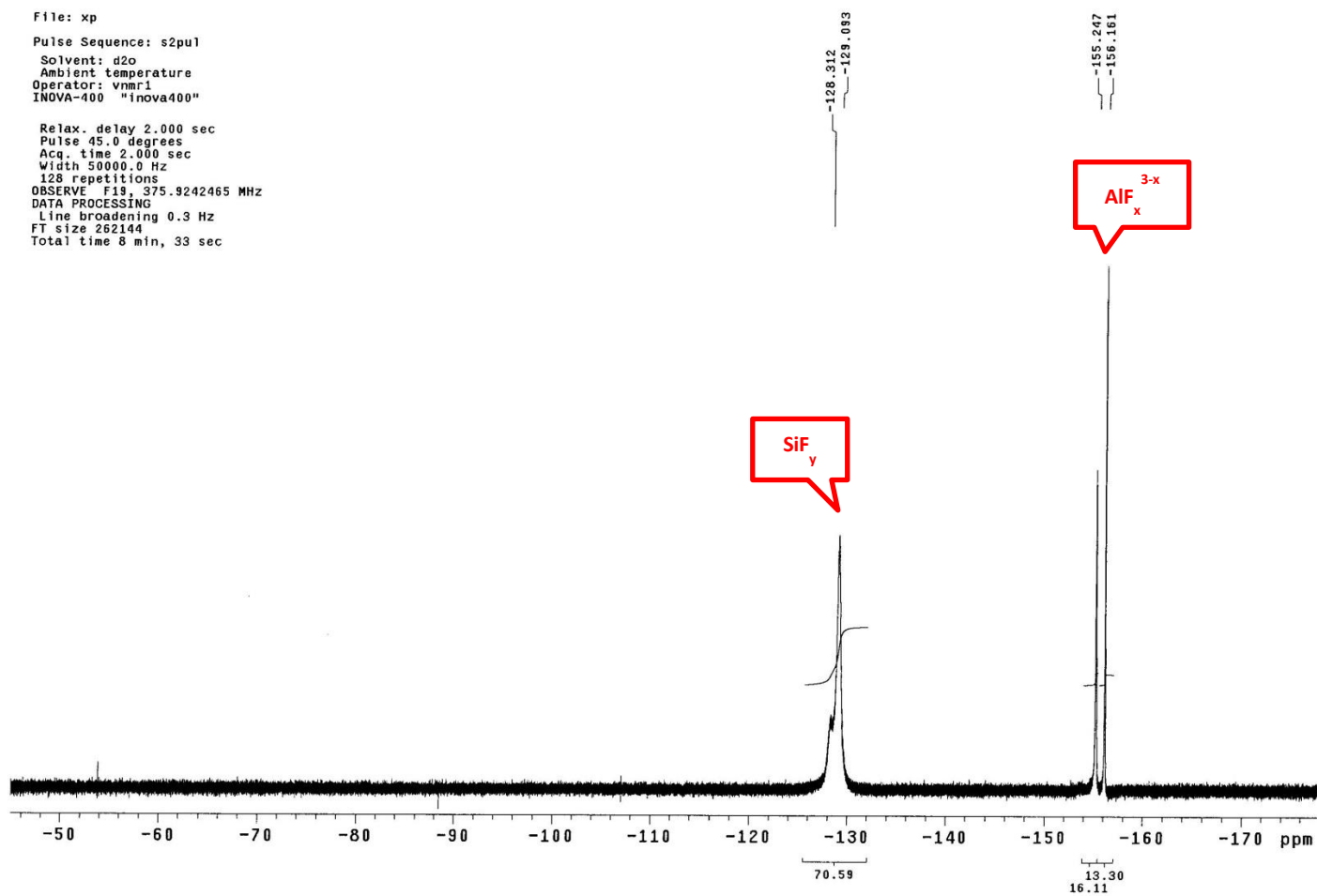


Figure 15:  $^{19}\text{F}$  NMR spectrum of 12-3 mud acid solution reacted with kaolinite at 75°F for 4 hours.

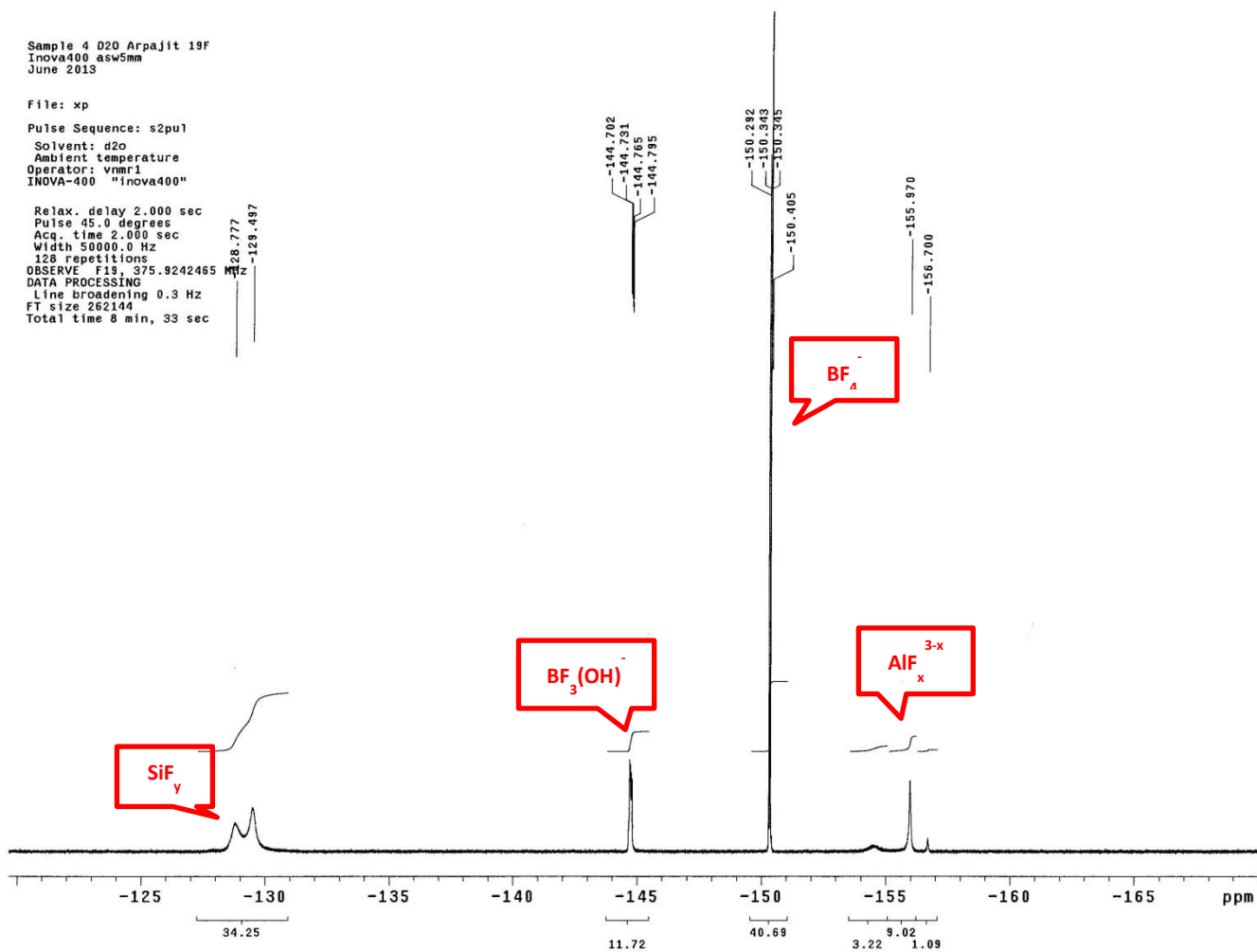


Figure 16:  $^{19}\text{F}$  NMR spectrum of 3%  $\text{HBF}_4$  solution reacted with kaolinite at 75°F for 4 hours.

ArpaJit Dlite + HBF<sub>4</sub> 4 hr 19F  
 Jan 2014

File: xp

Pulse Sequence: s2pul

Solvent: d2o

Ambient temperature

Operator: vmmr1

INOVA-400 "inova400"

Relax. delay 2.000 sec

Pulse 45.0 degrees

Acq. time 2.000 sec

Width 50000.0 Hz

32 repetitions

OBSERVE F19, 375.911875 MHz

DATA PROCESSING

Line broadening 0.3 Hz

FT size 262144

Total time 8 min, 33 sec

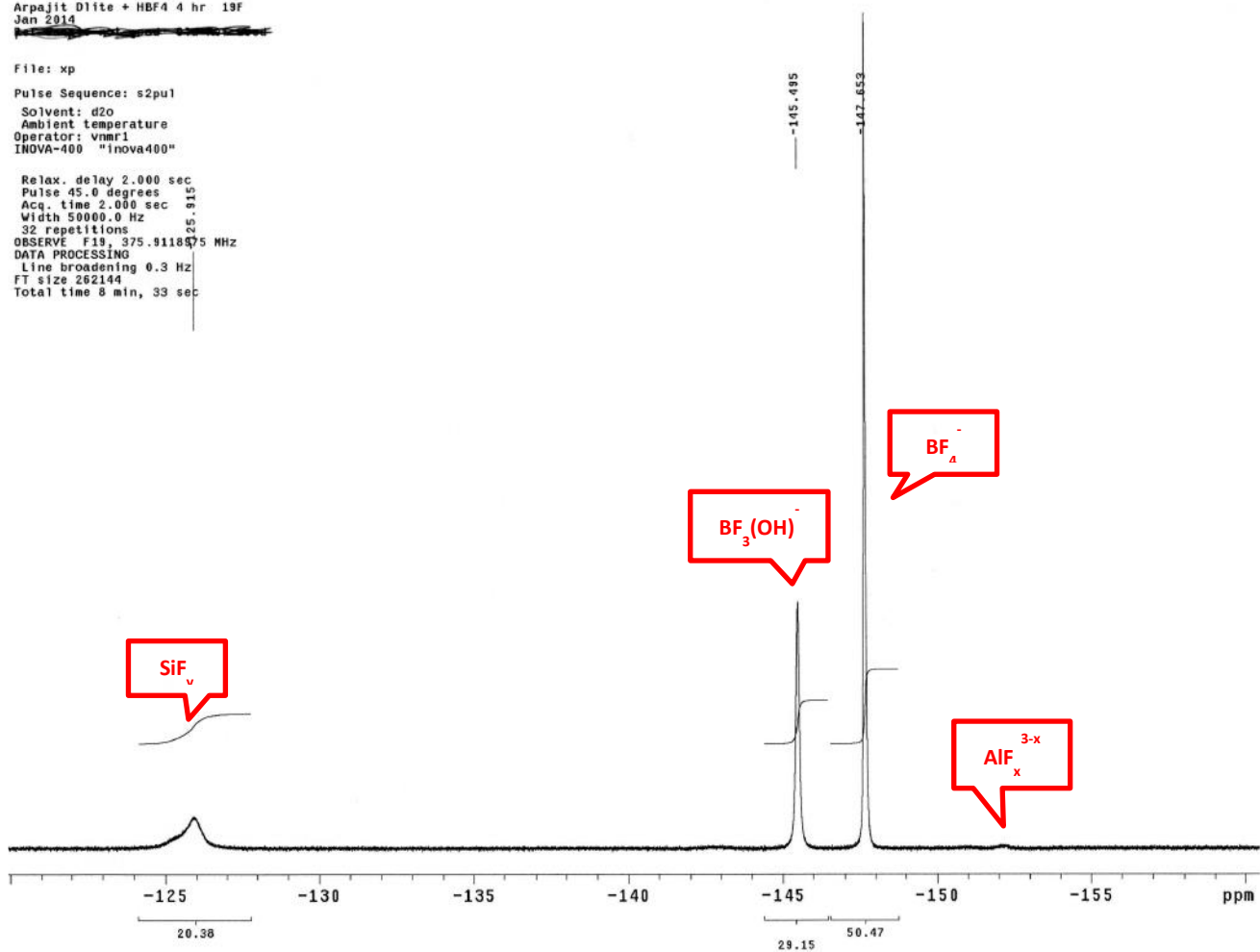


Figure 17: <sup>19</sup>F NMR spectrum of 3% HBF<sub>4</sub> solution reacted with illite at 75°F for 4 hours.



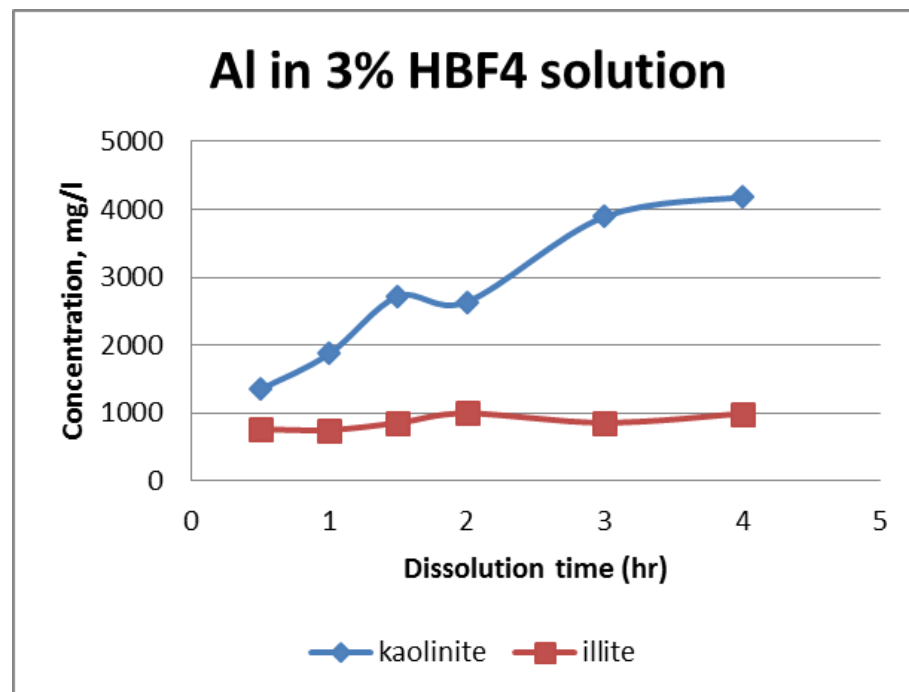


Figure 18: Al concentration available when reacting with different clay with 3% HBF<sub>4</sub> at 75°F.

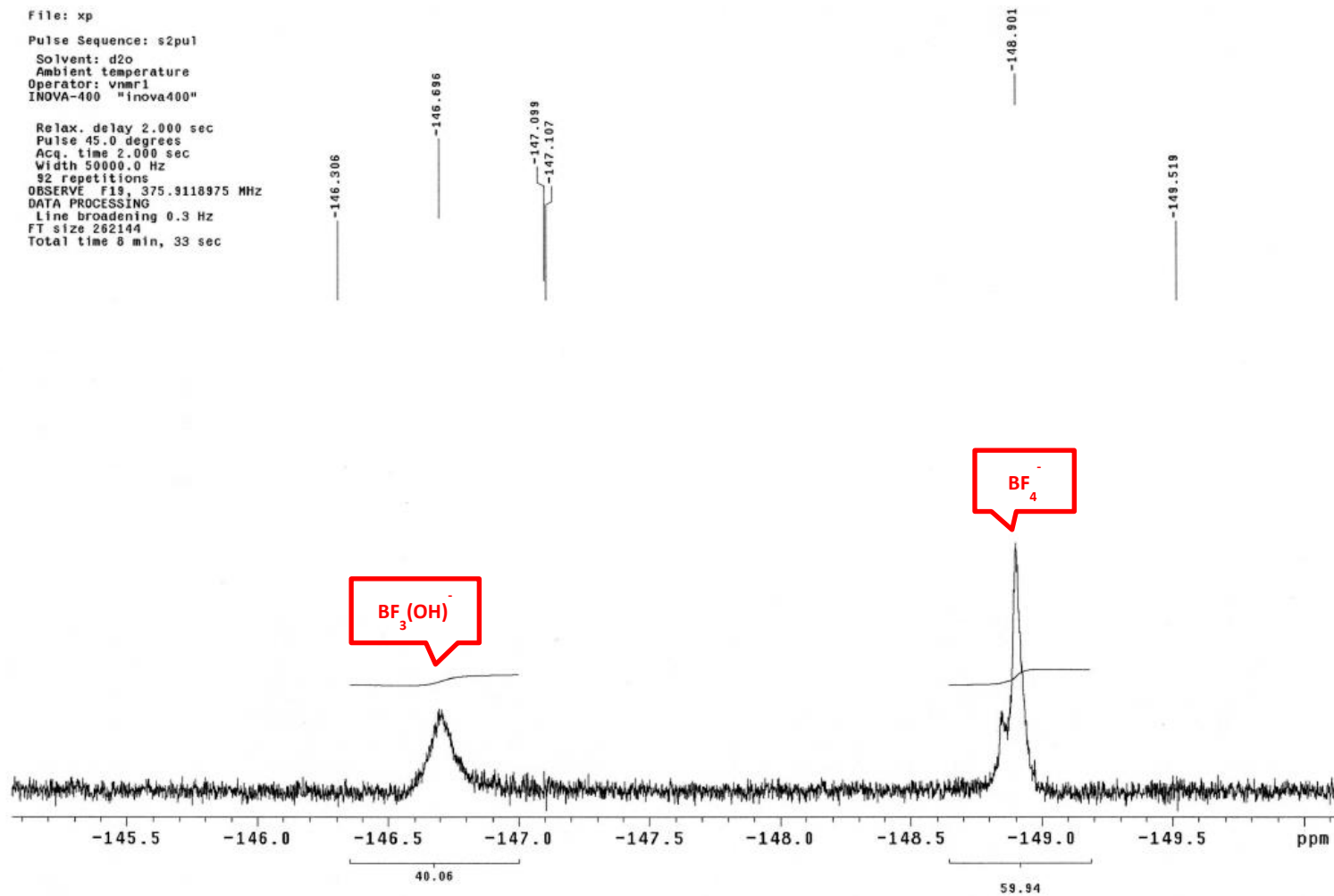


Figure 19:  $^{19}\text{F}$  NMR spectrum of 3%  $\text{HBF}_4$  solution reacted with bentonite at  $75^\circ\text{F}$  for 4 hours.

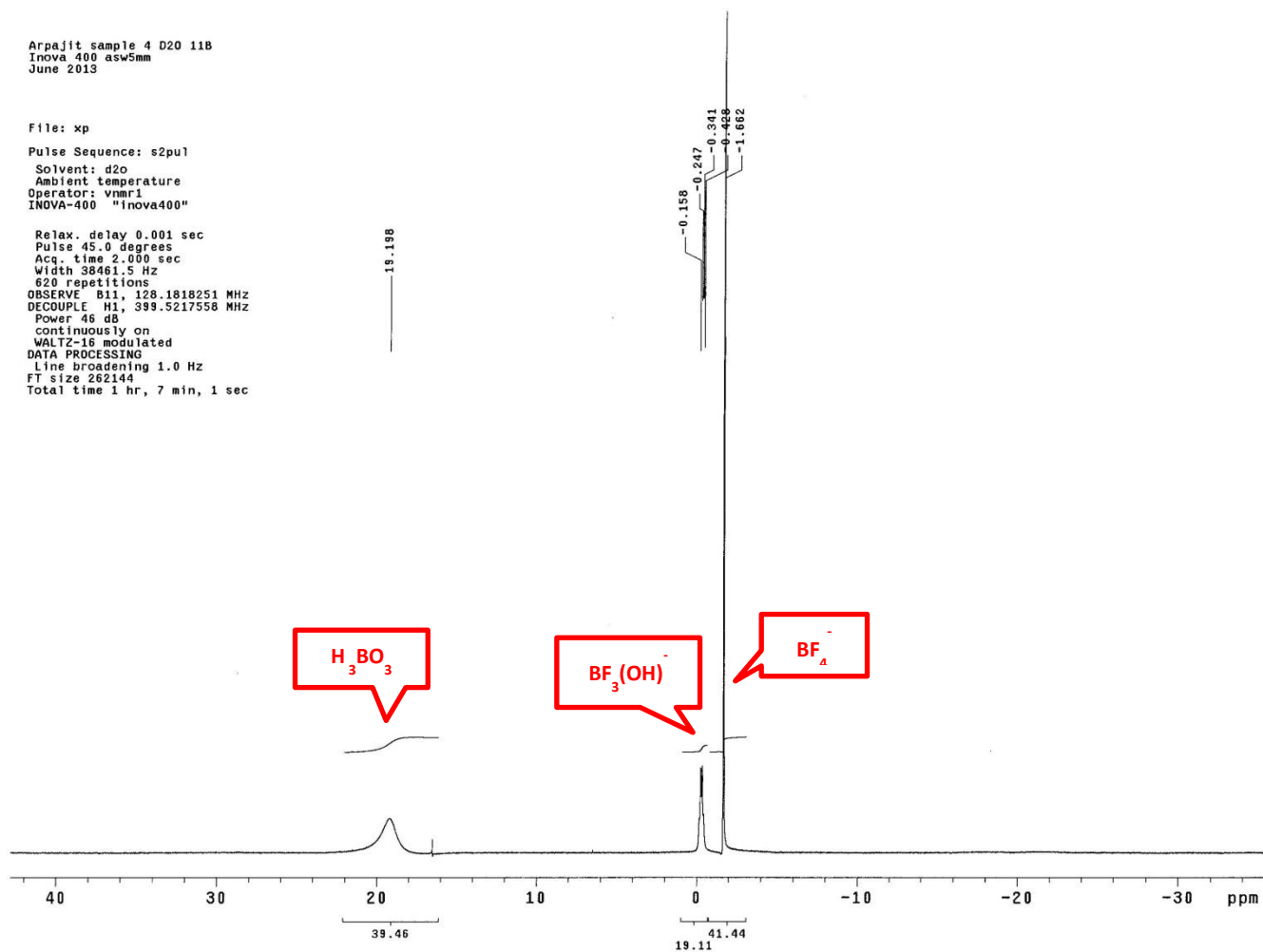


Figure 20:  $^{11}\text{B}$  NMR spectrum of 3%  $\text{HBF}_4$  solution reacted with kaolinite at 75°F for 4 hours.

Arpajit Dilite + HBF<sub>4</sub> 4hr  
1400 asw5mm  
Jan 2014 old ref data used  
Ref sample bad

File: xp

Pulse Sequence: s2pul

Solvent: d2o  
Ambient temperature  
Operator: vnmr1  
INNOVA-400 "inova400"

Relax. delay 0.001 sec  
Pulse 45.0 degrees  
Acq. time 2.000 sec  
Width 38461.5 Hz  
120 repetitions  
OBSERVE 811.128.1776451 MHz  
DATA PROCESSING  
Line broadening 1.0 Hz  
FT size 262144  
Total time 4 min, 19 sec

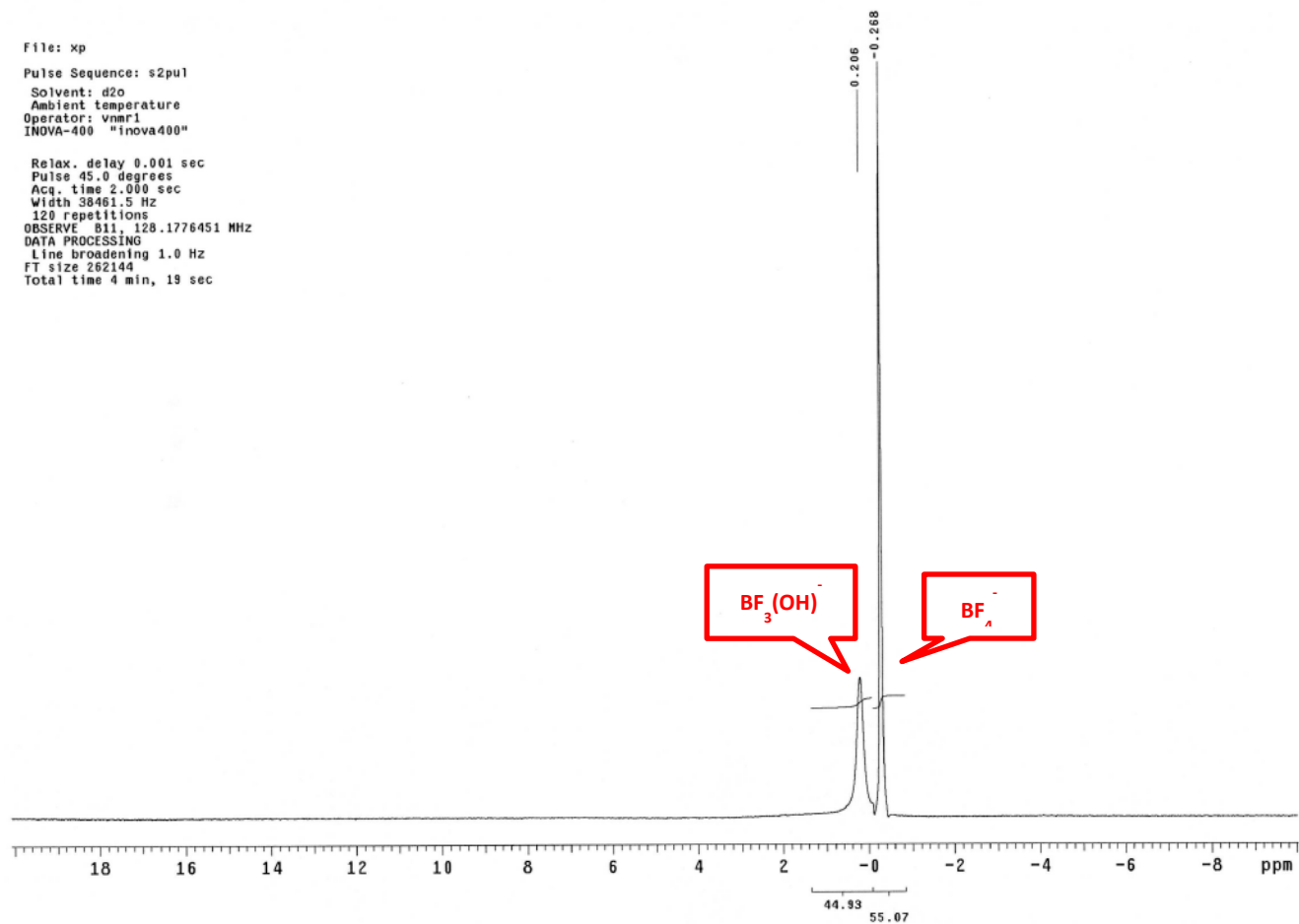


Figure 21: <sup>11</sup>B NMR spectrum of 3% HBF<sub>4</sub> solution reacted with illite at 75°F for 4 hours.

ArpaJit Bentonite HBF<sub>4</sub> 4hr B11  
I400 asw5mm  
Jan 2014 old ref data used  
Ref sample bad

File: xp

Pulse Sequence: s2pul  
Solvent: d2o  
Ambient temperature  
Operator: vnmr1  
INOVA-400 "inova400"

Relax. delay 0.001 sec  
Pulse 45.0 degrees  
Acq. time 2.000 sec  
Width 38461.5 Hz  
128 repetitions  
OBSERVE B11, 128.1776451 MHz  
DATA PROCESSING  
Line broadening 1.0 Hz  
FT size 262144  
Total time 4 min, 19 sec

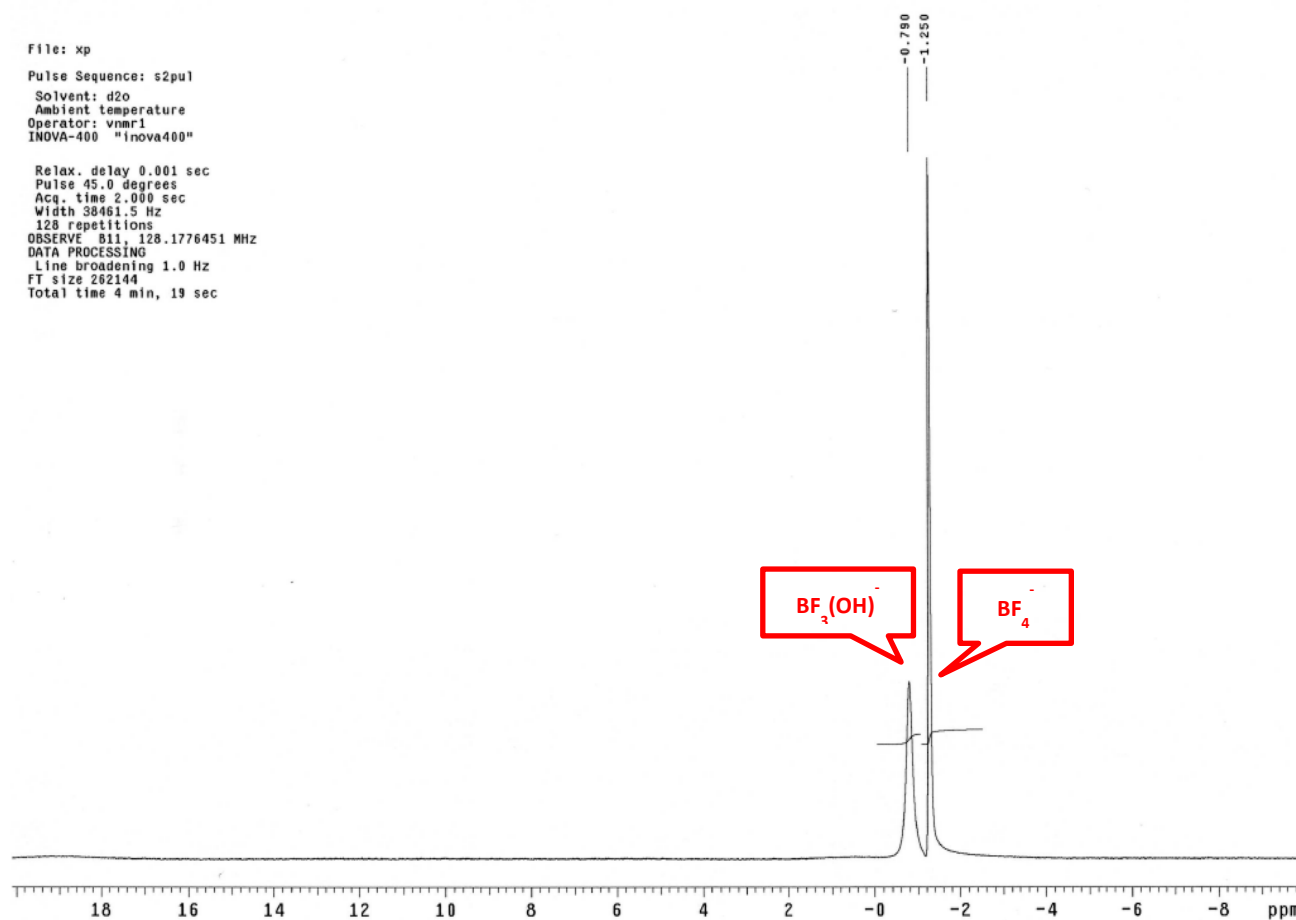
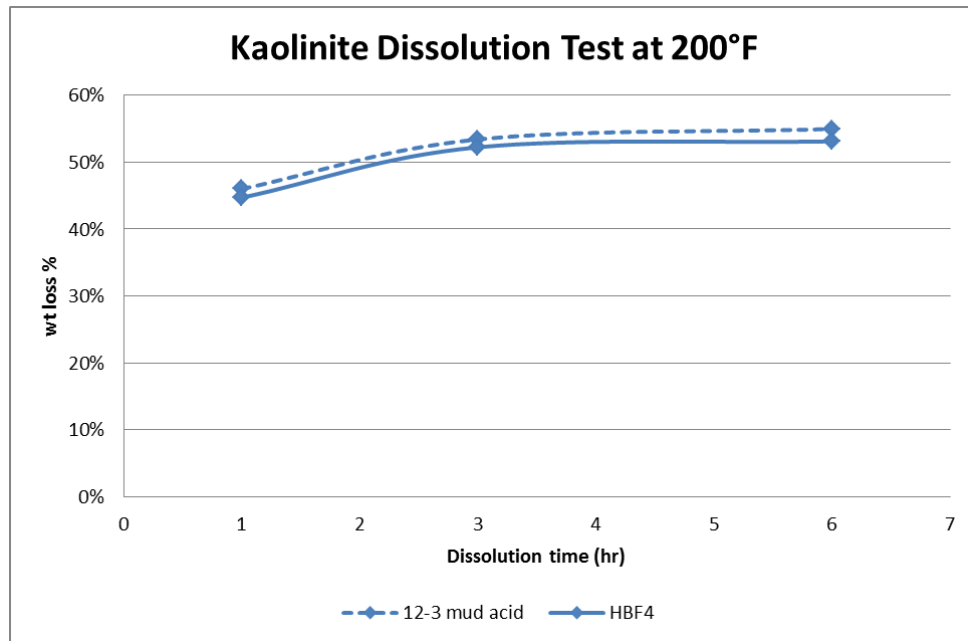


Figure 22: <sup>11</sup>B NMR spectrum of 3% HBF<sub>4</sub> solution reacted with bentonite at 75°F for 4 hours.

### Clay Dissolution Test at 200°F

Comparing to 12-3 mud acid dissolvability at 200°F, the retardation effect of  $\text{HBF}_4$  plunges down to about 2-3% as shown in Fig. 23.



**Figure 23: Kaolinite weight loss percent by 12-3 mud acid and 3%  $\text{HBF}_4$  at 200°F.**

Fig. 24 compares the reaction rate of  $\text{HBF}_4$  on different clays at high temperature. The reaction rate has been raised for every clay tested at this temperature. It was observed that Bentonite lost its weight more than illite with  $\text{HBF}_4$  at 200°F, and the opposite happened at 75°F.

The supernatant of  $\text{HBF}_4$  with illite precipitated a white substance at all dissolution times (1,3,6 hours) as shown in Fig. 25, which later was analyzed with XRD

and identified as  $\text{KBF}_4$ . A match of  $\text{KBF}_4$  from EVA database with XRD spectrum confirms its identity (Fig. 26).

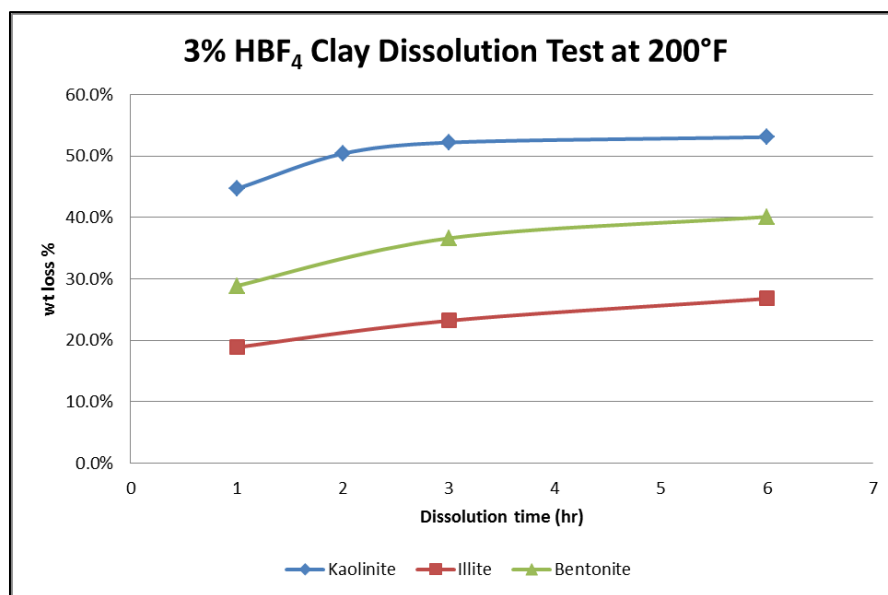


**Figure 24: Clay weight loss percent by 3%  $\text{HBF}_4$  at 200°F.**



**Figure 25: Precipitate from illite +  $\text{HBF}_4$  dissolution at 200°F for 6 hours.**

## 2014\_02\_07\_NED\_KBF4

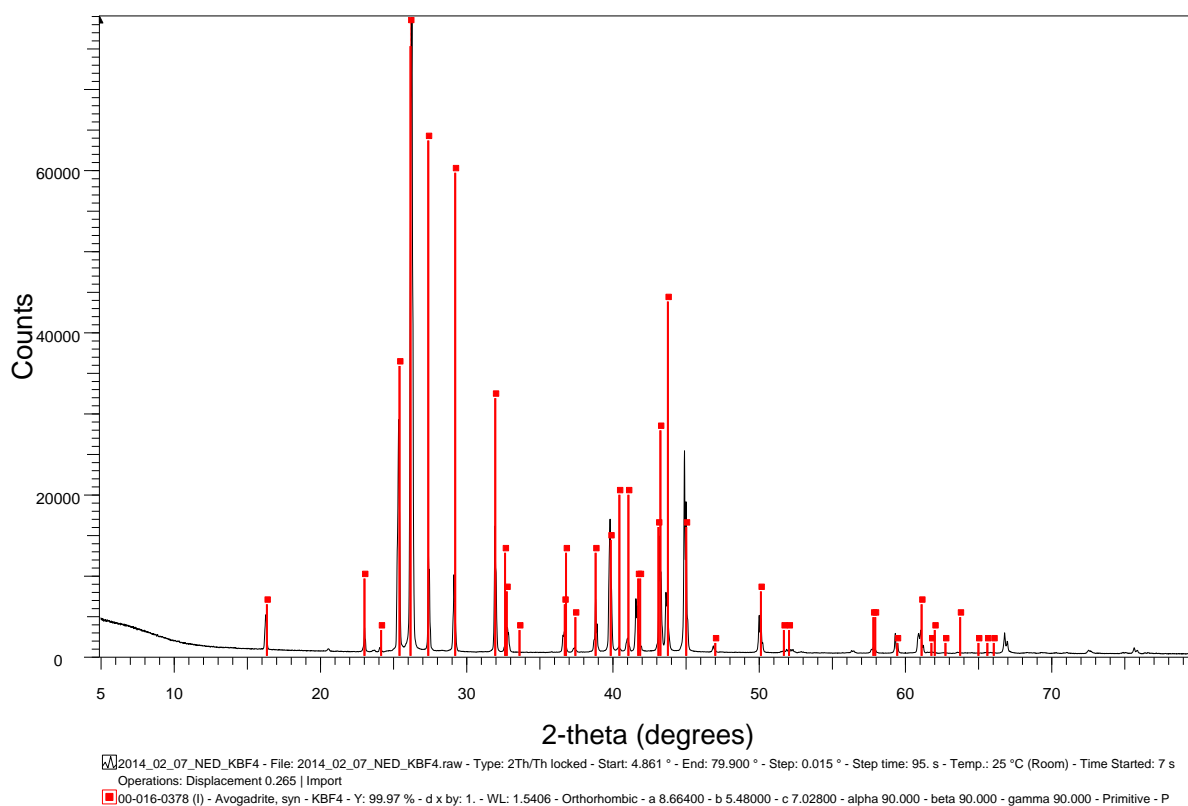


**Figure 26: XRD spectrum matched with KBF<sub>4</sub> using EVA database.**

The potassium concentration from 3% HBF<sub>4</sub> with illite at a higher temperature is lower. This can be accounted for due to the KBF<sub>4</sub> precipitation drawing K out of solution (Fig. 27).

Comparing key elements measured in the 3% HBF<sub>4</sub> supernatant of different clays (Fig. 28-30), a distinct falling trend of B in illite with acid solution is apparent. This is also resulted from KBF<sub>4</sub> precipitation.



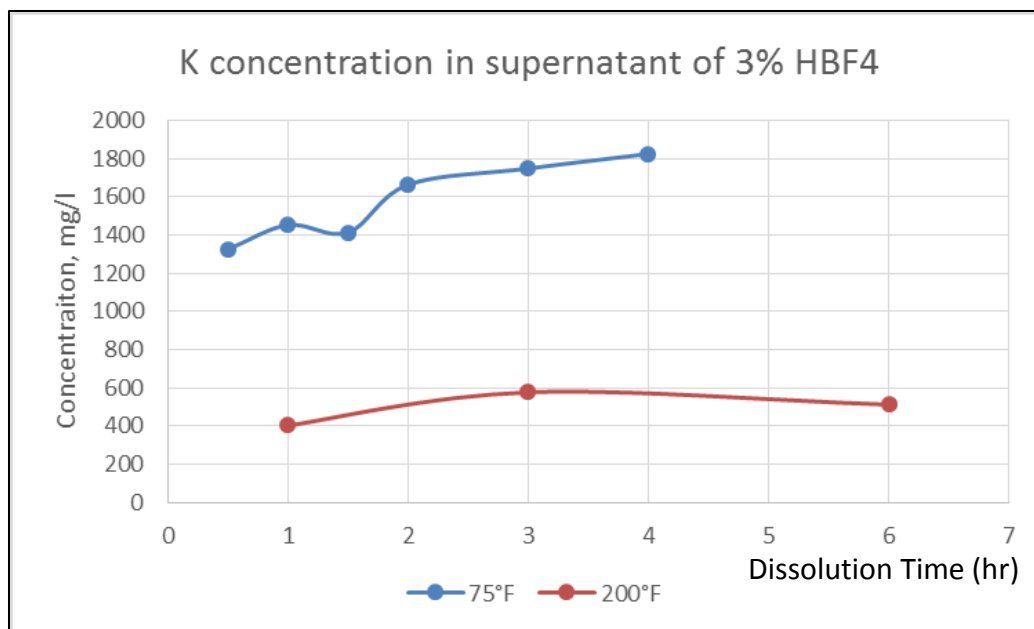


**Figure 27: Potassium concentration leached from illite by 3% HBF<sub>4</sub> at different temperatures.**

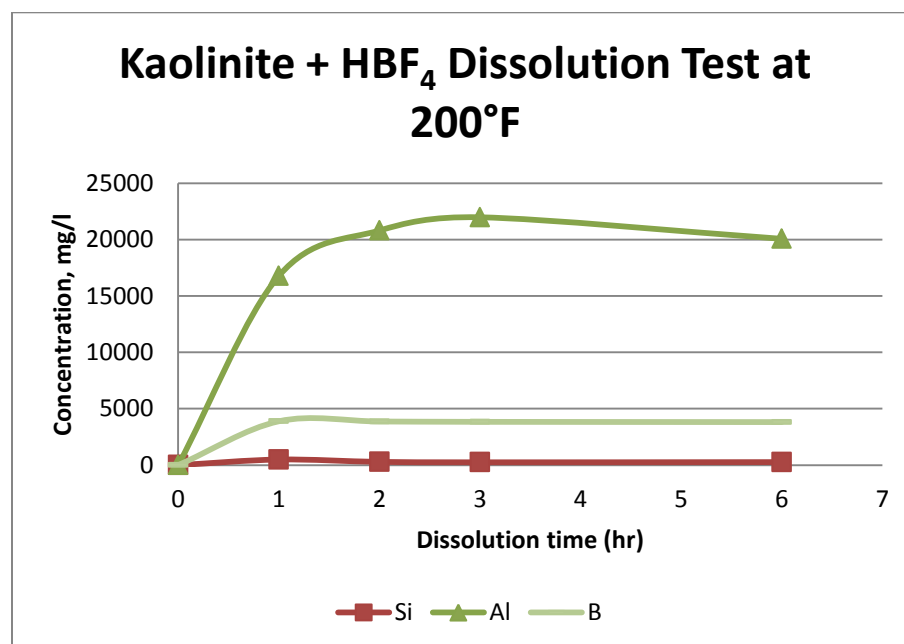


**Figure 28: Key elements concentration in supernatant of kaolinite reacted with HBF<sub>4</sub> at 200°F.**

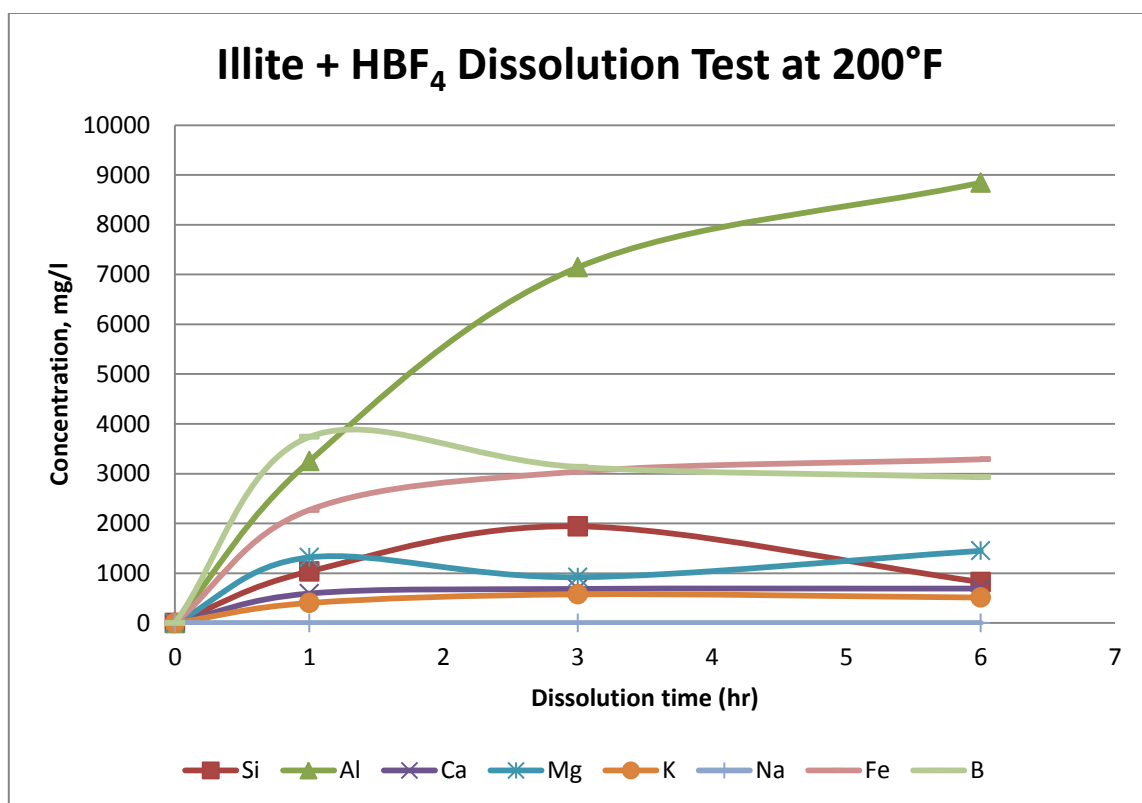


**Figure 29: Key elements concentration in supernatant of illite reacted with HBF<sub>4</sub> at 200°F.**

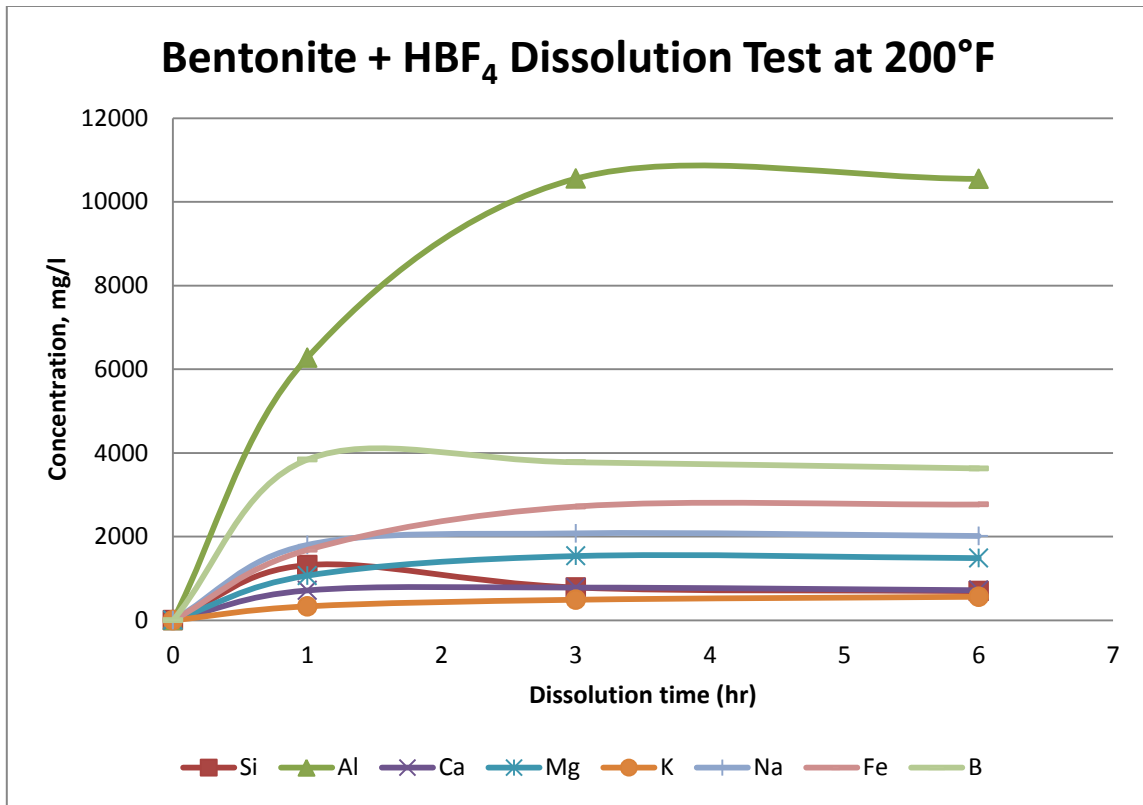


**Figure 30: Key elements concentration in supernatant of bentonite reacted with HBF<sub>4</sub> at 200°F.**

Fig. 31 contrasts the EDS spectrum of undissolved clays by 3% HBF<sub>4</sub> at 2 temperatures. At 200°F, HBF<sub>4</sub> leaches almost all Al from the clay structure (secondary reaction). Moreover, no SiF<sub>y</sub> or AlF<sub>x</sub><sup>(3-x)</sup> precipitated in any clay, and no NaBF<sub>4</sub> precipitate in Bentonite.

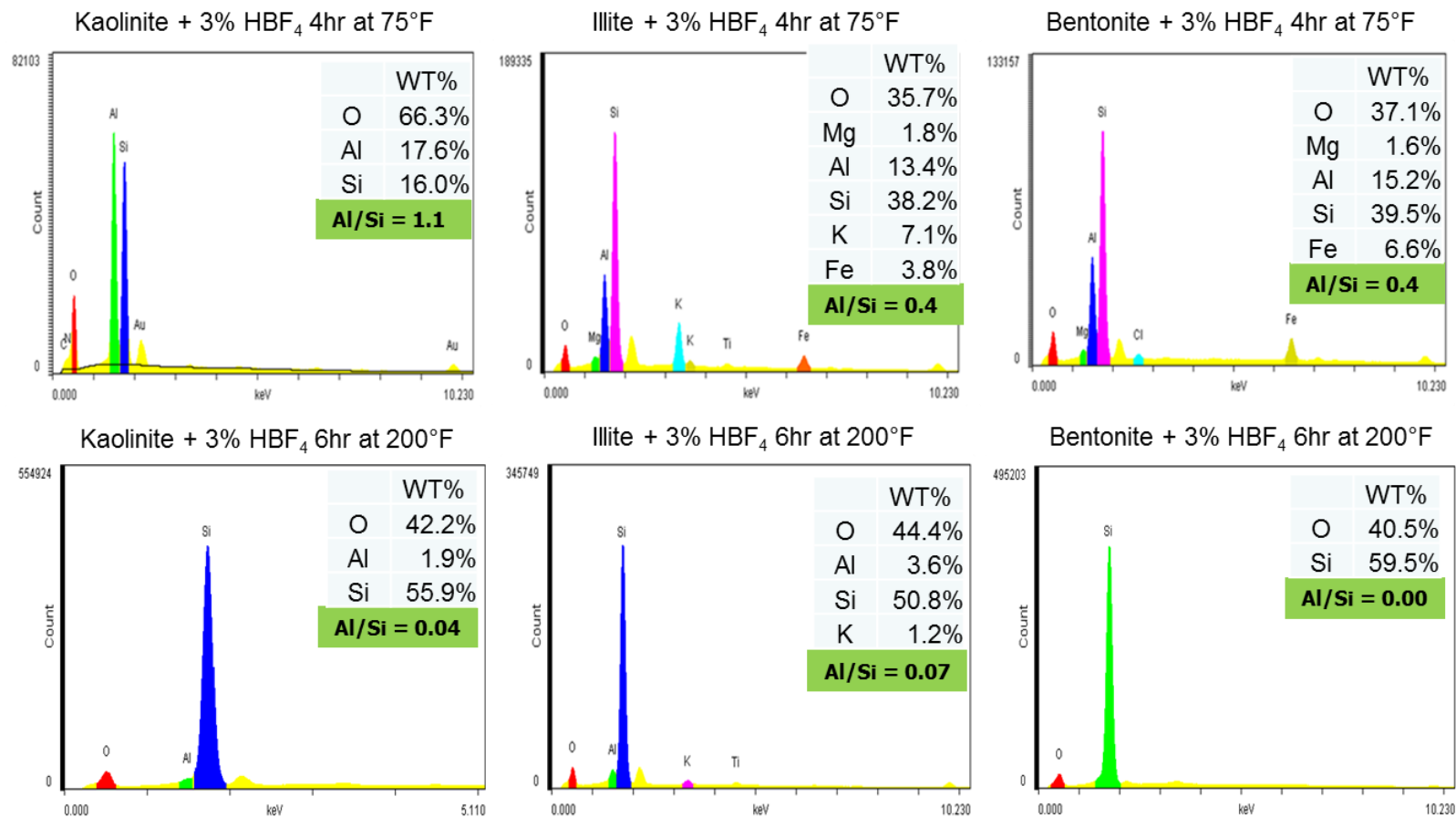


**Figure 31: EDS spectra of 3% HBF<sub>4</sub> dissolved clays at 75°F for 4 hours (top row) vs 3% HBF<sub>4</sub> dissolved clays at 200°F for 6 hours.**

Fig. 32-34 show comparisons of either Si or Al concentrations in 3%  $\text{HBF}_4$  acid that had completed secondary reaction (200°F) with tests at 75°F. All show decreases of Si due to precipitation as amorphous silica and large increases in the Al leached.

An increase in the  $\text{AlF}_x^{(3-x)}$  species noticed in Fig. 35 from Fig. 16 was due to a higher intensity of aluminum fluoride species compared to 75°F acid supernatant due to Al abundance in solution. A similar statement can also be implied on Fig. 36 and 37.

Fig. 38-40 yielded three similar species in every clay's supernatant (from left to right:  $\text{H}_3\text{BO}_3$ ,  $\text{BF}_3\text{OH}^-$  and  $\text{BF}_4^-$ ). It can then be concluded that a significant reaction is going on at this temperature for each clay with 3%  $\text{HBF}_4$ .

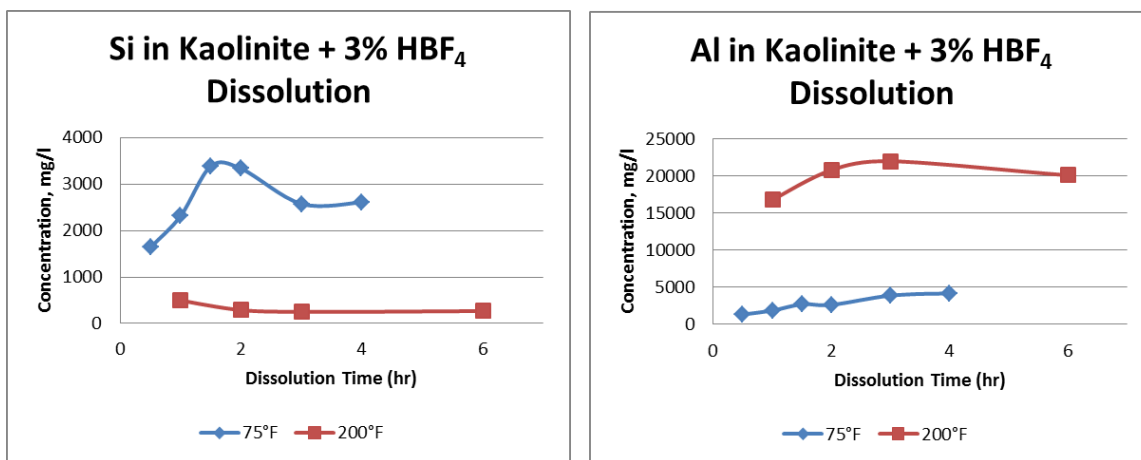


**Figure 32: Effect of temperature on Si and Al concentrations in 3%  $\text{HBF}_4$  supernatant with kaolinite.**

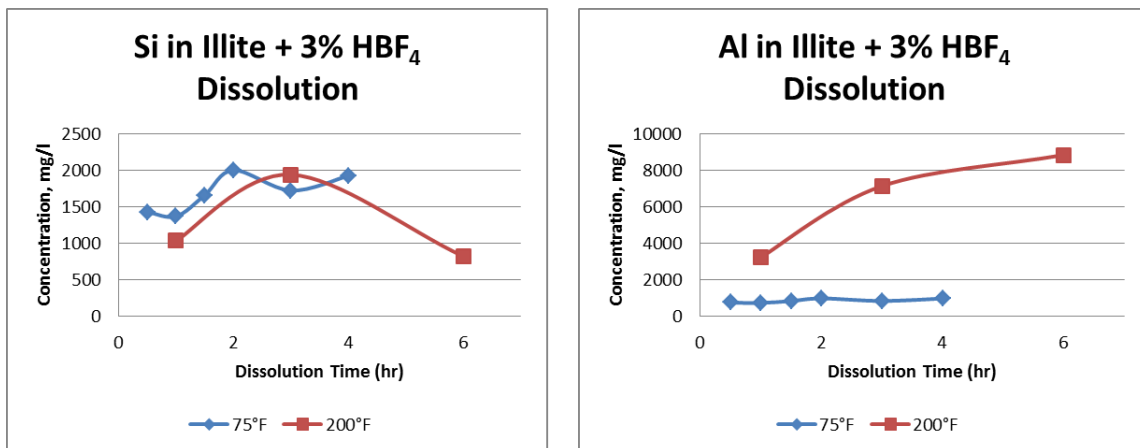


**Figure 33: Effect of temperature on Si and Al concentrations in 3% HBF<sub>4</sub> supernatant with illite.**

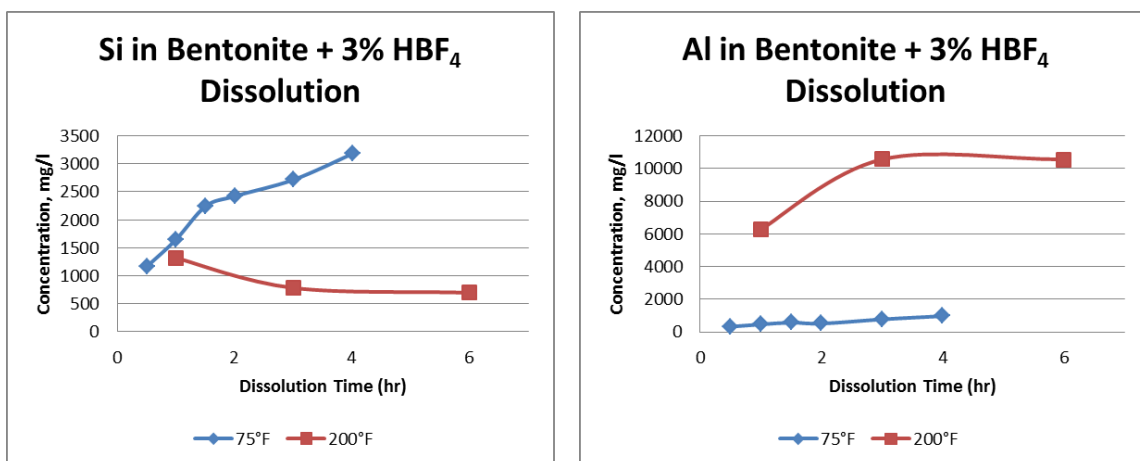


**Figure 34: Effect of temperature on Si and Al concentrations in 3% HBF<sub>4</sub> supernatant with bentonite.**

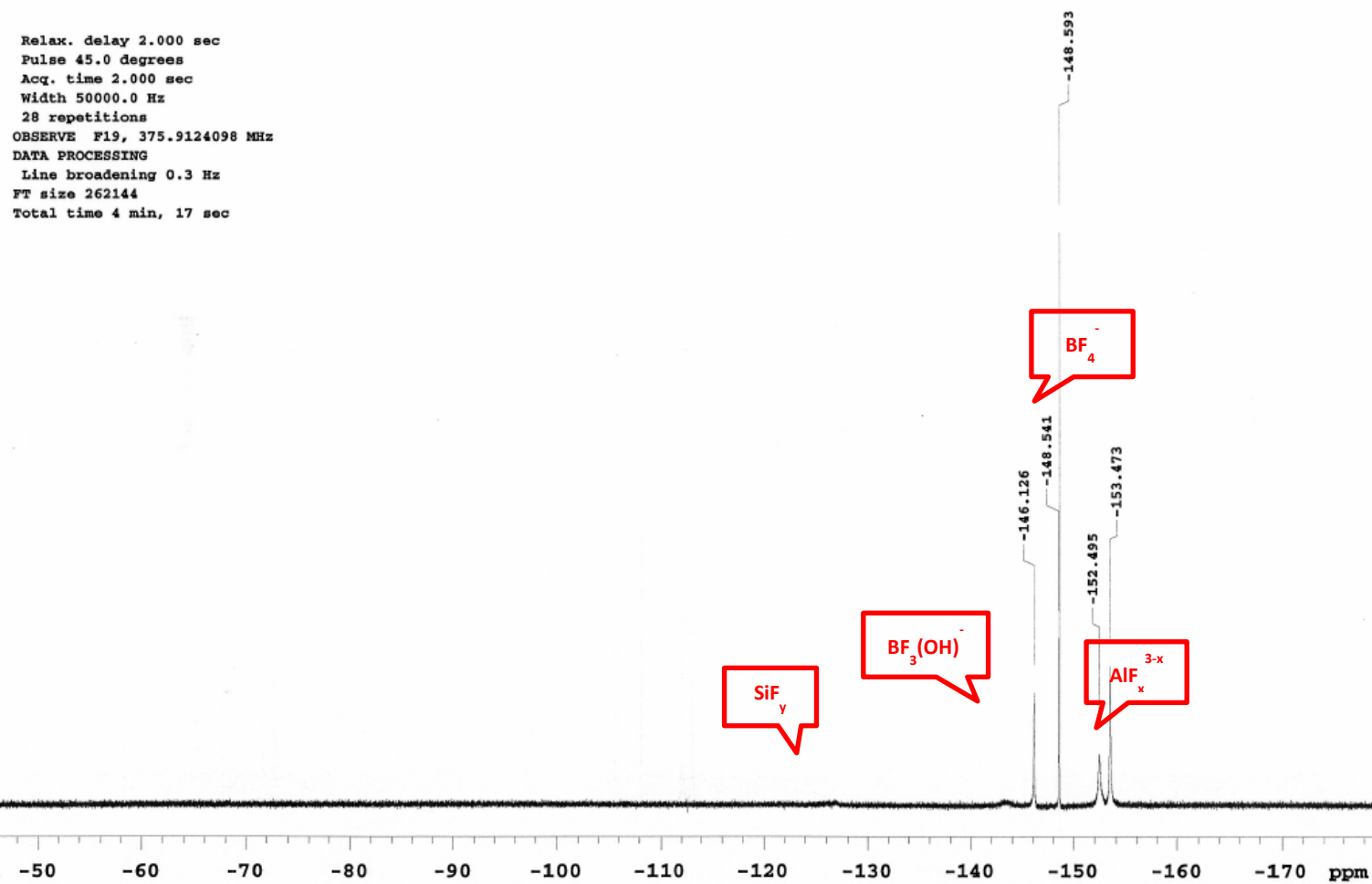


Figure 35:  $^{19}\text{F}$  NMR spectrum of 3%  $\text{HBF}_4$  solution reacted with kaolinite at 200°F for 6 hours.

Relax. delay 2.000 sec  
Pulse 45.0 degrees  
Acq. time 2.000 sec  
Width 50000.0 Hz  
48 repetitions  
OBSERVE F19, 375.9124098 MHz  
DATA PROCESSING  
Line broadening 0.3 Hz  
FT size 262144  
Total time 4 min, 17 sec

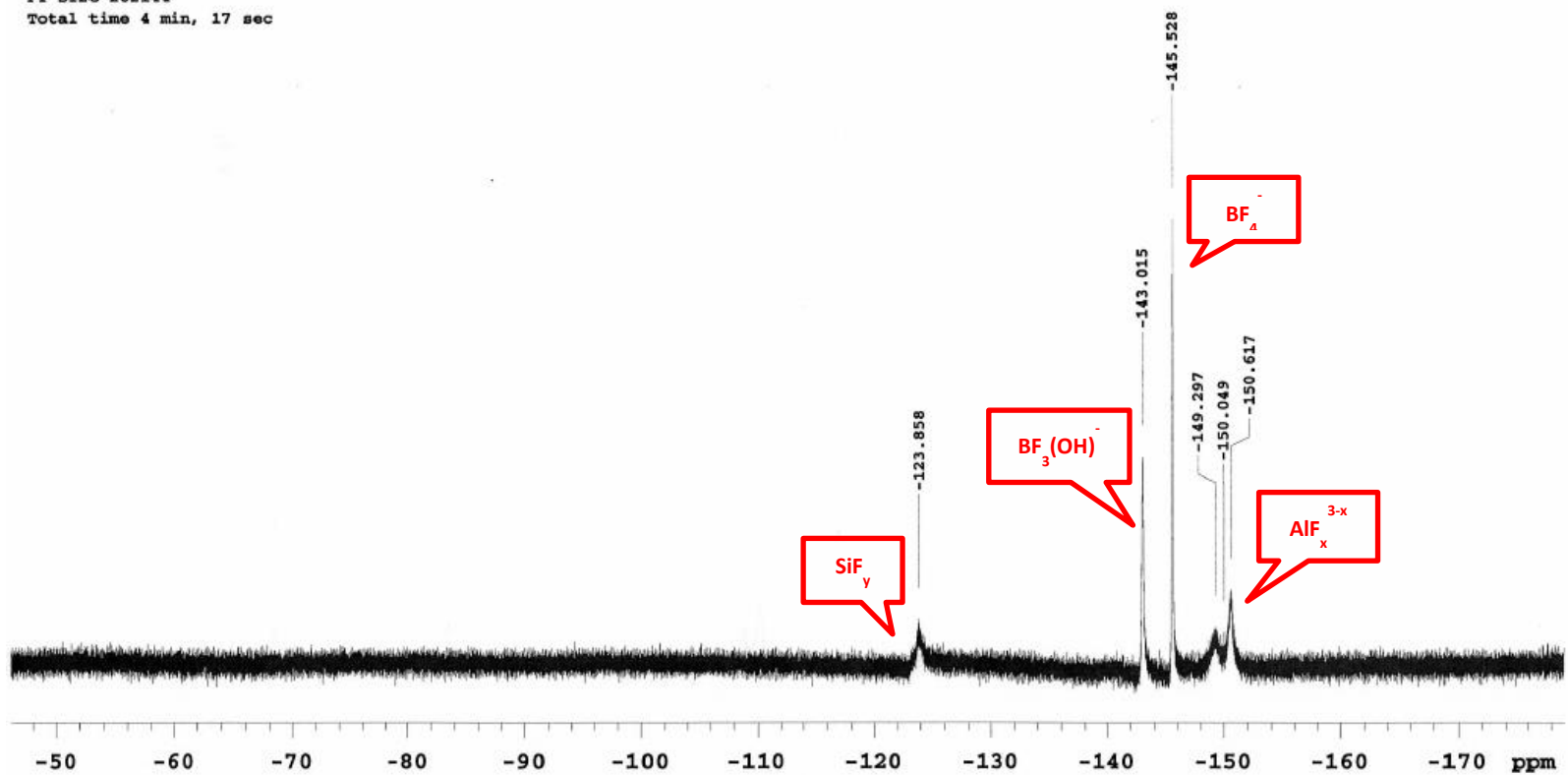


Figure 36:  $^{19}\text{F}$  NMR spectrum of 3%  $\text{HBF}_4$  solution reacted with illite at 200°F for 6 hours.



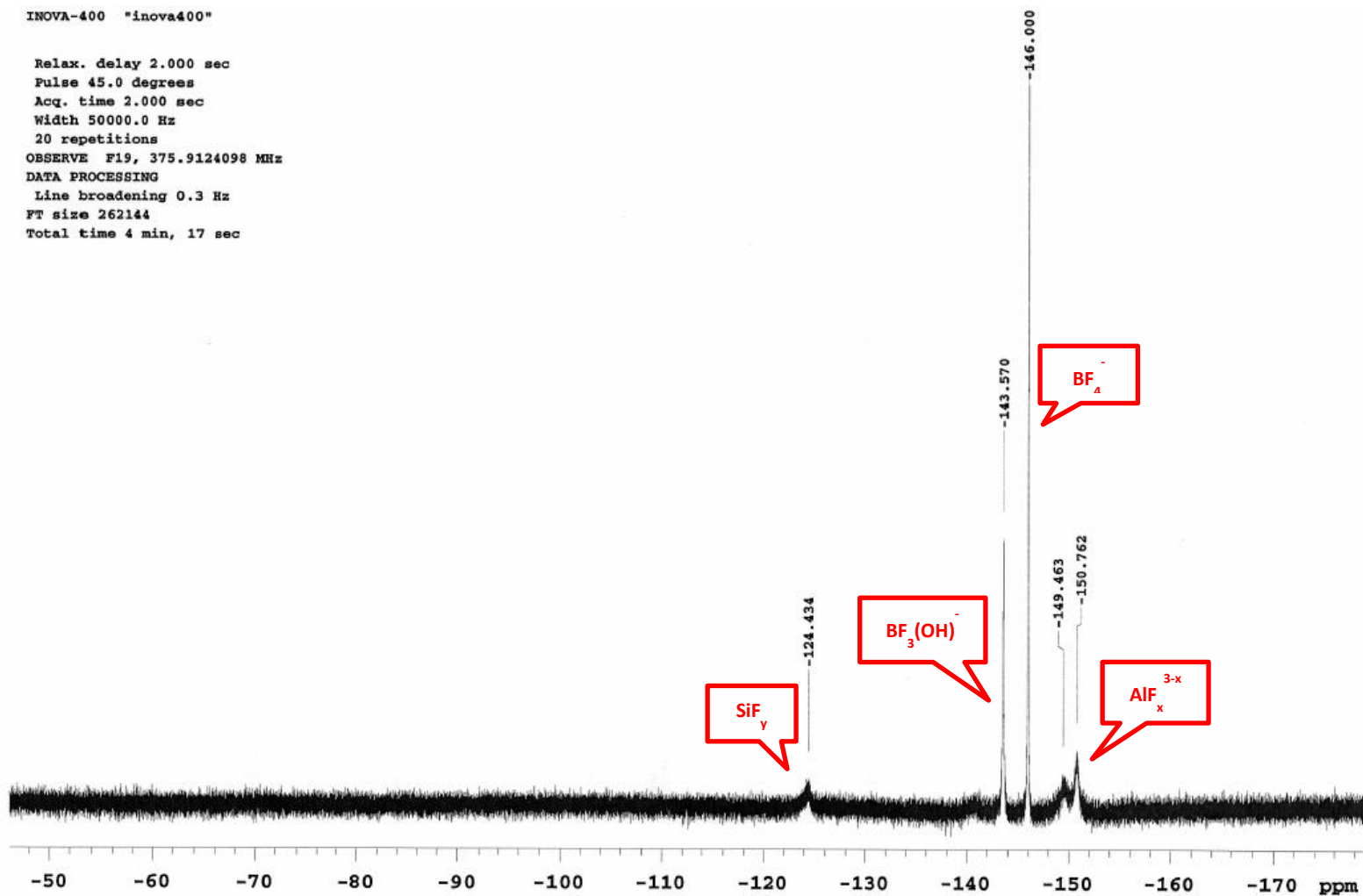


Figure 37:  $^{19}\text{F}$  NMR spectrum of 3%  $\text{HBF}_4$  solution reacted with bentonite at 200°F for 6 hours.

solvent: d2o  
Ambient temperature  
Operator: kchansae  
INOVA-400 "inova400"

Relax. delay 0.001 sec  
Pulse 45.0 degrees  
Acq. time 2.000 sec  
Width 38461.5 Hz  
52 repetitions  
OBSERVE B11, 128.1778459 MHz  
DECOUPLE H1, 399.5087270 MHz  
Power 46 dB  
continuously on  
WALTZ-16 modulated  
DATA PROCESSING  
Line broadening 1.0 Hz  
FT size 262144  
Total time 2 hr, 47 min, 31 sec

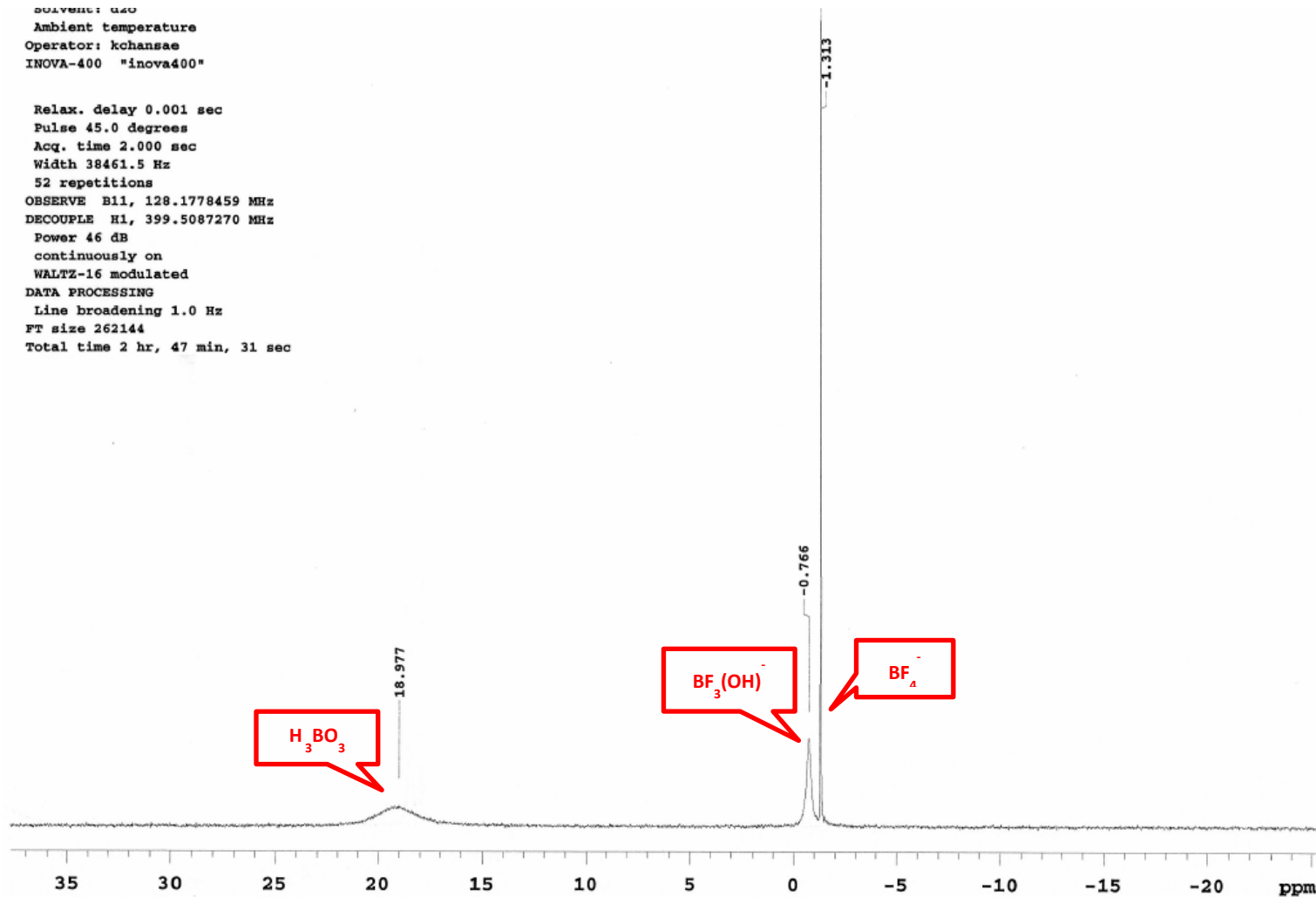


Figure 38:  $^{11}\text{B}$  NMR spectrum of 3%  $\text{HBF}_4$  solution reacted with kaolinite at 200°F for 6 hours.

Ambient temperature  
Operator: kchansae  
INOVA-400 "inova400"

Relax. delay 0.001 sec  
Pulse 45.0 degrees  
Acq. time 2.000 sec  
Width 38461.5 Hz  
96 repetitions  
OBSERVE B11, 128.1778459 MHz  
DECOUPLE H1, 399.5087270 MHz  
Power 46 dB  
continuously on  
WALTZ-16 modulated  
DATA PROCESSING  
Line broadening 1.0 Hz  
FT size 262144  
Total time 2 hr, 47 min, 31 sec

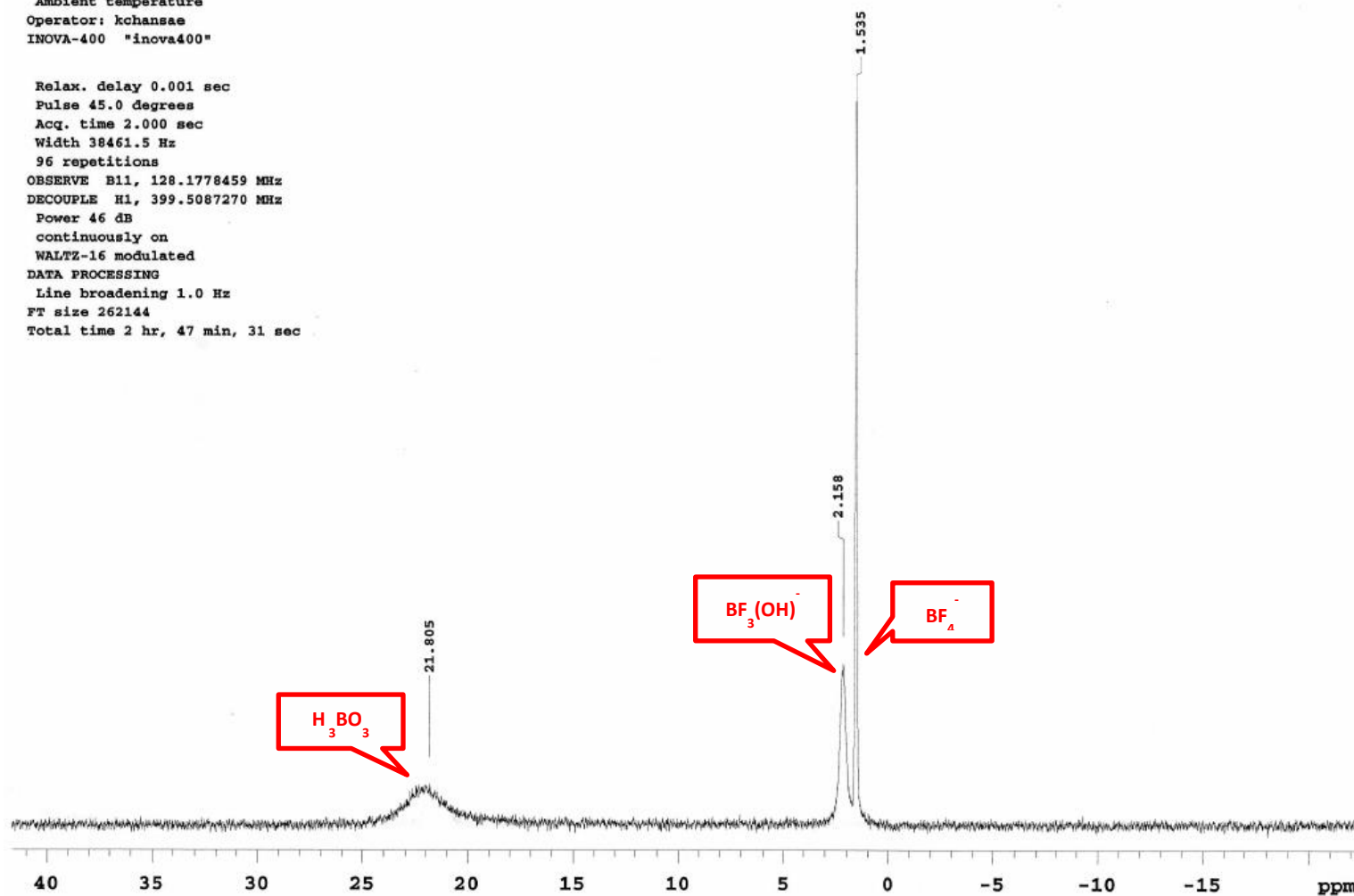


Figure 39:  $^{11}\text{B}$  NMR spectrum of 3%  $\text{HBF}_4$  solution reacted with illite at 200°F for 6 hours.

Solvent: d2o  
Ambient temperature  
Operator: kchansae  
INOVA-400 "inova400"

Relax. delay 0.001 sec  
Pulse 45.0 degrees  
Acq. time 2.000 sec  
Width 38461.5 Hz  
48 repetitions  
OBSERVE B11, 128.1778459 MHz  
DECOUPLE H1, 399.5087270 MHz  
Power 46 dB  
continuously on  
WALTZ-16 modulated  
DATA PROCESSING  
Line broadening 1.0 Hz  
FT size 262144  
Total time 2 hr, 47 min, 31 sec

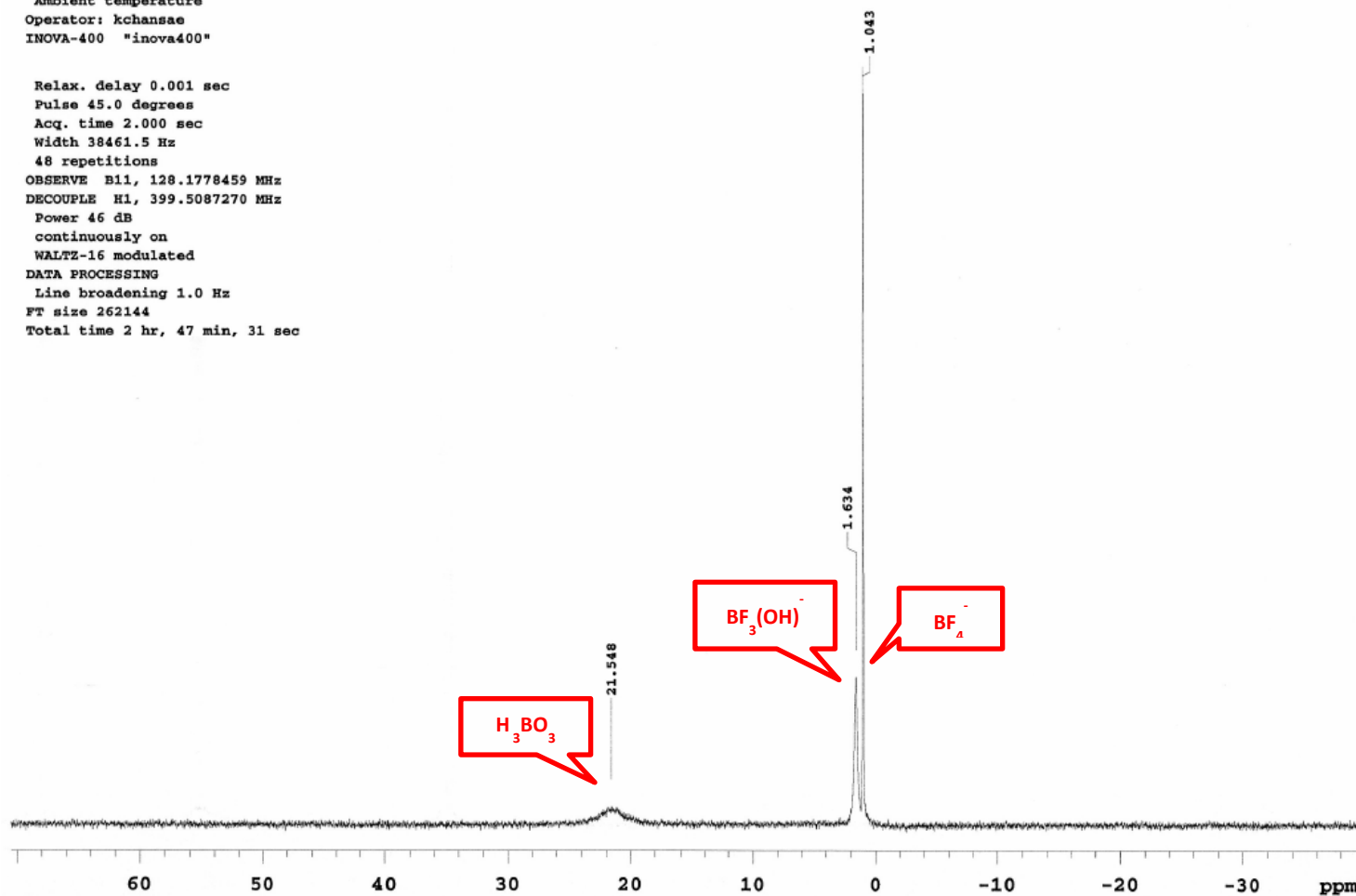
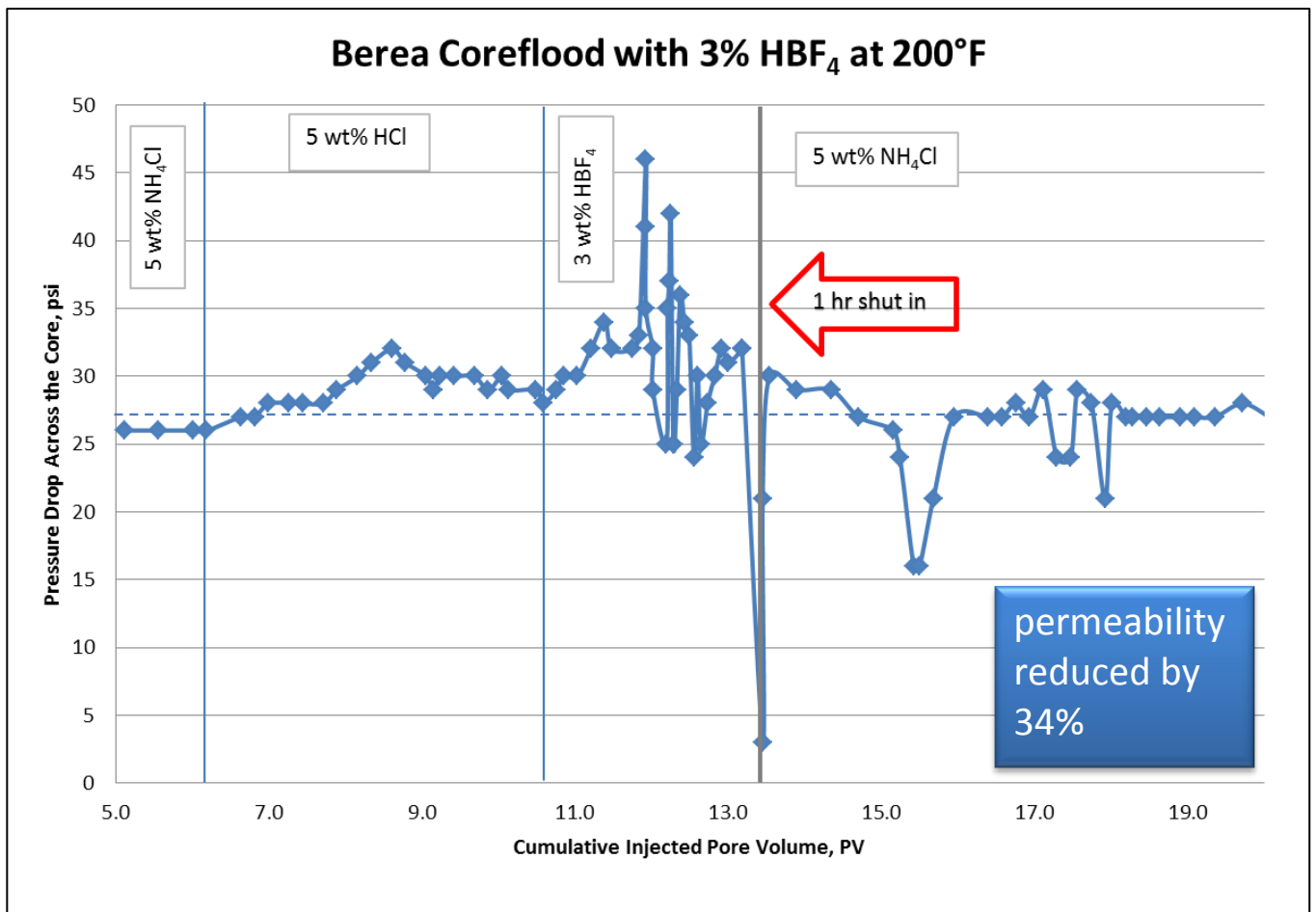


Figure 40:  $^{11}\text{B}$  NMR spectrum of 3%  $\text{HBF}_4$  solution reacted with bentonite at 200°F for 6 hours.

### **Berea Sandstone Coreflood at 200°F**

Corefloods in Berea sandstone with 3% and 8% mud acid resulted in a permeability reduction of 34% (Fig. 41) and 22% (Fig. 46) respectively. This is suspected to be caused by amorphous silica precipitation blocking pore throats. The falling of Si concentration in the effluent samples after 1 hour acid shut-in in both corefloods in Fig. 42 and 47 can support this thinking. All other key elements concentration are shown in Fig. 44-45 and Fig. 49-50.

A 5 wt% HCl preflush of 5 PV has proven to be sufficient judging from the low level of Ca even before that stage is done (Fig. 43,48 and 53). Fig. 52 illustrates how the Si trend should look if the core was stimulated with 12-3 mud acid and HF was not shut-in, which would induce less precipitation and would not damage the core (Fig. 51). All other key elements concentration from mud acid coreflood are shown in Fig. 54-55.



**Figure 41: Pressure drop across the core during injection in Berea sandstone with 3%  $\text{HBF}_4$  main acid at 200°F.**

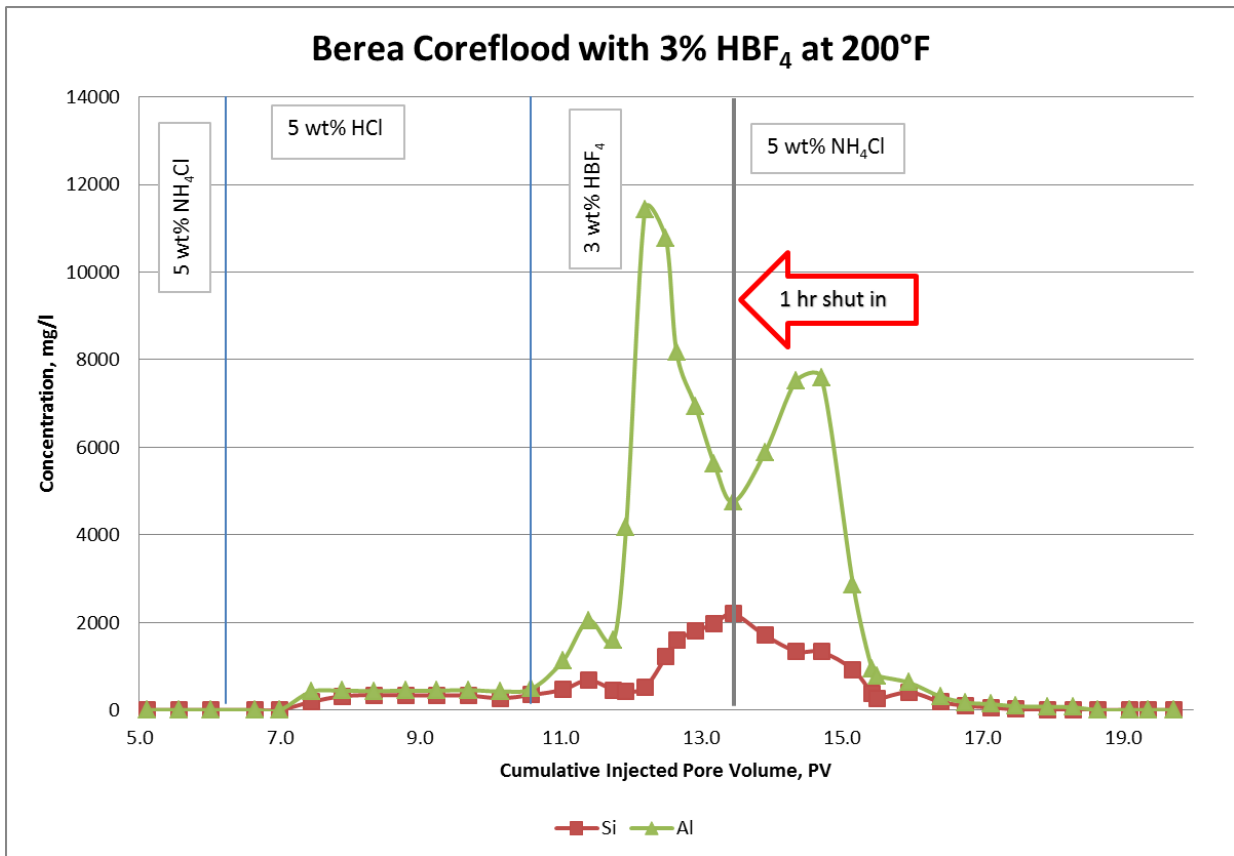


**Figure 42: Si and Al concentrations in Berea coreflood effluent samples at 200°F with 3%  $\text{HBF}_4$  main acid.**

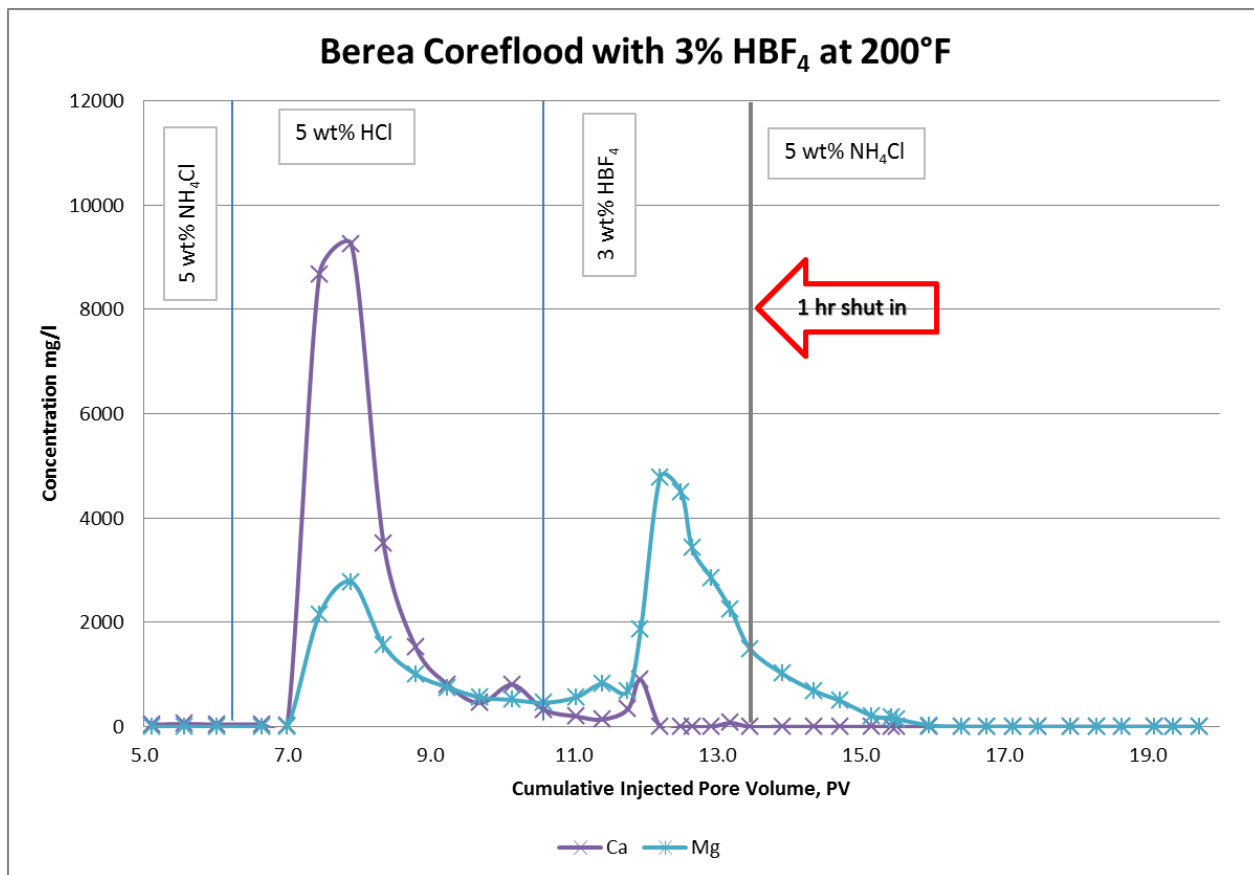


**Figure 43: Ca and Mg concentrations in Berea coreflood effluent samples at 200°F with 3%  $\text{HBF}_4$  main acid.**



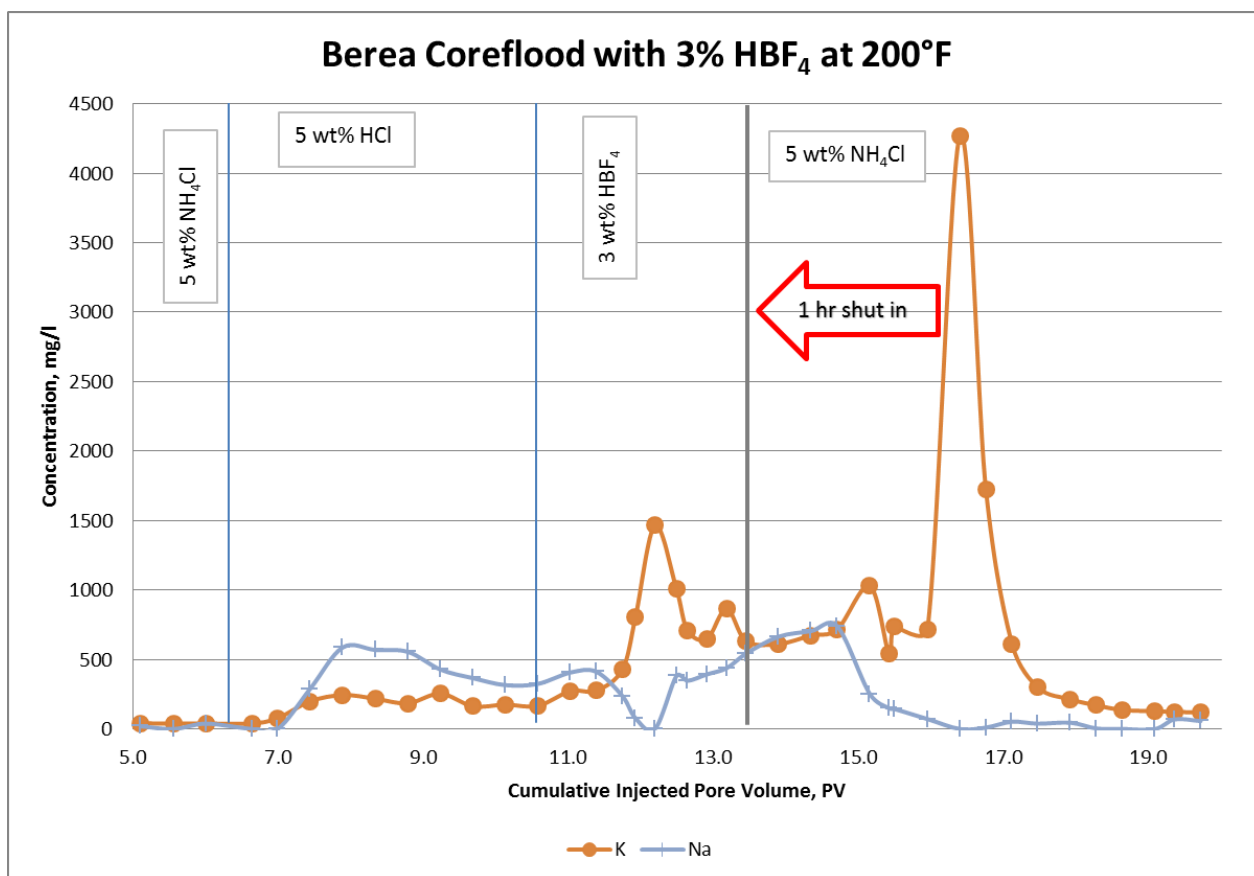


**Figure 44: K and Na concentrations in Berea coreflood effluent samples at 200°F with 3%  $\text{HBF}_4$  main acid.**

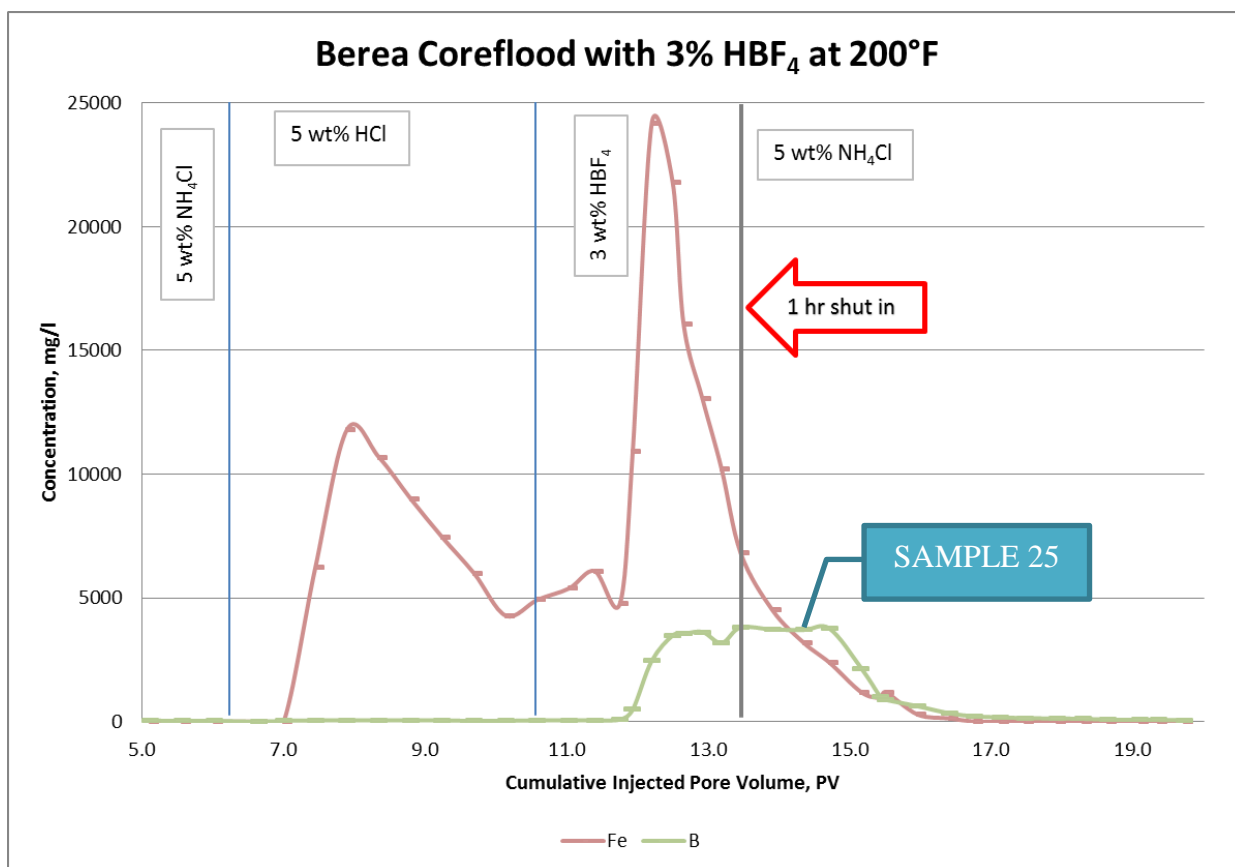


**Figure 45: Fe and B concentrations in Berea coreflood effluent samples at 200°F with 3%  $\text{HBF}_4$  main acid.**

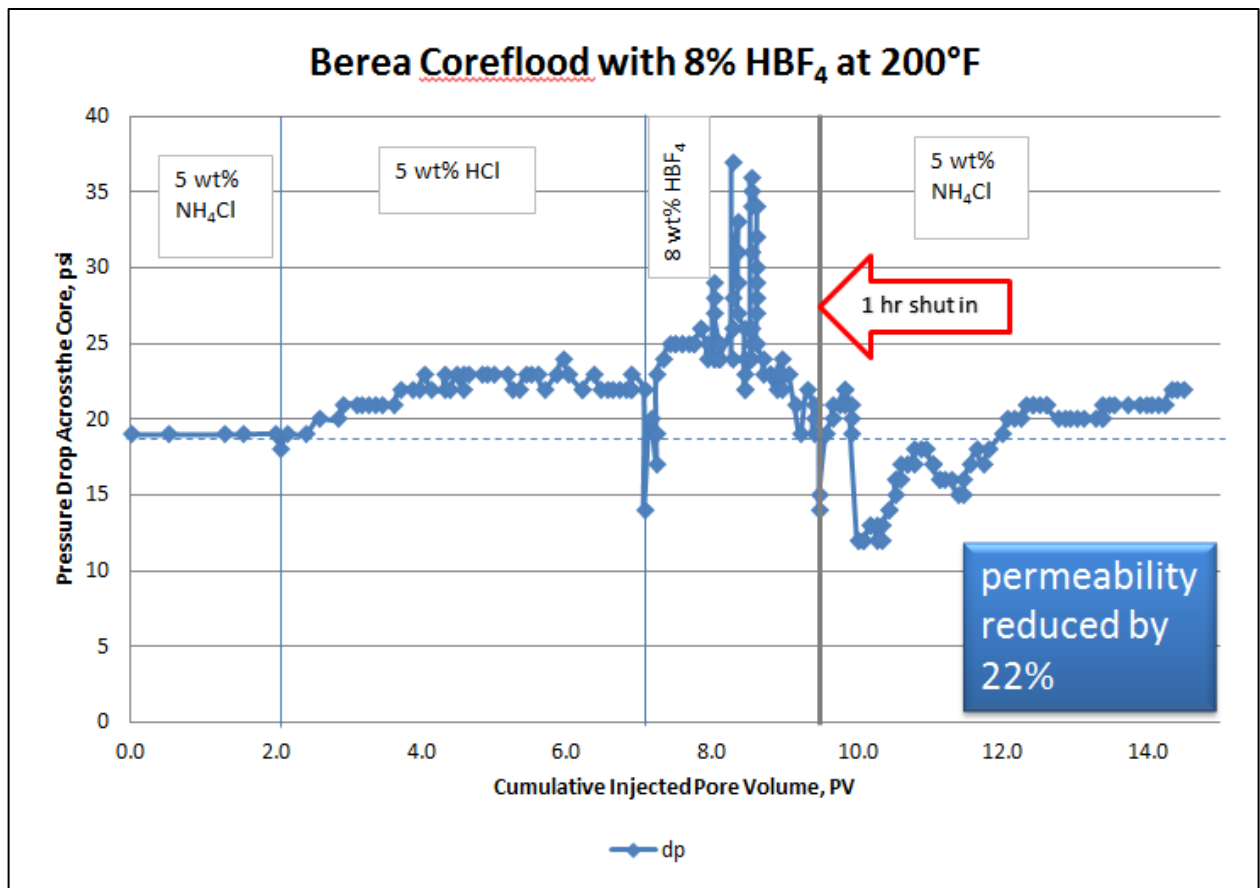


**Figure 46: Pressure drop across the core during injection in Berea sandstone with 8%  $\text{HBF}_4$  main acid at 200°F.**

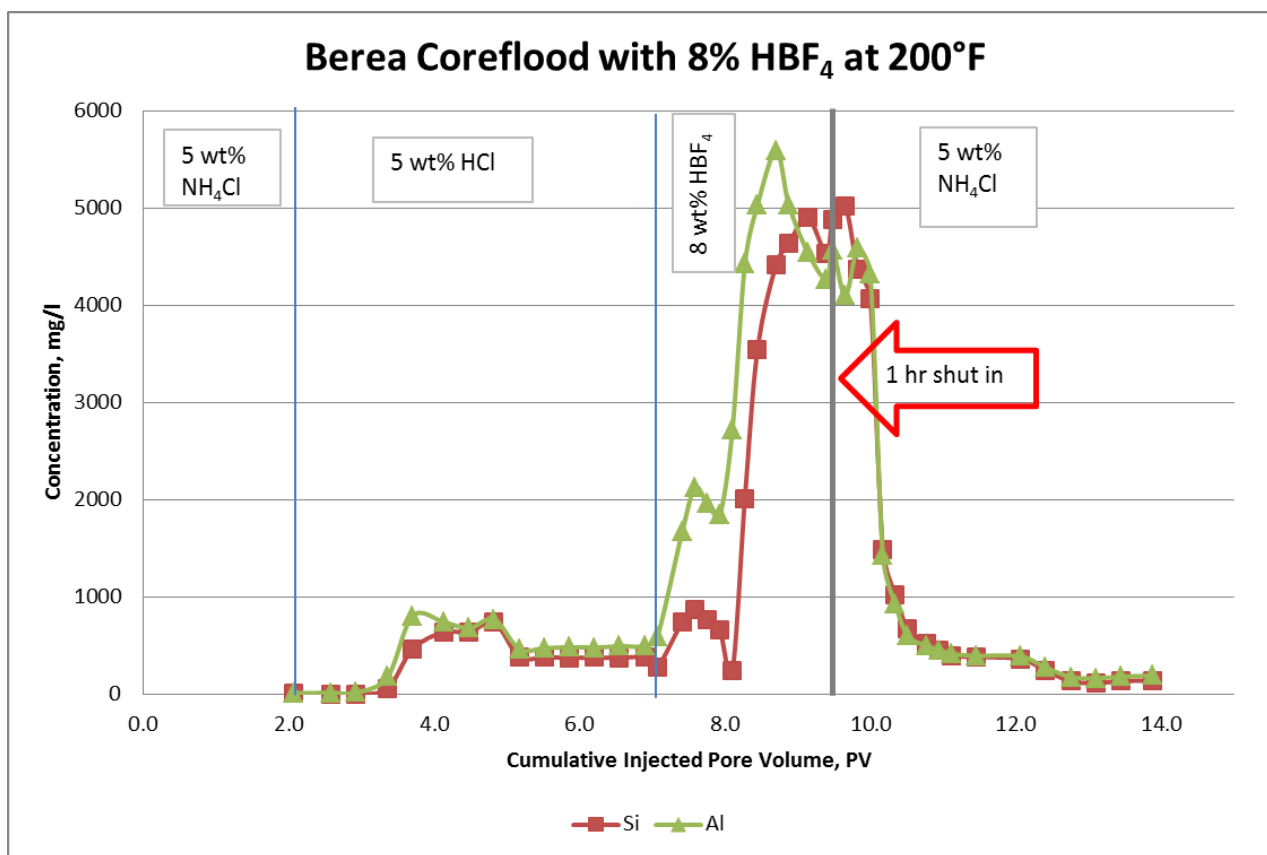


**Figure 47: Si and Al concentrations in Berea coreflood effluent samples at 200°F with 8%  $\text{HBF}_4$  main acid.**

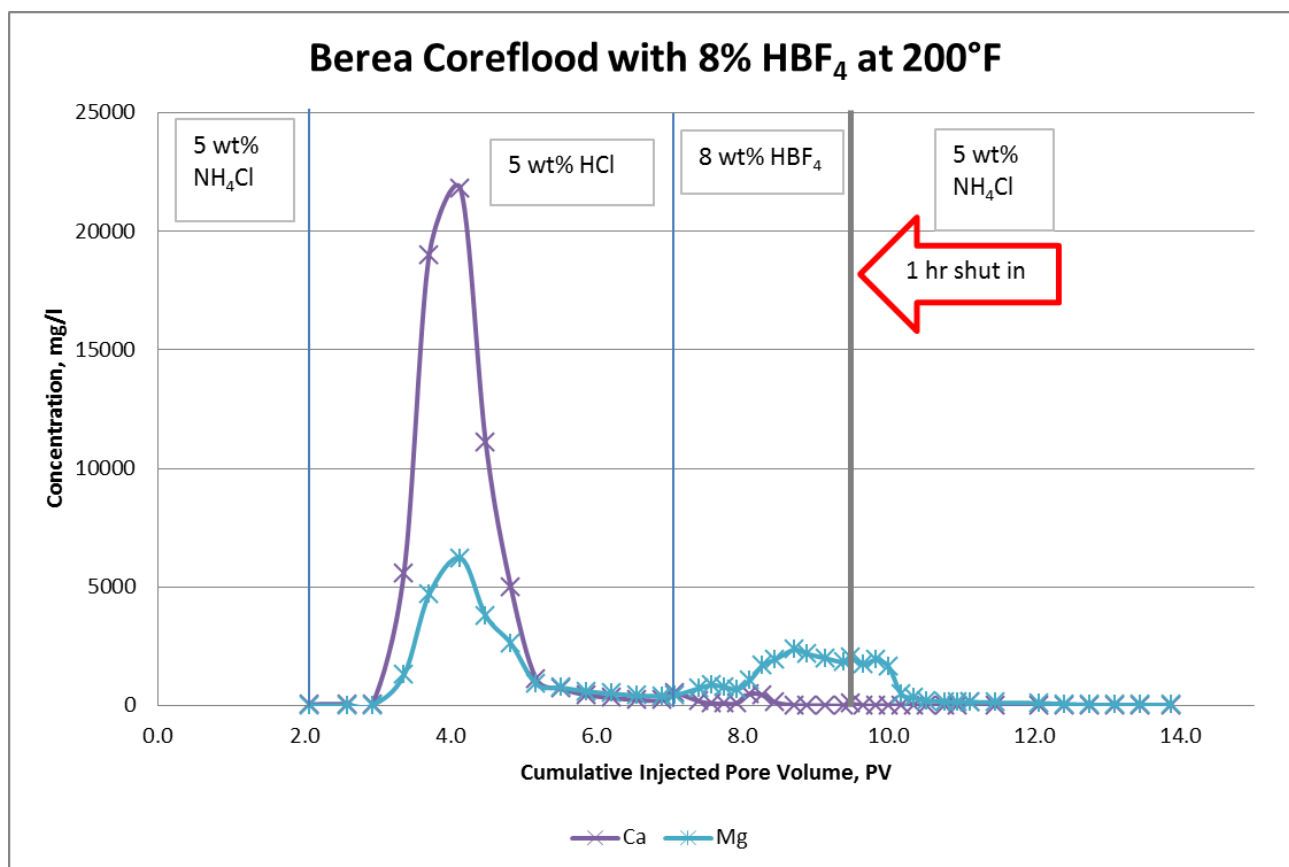


**Figure 48: Ca and Mg concentrations in Berea coreflood effluent samples at 200°F with 8% HBF<sub>4</sub> main acid.**

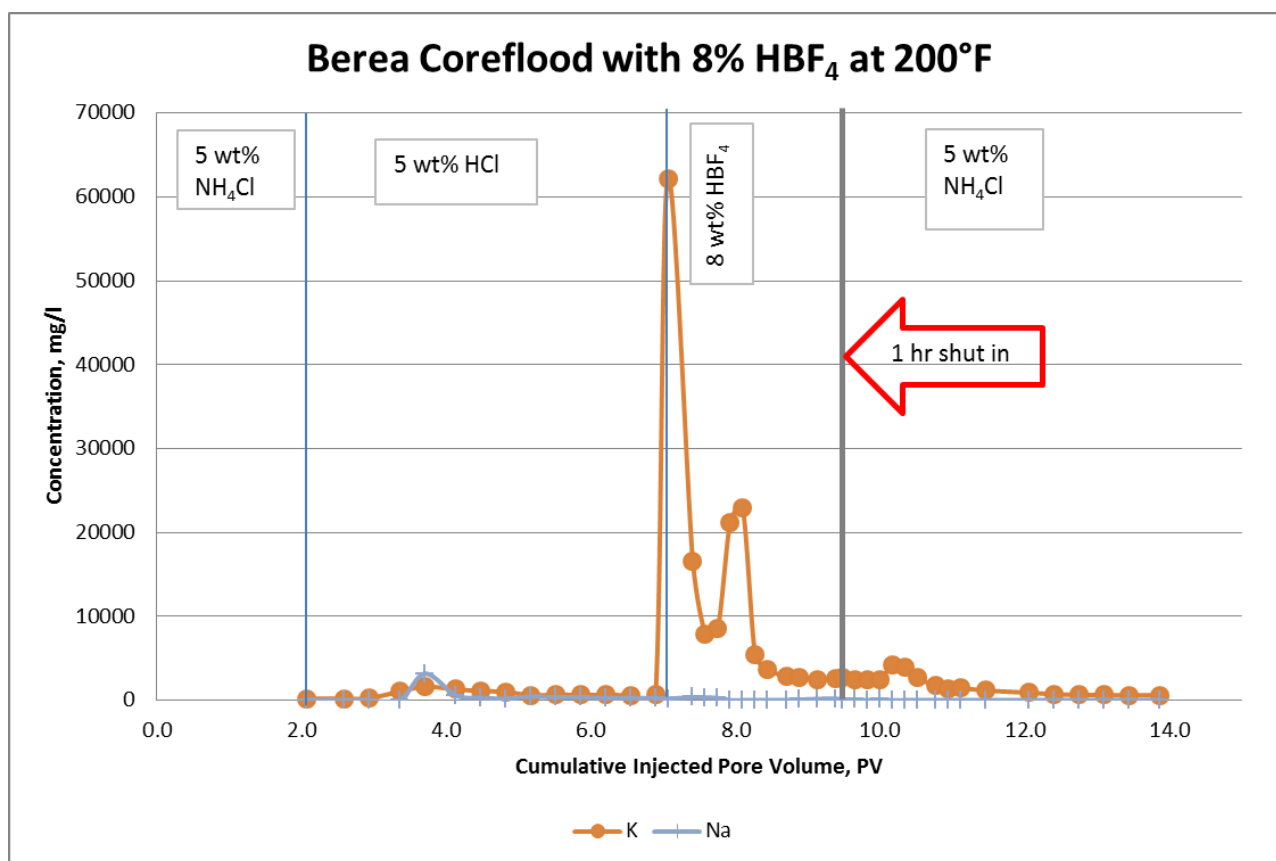


**Figure 49: K and Na concentrations in Berea coreflood effluent samples at 200°F with 8%  $\text{HBF}_4$  main acid.**

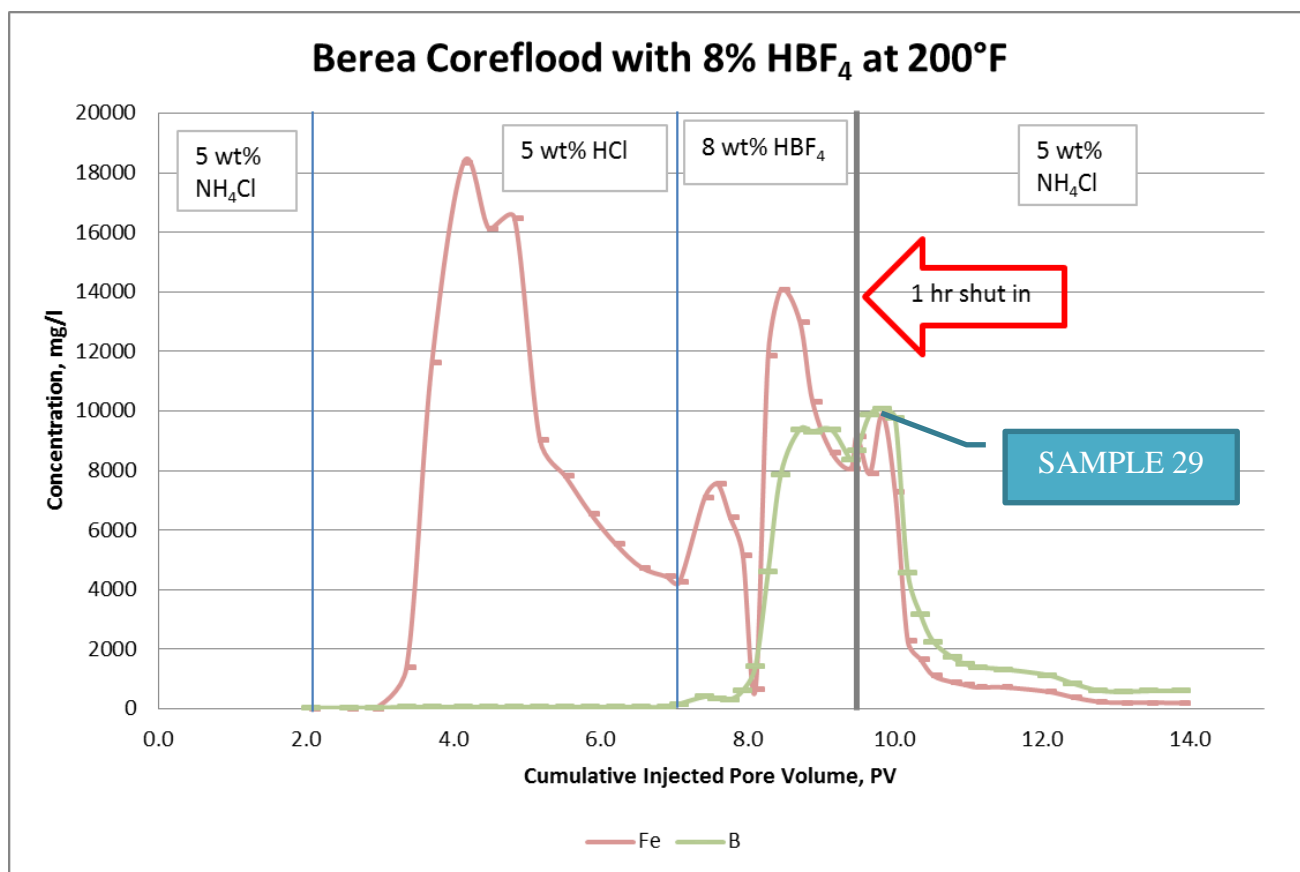


**Figure 50: Fe and B concentrations in Berea coreflood effluent samples at 200°F with 8%  $\text{HBF}_4$  main acid.**

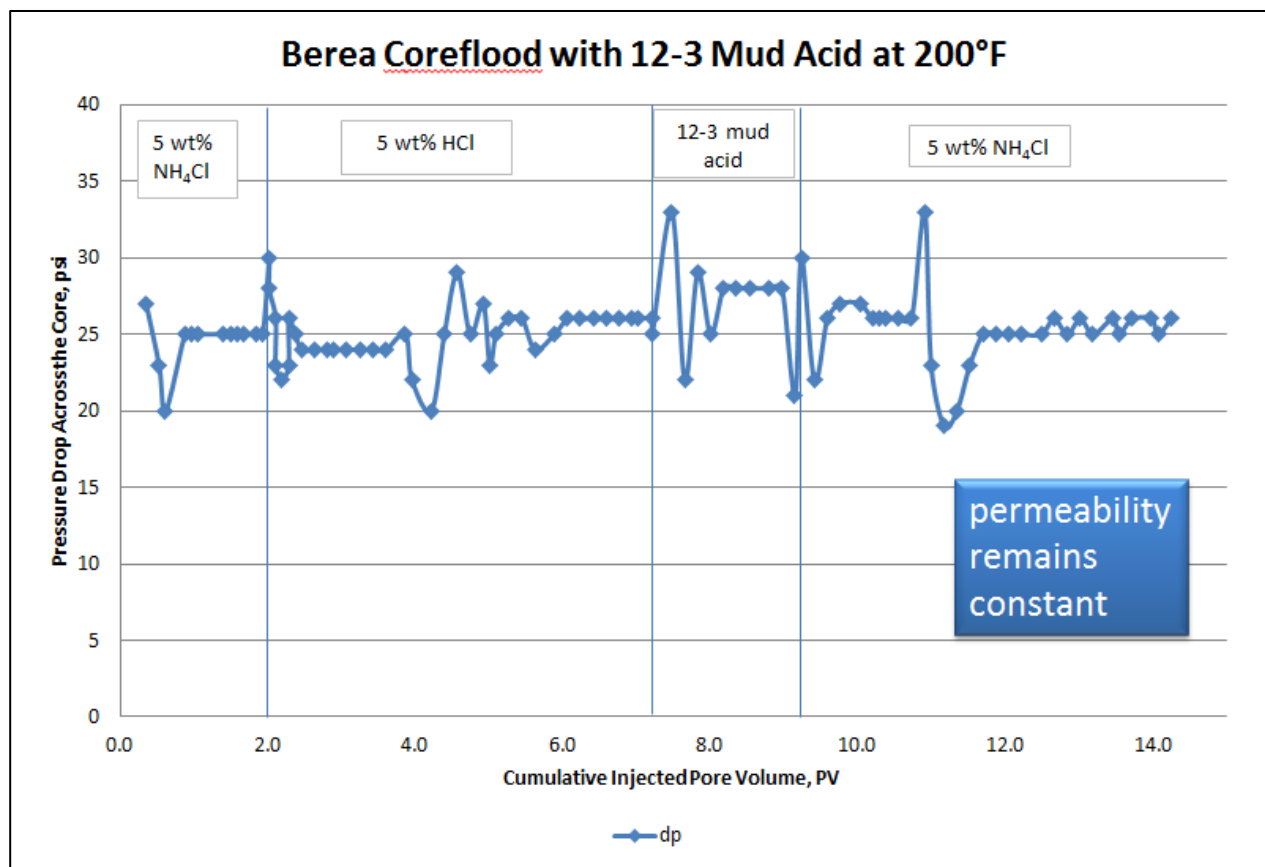


**Figure 51: Pressure drop across the core during injection in Berea sandstone with 3%  $\text{HBF}_4$  main acid at 200°F.**



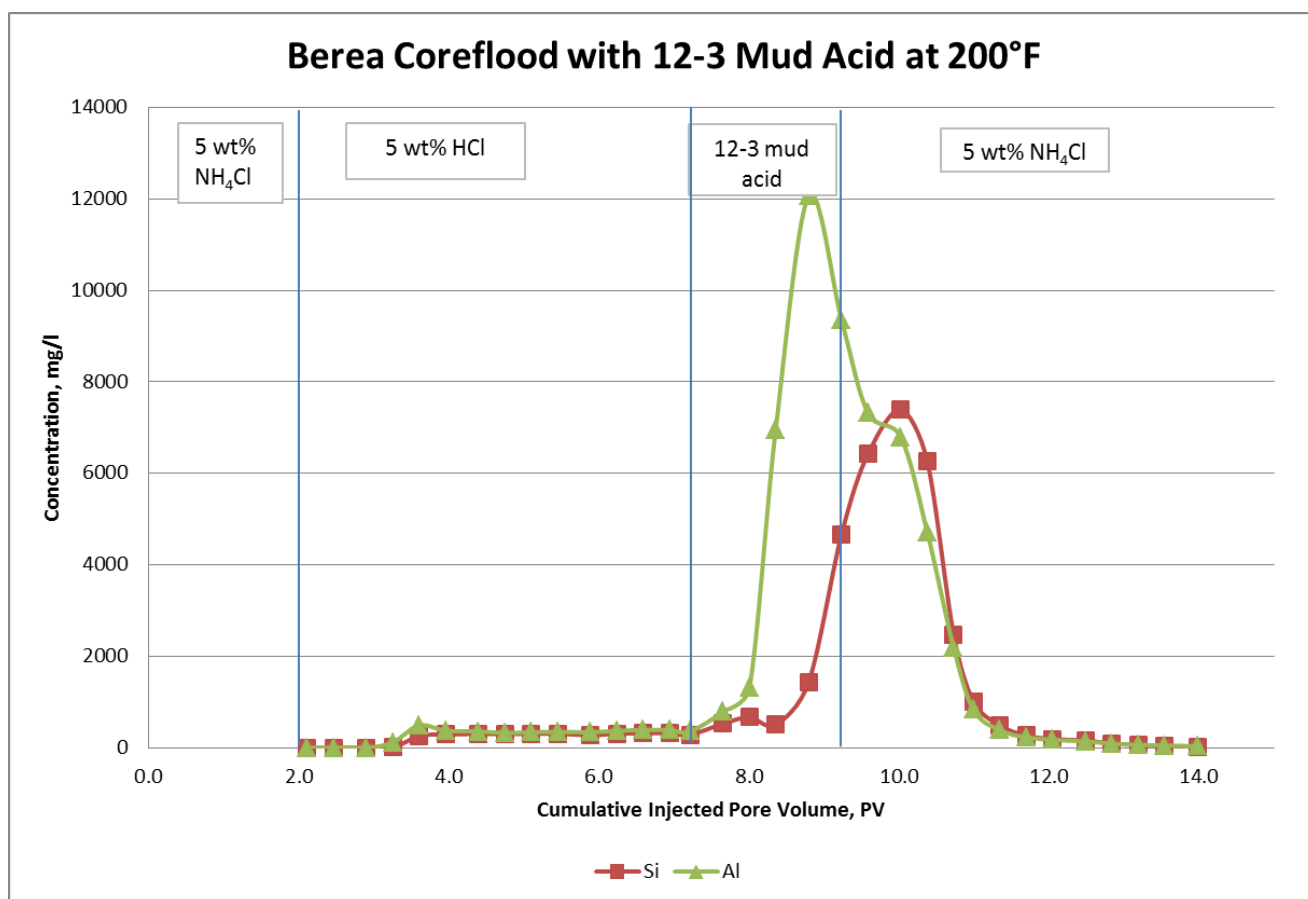


**Figure 52: Si and Al concentrations in Berea coreflood effluent samples at 200°F with 12-3 mud acid as main acid.**

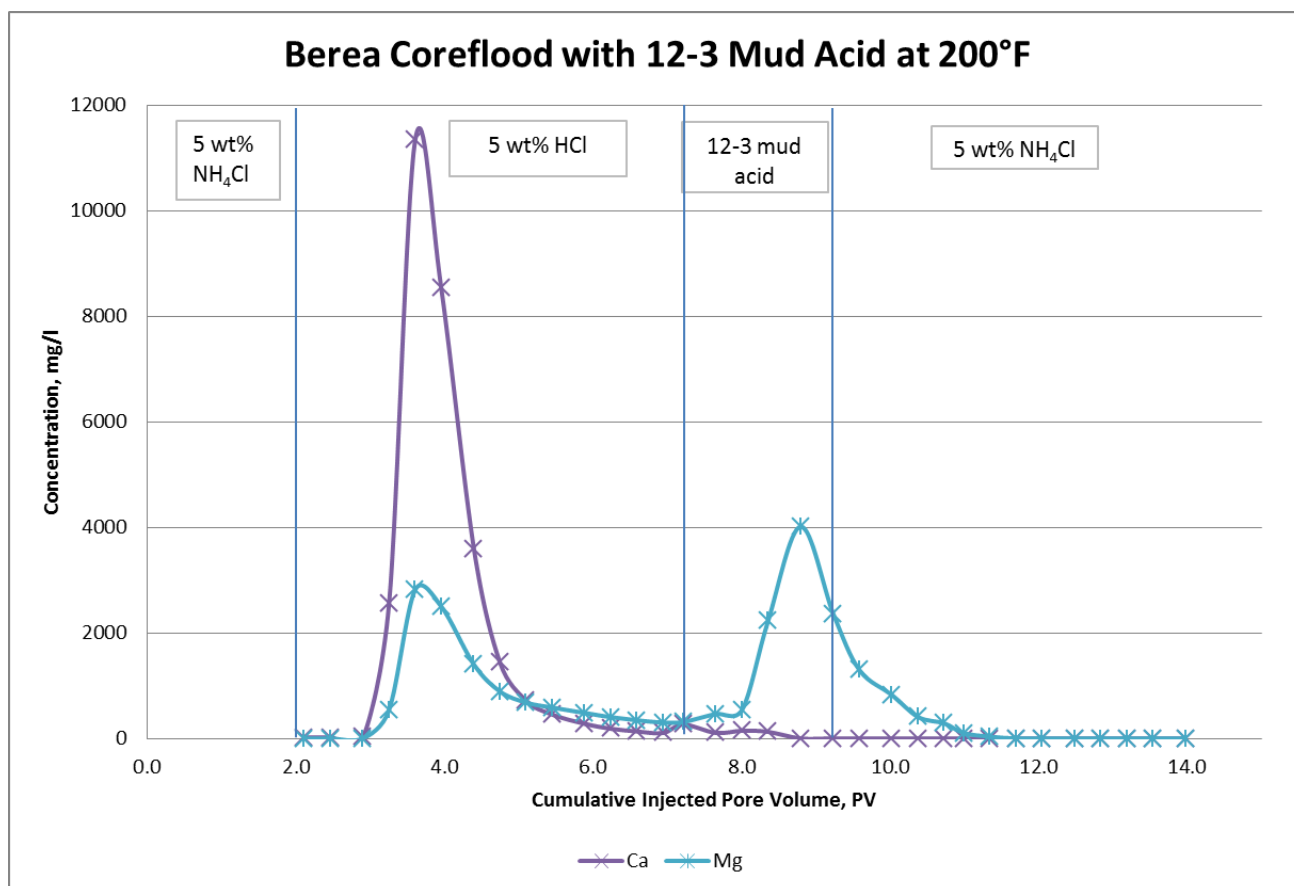


**Figure 53: Ca and Mg concentrations in Berea coreflood effluent samples at 200°F with 12-3 mud acid as main acid.**

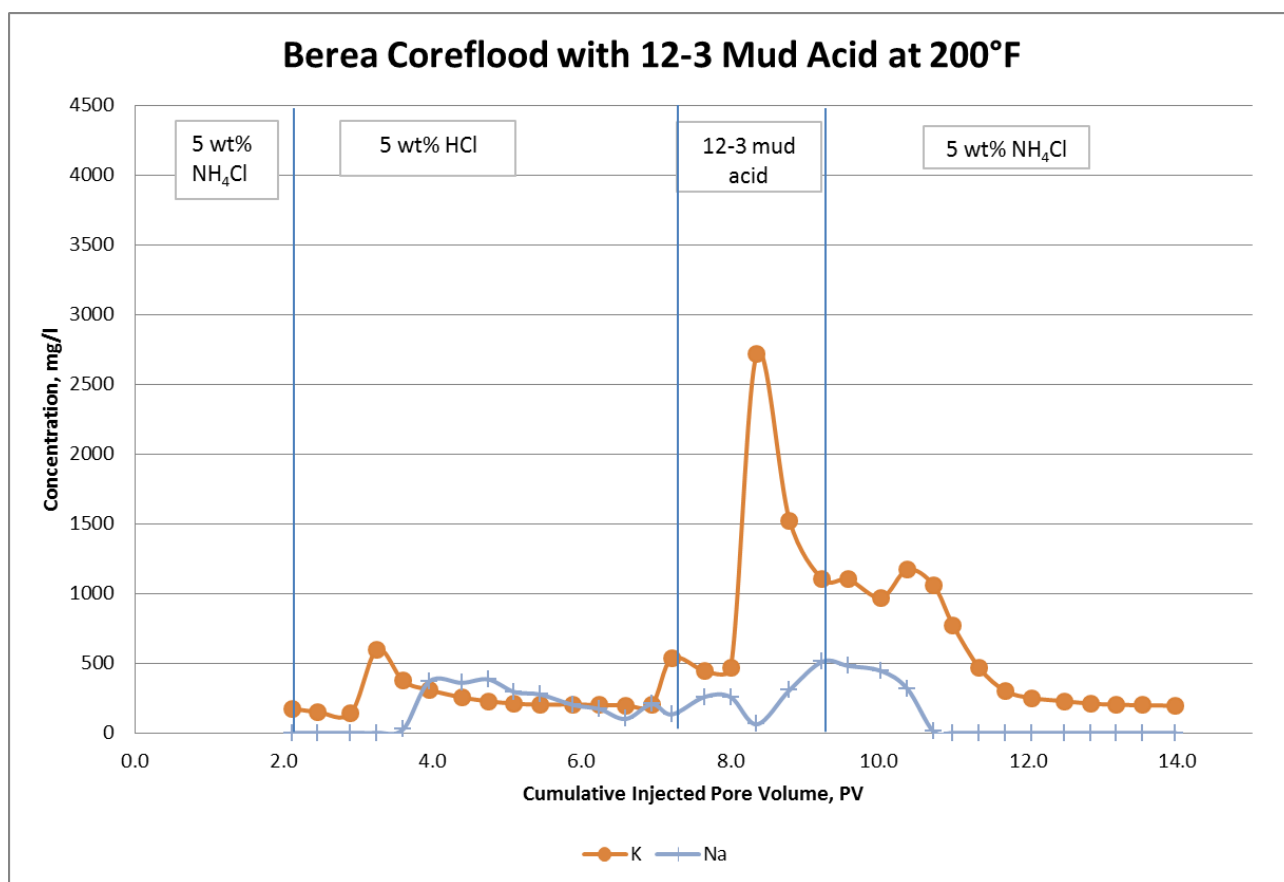


**Figure 54: K and Na concentrations in Berea coreflood effluent samples at 200°F with 12-3 mud acid as main acid.**

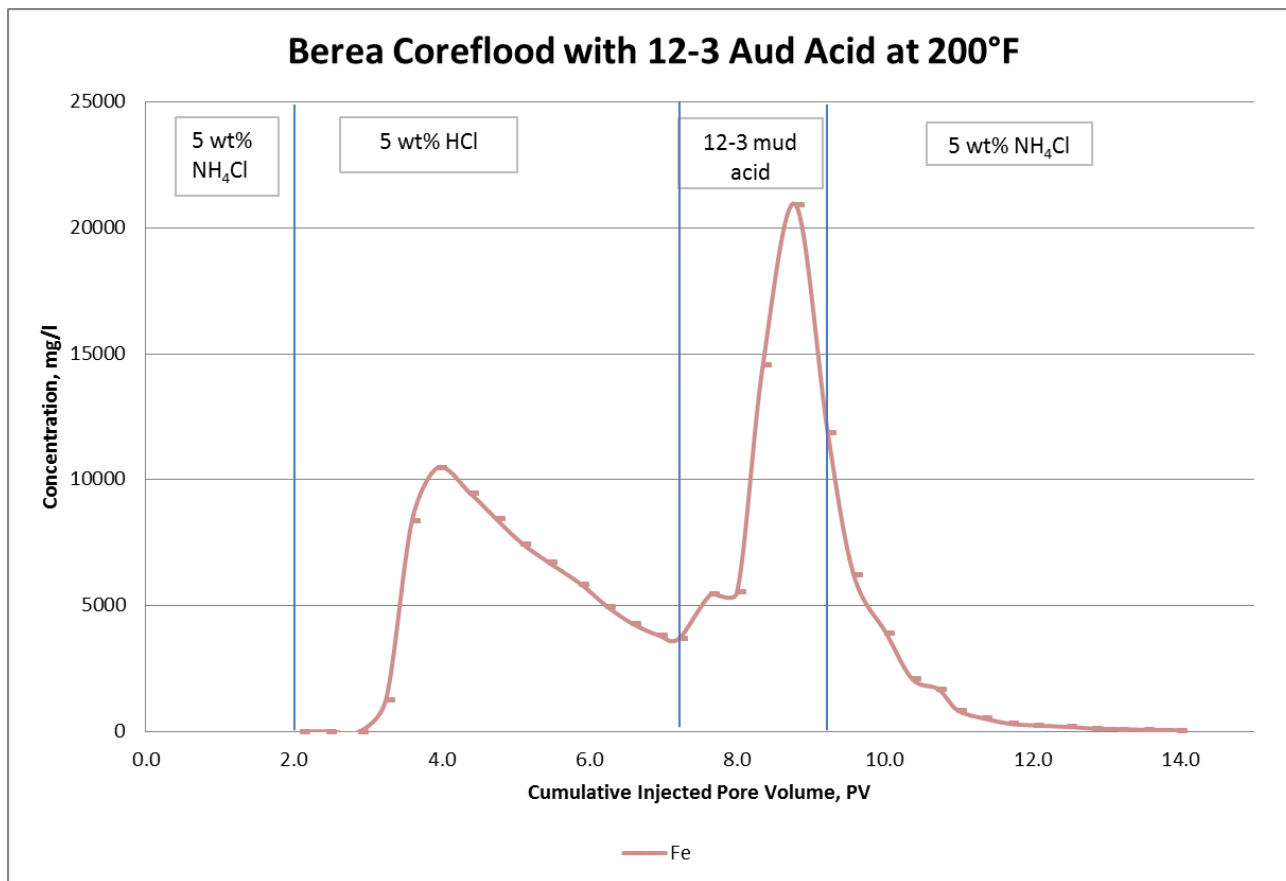


**Figure 55: Fe concentration in Berea coreflood effluent samples at 200°F with 12-3 mud acid as main acid.**

Both  $^{11}\text{B}$  and  $^{19}\text{F}$  NMR spectrum of the effluent samples from 3%  $\text{HBF}_4$  coreflood show common species as the previous analysis of acid solutions from clay dissolution tests (Fig. 56-57), whereas the effluent samples from 8%  $\text{HBF}_4$  coreflood gives a different spectrum. Peaks in Fig. 59 are assigned as  $\text{H}_3\text{BO}_3$  at  $\delta_{\text{B}} = 21$  ppm,  $\text{BF}_3(\text{OH})^-$  at  $\delta_{\text{B}} = 0$  ppm, and a third minor species at  $\delta_{\text{B}} = 3.5$  ppm assigned as  $\text{BF}_2(\text{OH})_2^-$  to be in equilibrium with  $\text{BF}_3(\text{OH})^-$ . Both species also appear in Fig. 58. Therefore, a peak at  $\delta_{\text{F}} = -131$  ppm is assigned as  $\text{BF}_2(\text{OH})_2^-$  and a peak at  $\delta_{\text{F}} = -139$  ppm is assigned as  $\text{BF}_3(\text{OH})^-$ .

Solvent: d2o  
Ambient temperature  
Operator: kchansae  
INOVA-400 "inova400"

Relax. delay 2.000 sec  
Pulse 45.0 degrees  
Acq. time 2.000 sec  
Width 50000.0 Hz  
28 repetitions  
OBSERVE F19, 375.9124098 MHz  
DATA PROCESSING  
Line broadening 0.3 Hz  
FT size 262144  
Total time 4 min, 17 sec

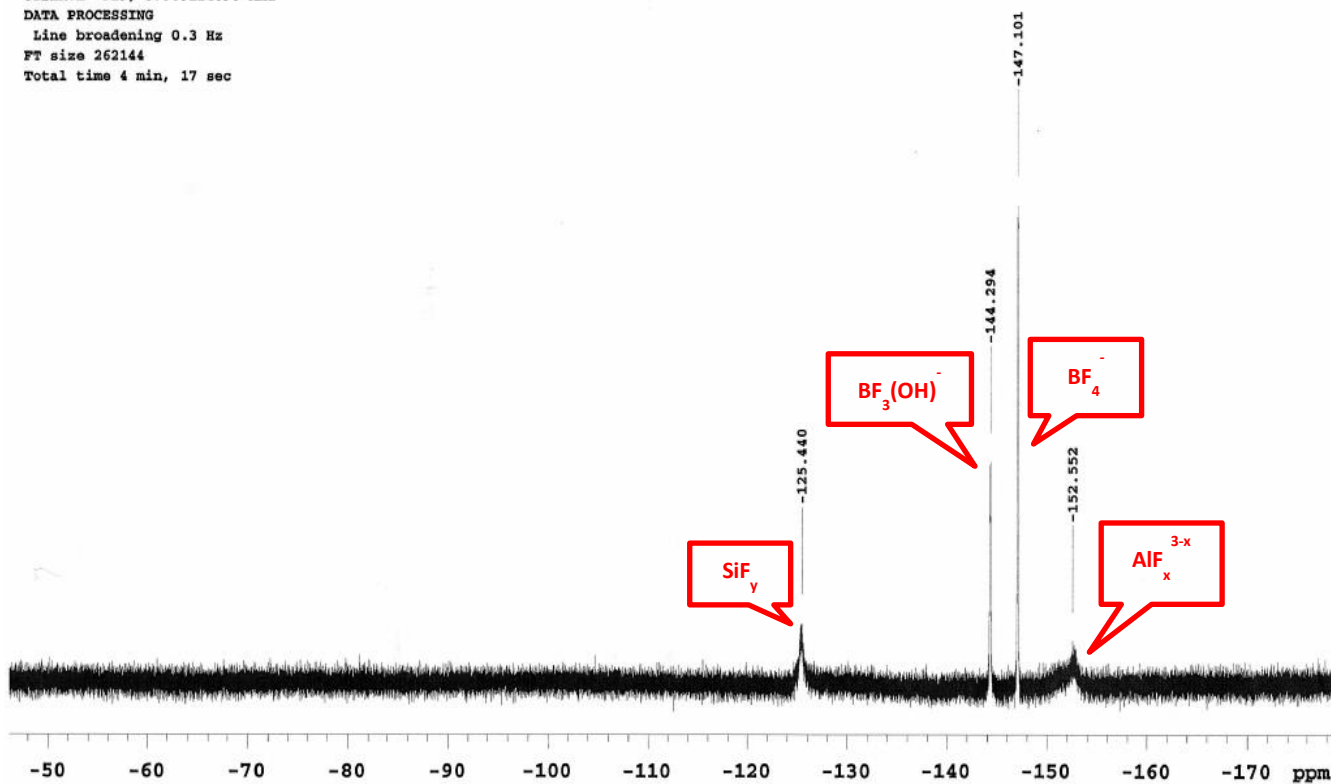


Figure 56:  $^{19}\text{F}$  NMR spectrum of effluent sample 25 from Berea coreflood at 200°F with 3%  $\text{HBF}_4$  main acid.

solvent: d2o  
Ambient temperature  
Operator: kchansae  
INOVA-400 "inova400"  
  
Relax. delay 0.001 sec  
Pulse 45.0 degrees  
Acq. time 2.000 sec  
Width 38461.5 Hz  
68 repetitions  
OBSERVE B11, 128.1778459 MHz  
DECOUPLE H1, 399.5087270 MHz  
Power 46 dB  
continuously on  
WALTZ-16 modulated  
DATA PROCESSING  
Line broadening 1.0 Hz  
FT size 262144  
Total time 2 hr, 47 min, 31 sec

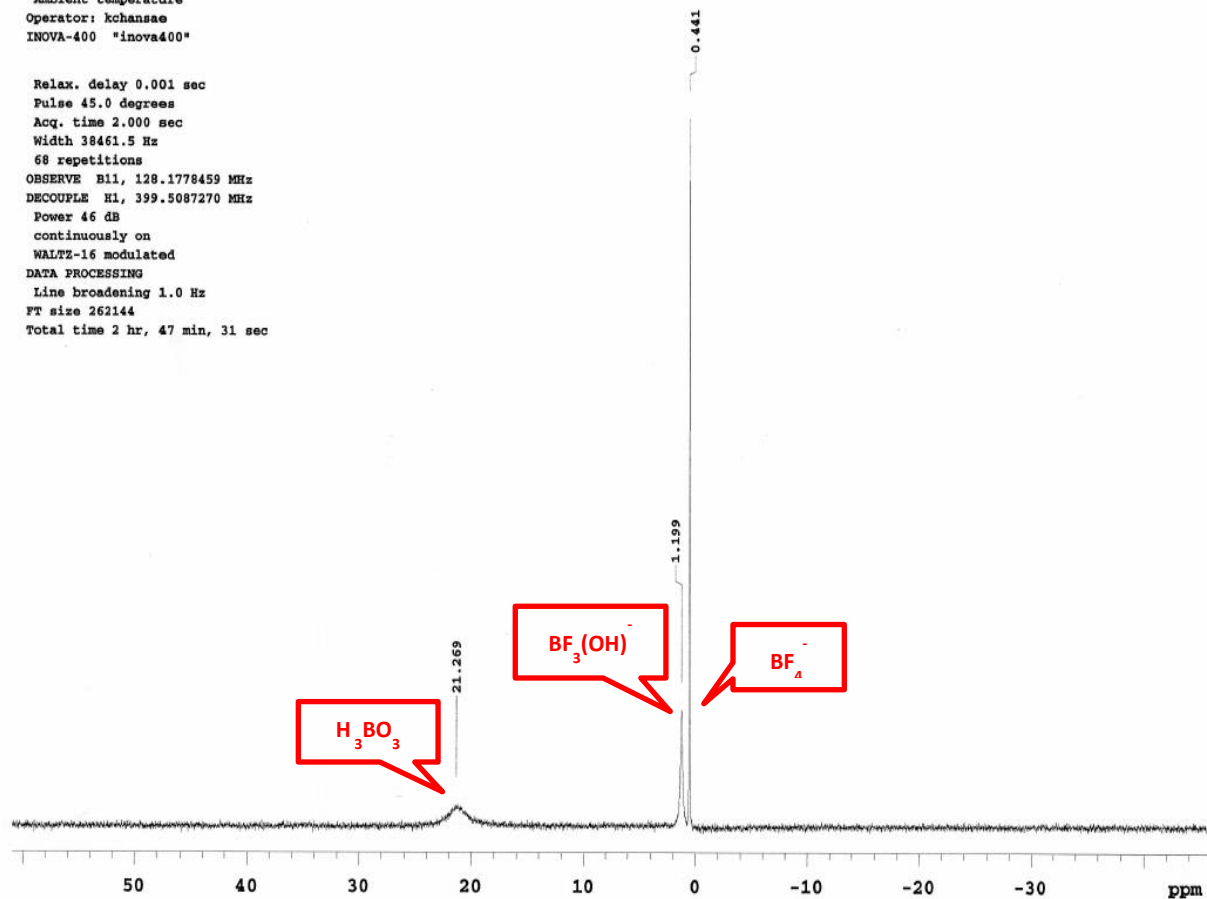


Figure 57:  $^{11}\text{B}$  NMR spectrum of effluent sample 25 from Berea coreflood at 200°F with 3%  $\text{HBF}_4$  main acid.

Pulse Sequence: s2pul  
Solvent: d2o  
Ambient temperature  
Operator: kchansae  
INOVA-400 "inova400"  
  
Relax. delay 2.000 sec  
Pulse 45.0 degrees  
Acq. time 2.000 sec  
Width 50000.0 Hz  
20 repetitions  
OBSERVE F19, 375.9124098 MHz  
DATA PROCESSING  
Line broadening 0.3 Hz  
FT size 262144  
Total time 4 min, 17 sec

sample 67

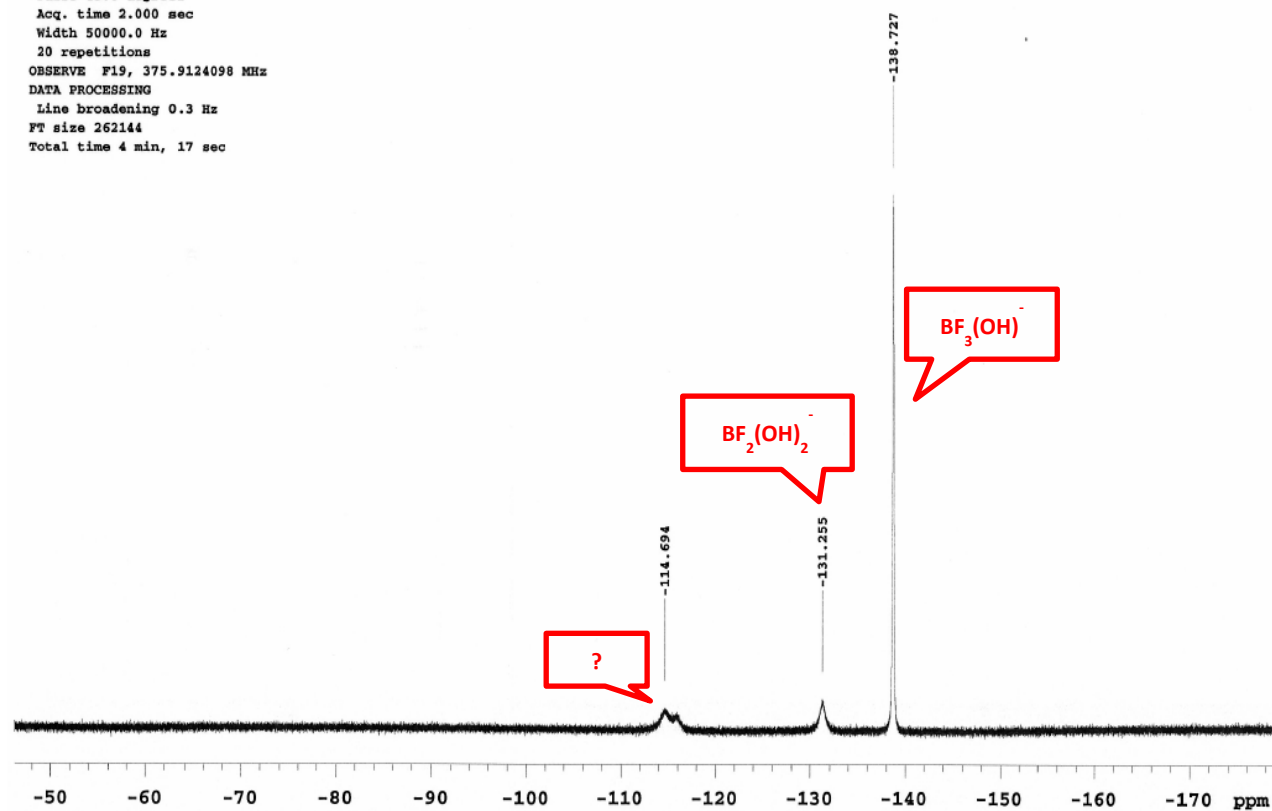


Figure 58:  $^{19}\text{F}$  NMR spectrum of effluent sample 29 from Berea coreflood at 200°F with 8%  $\text{HBF}_4$  main acid.

Pulse Sequence: s2pul  
Solvent: d2o  
Ambient temperature  
Operator: kchansae  
INOVA-400 "inova400"  
  
Relax. delay 0.001 sec  
Pulse 45.0 degrees  
Acq. time 2.000 sec  
Width 38461.5 Hz  
104 repetitions  
OBSERVE B11, 128.1787778 MHz  
DECOUPLE H1, 399.5087270 MHz  
Power 46 dB  
continuously on  
WALTZ-16 modulated  
DATA PROCESSING  
Line broadening 1.0 Hz  
FT size 262144  
Total time 2 hr, 47 min, 31 sec

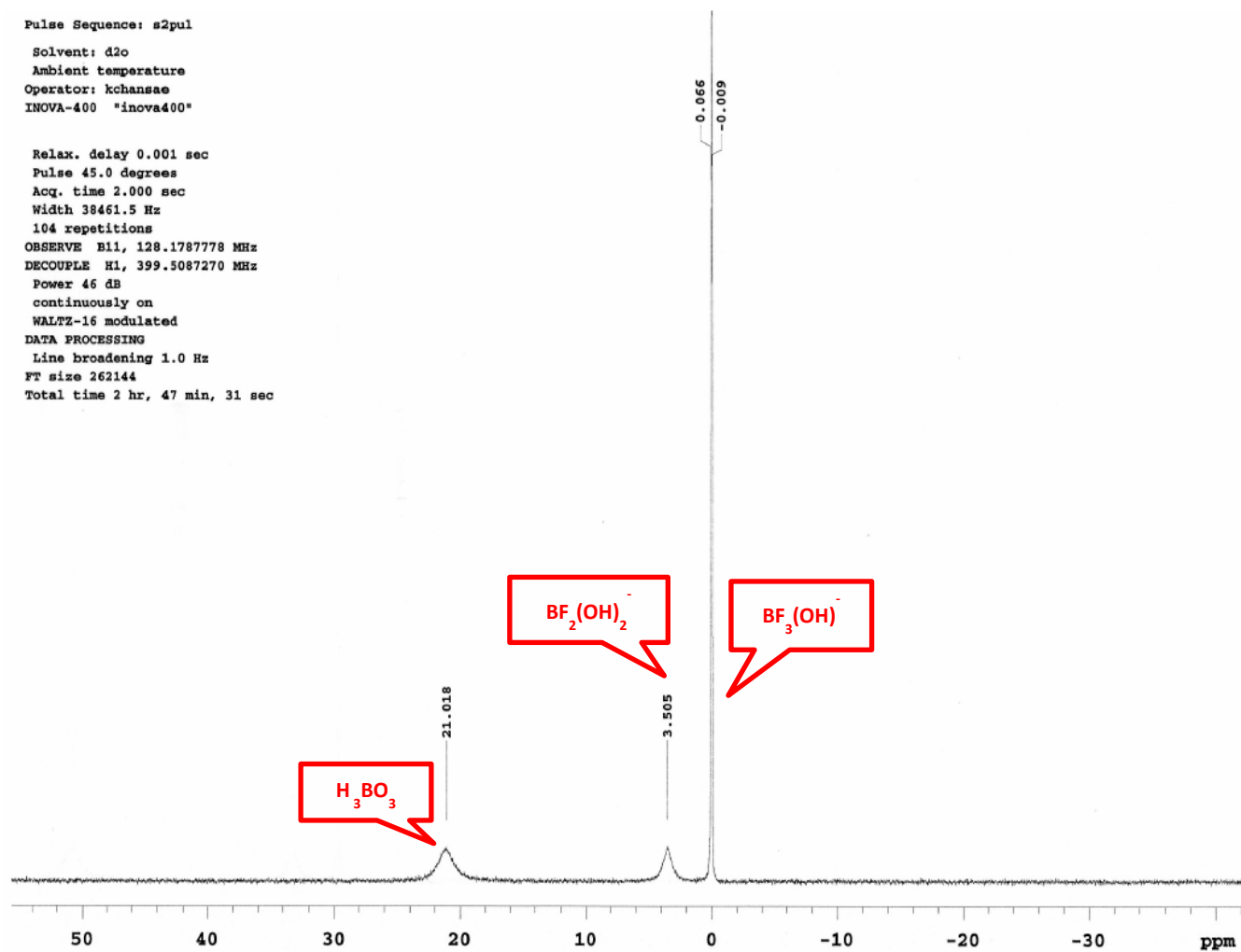


Figure 59:  $^{11}\text{B}$  NMR spectrum of effluent sample 29 from Berea coreflood at 200°F with 8%  $\text{HBF}_4$  main acid.



## CHAPTER IV

### FUTURE WORK

The borosilicate formation expected from the reaction of  $\text{HBF}_4$  and sandstone mentioned in literature has not been investigated as of current progress. Given that this is one distinguishable benefit of  $\text{HBF}_4$ , plans have been made to accommodate it in the scope of future experimental work.

In addition, to discover the limited retardation effect of  $\text{HBF}_4$  and to define its effective working temperature window, another set of experiments should be conducted in detail over a fine grid of temperature to pinpoint the precise temperature limit of  $\text{HBF}_4$  for formation treatment purposes.

An effort should also be made to explain the fact why illite and bentonite responded differently to  $\text{HBF}_4$  acid under different temperatures. With the current knowledge, this phenomenon still cannot be comprehended.

Most important of all is to continue exploring the parameters/conditions that will make  $\text{HBF}_4$  coreflood stimulation successful in addition to understanding the relevant reactions. This would be done in comparison with mud acid and evaluated using suitable techniques to demonstrate the claimed benefits of  $\text{HBF}_4$  over traditional mud acid.

## CHAPTER V

### CONCLUSIONS

It was shown in this study that the dissolution of aluminosilicates with 3%  $\text{HBF}_4$  at 75°F will dissolve Al and Si at an equal ratio for all three clays at an effectively retarded rate and will have minor  $\text{KBF}_4$  precipitate only in the case of illite. When reaction temperature is raised to 200°F,  $\text{HBF}_4$  has developed a different reaction and leached all other elements from the clay structure except silica. This behavior matches the secondary reaction discussed by Gdanski.

Fresh  $\text{HBF}_4$  hydrolytic equilibrium is established soon as it is prepared at room temperature at the given  $\text{H}^+$  concentration. It contains three species ( $\text{BF}_4^-$ ,  $\text{BF}_3(\text{OH})^-$  and  $\text{HF}$ ) with  $\text{BF}_4^-$  being predominant and only a limited amount of  $\text{HF}$ .

The retardation effect of  $\text{HBF}_4$  is evidently a strong function of temperature. Even though reaction retardation is witnessed at room temperature, it does not persist at 200°F as exhibited by the kaolinite dissolution rate of  $\text{HBF}_4$  at 200°F, which was approximately the same as regular mud acid at this temperature. Therefore it is not recommended to apply this acid where bottomhole circulating temperature is close to or greater than 200°F.

The use of  $\text{HBF}_4$  in formations that contains illite clay or potassium feldspar should be strictly prohibited due to the risk of  $\text{KBF}_4$  precipitation, which can potentially cause formation damage.

Treating a six inches Berea core with 12-3 mud acid at 200°F with no shut-in did not improve the core's permeability. When using  $\text{HBF}_4$  to treat the core at the same conditions, both 3% and 8%  $\text{HBF}_4$  damaged the core after 1 hour of shut-in. This damage is probably due to silica precipitation, as it is a known product of the secondary reaction which goes to completion at this temperature. The different responses of core's final permeability after mud acid and  $\text{HBF}_4$  is believed to be induced by silica-precipitate-blocked pore throats developed over the period of HF being shut-in in the case of  $\text{HBF}_4$ .

## REFERENCES

- Al-Dahlan, M. N., H. A. Nasr-El-Din, A. A. Al-Qahtani. 2001. Evaluation of Retarded HF Acid Systems. Proc., SPE International Symposium on Oilfield Chemistry, Houston, Texas.
- Ayorinde, C. Granger, R. L. Thomas. 1992. The Application of Fluoboric Acid in Sandstone Matrix Acidizing: A Case Study. *Indonesian Petroleum Association 21st Annual Convention Proceedings* **2**: 235-261.
- Bertaux, J. 1989. Treatment-Fluid Selection for Sandstone Acidizing: Permeability Impairment in Potassic Mineral Sandstones. *SPE Production Engineering* **4** (1): 41-48.
- Boyer, R. C., Chia-Hsin Wu. 1983. The Role of Reservoir Lithology in Design of an Acidization Program: Kuparuk River Formation, North Slope, Alaska. Proc., SPE California Regional Meeting, Ventura, California.
- Dewar, Michael JS, Richard Jones. 1967. New Heteroaromatic Compounds. XXV. Studies of Salt Formation in Boron Oxyacids by  $^{11}\text{B}$  Nuclear Magnetic Resonance. *Journal of the American Chemical Society* **89** (10): 2408-2410.
- Dungan, C.H., J.R. Van Wazer. 1970. *Compilation of Reported  $^{19}\text{F}$  NMR Chemical Shifts, 1951 to mid-1967*. New York, Wiley-Interscience (Reprint).
- Feng, Puyong, Da Wang, Gangzhi Liu et al. 2011. Sandstone Reservoir Stimulation Using High-Temperature Deep-Penetrating Acid. Proc., SPE Western North American Region Meeting, Anchorage, Alaska.
- Gdanski, R.D. 1999. Kinetics of the Secondary Reaction of HF on Alumino-Silicates. *SPE Production & Operations* **14** (4): 260-268.
- Gdanski, Rick. 1998. Kinetics of Tertiary Reactions of Hydrofluoric Acid on Aluminosilicates. *SPE Production & Operations* **13** (2): 75-80.

- Gomaa, Ahmed M., Jennifer Cutler, Joel Boles et al. 2013. Matrix Stimulation: An Effective One-Step Sandstone Acid System. Proc., 2013 SPE Production and Operations Symposium, Oklahoma City, Oklahoma.
- Gray, DH, RW Rex. 1990. Formation Damage in Sandstones Caused by Clay Dispersion and Migration. *Formation Damage, SPE Reprint Series* (29): 82-95.
- Hartman, Ryan L., Bruno Lecerf, Wayne W. Frenier et al. 2006. Acid-Sensitive Aluminosilicates: Dissolution Kinetics and Fluid Selection for Matrix-Stimulation Treatments. *SPE Production & Operations* **21** (2): pp. 194-204.
- Jaramillo, Oscar Julian, Ricardo Romero, Alexis Ortega et al. 2010. Matrix Acid Systems for Formations With High Clay Content. Proc., SPE International Symposium and Exhibiton on Formation Damage Control, Lafayette, Louisiana.
- Kume, Nicholas, Robert Van Melsen, Luckie Erhahon et al. 1999. New HF Acid System Improves Sandstone Matrix Acidizing Success Ratio By 400% Over Conventional Mud Acid System in Niger Delta Basin. Proc., SPE Annual Technical Conference and Exhibition, Houston, Texas.
- Kunze, Kenneth R., Chris M. Shaughnessy. 1983. Acidizing Sandstone Formations With Fluoboric Acid. *Society of Petroleum Engineers Journal* **23** (1): 65-72.
- McBride, J.R., M.J. Rathbone, R.L. Thomas. 1979. Evaluation of Fluoboric Acid Treatment in the Grand Isle Offshore Area Using Multiple Rate Flow Test. Proc., SPE Annual Technical Conference and Exhibition, Las Vegas, Nevada.
- Paccaloni, Giovanni, Mauro Tambini. 1993. Advances in Matrix Stimulation Technology. *Journal of Petroleum Technology* **45** (3): 256-263.
- Prakash, GK Surya, Fabrizio Pertusati, George A Olah. 2011. HF-Free, Direct Synthesis of Tetrabutylammonium Trifluoroborates. *Synthesis* **2011** (02): 292-302.
- Radosavljević, S, V Šćepanović, S Stević et al. 1979. Effect of Boric Acid on Tetrafluoroborate Ion Hydrolysis in Solutions of Tetrafluoroboric Acid. *Journal of Fluorine Chemistry* **13** (6): 465-471.

- Restrepo, Alejandro, Manuel Lastre, Arthur William Milne et al. 2012. Effective Kaolinite Damage Control Under Unfavorable Chemical Environment: Field Case. Proc., SPE International Symposium and Exhibition on Formation Damage Control, Lafayette, Louisiana.
- Reyes, E.A. 2012. *Treatment Fluids Containing a Boron Trifluoride Complex and Methods for Use Thereof*, US Patent 2012/0115759 (Reprint).
- Ryss, I. G. 1956. *The Chemistry of Fluorine and Its Inorganic Compounds*. Moscow, State Publishing House of Scientific, Technical, and Chemical Literature (Reprint). Eng. trans., AEC-tr-3927, Office of Technical Services, U.S. Dept. of Commerce, Washington D.C., 1960.
- Shuchart, C.E., R.D. Gdanski. 1996. Improved Success in Acid Stimulations with a New Organic-HF System. Proc., European Petroleum Conference, Milan, Italy.
- Shuchart, Chris E., Douglas C. Buster. 1995. Determination of the Chemistry of HF Acidizing with the Use of F NMR Spectroscopy. Proc., SPE International Symposium on Oilfield Chemistry, San Antonio, Texas.
- Smith, C.F., A.R. Hendrickson. 1965. Hydrofluoric Acid Stimulation of Sandstone Reservoirs. *Journal of Petroleum Technology* **17** (02): 215 - 222.
- Thomas, R. L., C. W. Crowe, W. Chmilowski. 1978. Single-Stage Chemical Treatment Provides Stimulation And Clay Control In Sandstone Formations. Proc., Annual Technical Meeting, Calgary, Alberta, Canada.
- Thomas, R.L., C.W. Crowe. 1978. Matrix Treatment Employs New Acid System for Stimulation and Control of Fines Migration in Sandstone Formations. *Journal of Petroleum Technology* **33** (8): 1491-1500.
- Travers, A.; Malapradr, L. 1930. New Fluoboric Complexes. *Bulletin de la Societe Chimique de France*: **47**, 788-801.
- Wamser, Christian A. 1948. Hydrolysis of Fluoboric Acid in Aqueous Solution. *Journal of the American Chemical Society* **70** (3): 1209-1215.

Wamser, Christian A. 1951. Equilibria in the System Boron Trifluoride-Water at 25°. *Journal of the American Chemical Society* **73** (1): 409-416.

## APPENDIX A

### A-1. Fluoboric Acid Material Safety Data Sheet



Health	3
Fire	0
Reactivity	0
Personal Protection	

## Material Safety Data Sheet Fluoboric acid MSDS

Wednesday, March 5, 2014 at 8:45pm		<b>Product and Company Identification</b>	
<b>Product Name:</b> Fluoboric acid		<b>Contact Information:</b>	
<b>Catalog Codes:</b> SLF1771		<b>Sciencelab.com, Inc.</b>	
<b>CAS#:</b> 16872-11-0		14025 Smith Rd.	
<b>RTECS:</b> ED2685000		Houston, Texas 77396	
<b>TSCA:</b> TSCA 8(b) inventory: Fluoboric acid		US Sales: 1-800-901-7247	
<b>Cl#:</b> Not available.		International Sales: 1-281-441-4400	
<b>Synonym:</b> Tetrafluoroboric acid		Order Online: <a href="http://ScienceLab.com">ScienceLab.com</a>	
<b>Chemical Formula:</b> HBF <sub>4</sub>		<b>CHEMTREC (24HR Emergency Telephone), call:</b>	
		1-800-424-9300	
		<b>International CHEMTREC, call:</b> 1-703-527-3887	
		<b>For non-emergency assistance, call:</b> 1-281-441-4400	

Section 2: Composition and Information on Ingredients		
<b>Composition:</b>		
Name	CAS #	% by Weight
Fluoboric acid	16872-11-0	100
Toxicological Data on Ingredients: Fluoboric acid LD50: Not available. LC50: Not available.		

Section 3: Hazards Identification
<p><b>Potential Acute Health Effects:</b> Extremely hazardous in case of skin contact (irritant), of eye contact (irritant), of ingestion, of inhalation. Corrosive to skin and eyes on contact. Liquid or spray mist may produce tissue damage particularly on mucous membranes of eyes, mouth and respiratory tract. Skin contact may produce burns. Inhalation of the spray mist may produce severe irritation of respiratory tract, characterized by coughing, choking, or shortness of breath. Inflammation of the eye is characterized by redness, watering, and itching. Skin inflammation is characterized by itching, scaling, reddening, or, occasionally, blistering.</p> <p><b>Potential Chronic Health Effects:</b> Extremely hazardous in case of skin contact (irritant), of eye contact (irritant), of ingestion, of inhalation. CARCINOGENIC EFFECTS: Not available. MUTAGENIC EFFECTS: Not available. TERATOGENIC EFFECTS: Not available. DEVELOPMENTAL TOXICITY: Not available. The substance is toxic to lungs, mucous membranes. Repeated or prolonged exposure to the substance can produce target organs damage. Repeated or prolonged contact with spray mist may produce chronic eye irritation and severe skin irritation. Repeated or prolonged exposure to spray mist may produce respiratory tract irritation leading to frequent attacks of bronchial infection. Repeated or prolonged inhalation of vapors may lead to chronic respiratory irritation.</p>



#### Section 4: First Aid Measures

**Eye Contact:**

Check for and remove any contact lenses. Immediately flush eyes with running water for at least 15 minutes, keeping eyelids open. Cold water may be used. Do not use an eye ointment. Seek medical attention.

**Skin Contact:**

If the chemical got onto the clothed portion of the body, remove the contaminated clothes as quickly as possible, protecting your own hands and body. Place the victim under a deluge shower. If the chemical got on the victim's exposed skin, such as the hands : Gently and thoroughly wash the contaminated skin with running water and non-abrasive soap. Be particularly careful to clean folds, crevices, creases and groin. Cold water may be used. If irritation persists, seek medical attention. Wash contaminated clothing before reusing.

**Serious Skin Contact:**

Wash with a disinfectant soap and cover the contaminated skin with an anti-bacterial cream. Seek medical attention.

**Inhalation:** Allow the victim to rest in a well ventilated area. Seek immediate medical attention.

**Serious Inhalation:**

Evacuate the victim to a safe area as soon as possible. Loosen tight clothing such as a collar, tie, belt or waistband. If breathing is difficult, administer oxygen. If the victim is not breathing, perform mouth-to-mouth resuscitation. WARNING: It may be hazardous to the person providing aid to give mouth-to-mouth resuscitation when the inhaled material is toxic, infectious or corrosive. Seek immediate medical attention.

**Ingestion:**

Do not induce vomiting. Loosen tight clothing such as a collar, tie, belt or waistband. If the victim is not breathing, perform mouth-to-mouth resuscitation. Seek immediate medical attention.

**Serious Ingestion:** Not available.

#### Section 5: Fire and Explosion Data

**Flammability of the Product:** Non-flammable.

**Auto-Ignition Temperature:** Not applicable.

**Flash Points:** Not applicable.

**Flammable Limits:** Not applicable.

**Products of Combustion:** Not available.

**Fire Hazards in Presence of Various Substances:** Not applicable.

**Explosion Hazards in Presence of Various Substances:**

Risks of explosion of the product in presence of mechanical impact: Not available. Risks of explosion of the product in presence of static discharge: Not available.

**Fire Fighting Media and Instructions:** Not applicable.

**Special Remarks on Fire Hazards:** Not available.

**Special Remarks on Explosion Hazards:** Not available.

#### Section 6: Accidental Release Measures

**Small Spill:**

Dilute with water and mop up, or absorb with an inert dry material and place in an appropriate waste disposal container.

**Large Spill:**

Corrosive liquid. Stop leak if without risk. Absorb with DRY earth, sand or other non-combustible material. Do not get water inside container. Do not touch spilled material. Use water spray curtain to divert vapor drift. Prevent entry into sewers, basements or confined areas; dike if needed. Call for assistance on disposal.

### Section 7: Handling and Storage

**Precautions:**

Keep container dry. Do not breathe gas/fumes/ vapour/spray. Never add water to this product. In case of insufficient ventilation, wear suitable respiratory equipment. If ingested, seek medical advice immediately and show the container or the label. Avoid contact with skin and eyes. Keep away from incompatibles such as metals, alkalis. May corrode glass. Store in an appropriate container.

**Storage:**

May corrode metallic surfaces. Store in a metallic or coated fiberboard drum using a strong polyethylene inner package. May corrode glass. Store in an appropriate container. Corrosive materials should be stored in a separate safety storage cabinet or room.

### Section 8: Exposure Controls/Personal Protection

**Engineering Controls:**

Provide exhaust ventilation or other engineering controls to keep the airborne concentrations of vapors below their respective threshold limit value.

**Personal Protection:**

Face shield. Full suit. Vapor respirator. Be sure to use an approved/certified respirator or equivalent. Gloves. Boots.

**Personal Protection in Case of a Large Spill:**

Splash goggles. Full suit. Vapor respirator. Boots. Gloves. A self contained breathing apparatus should be used to avoid inhalation of the product. Suggested protective clothing might not be sufficient; consult a specialist BEFORE handling this product.

**Exposure Limits:** Not available.

### Section 9: Physical and Chemical Properties

**Physical state and appearance:** Liquid.

**Odor:** Odorless.

**Taste:** Not available.

**Molecular Weight:** 87.81 g/mole

**Color:** Colorless.

**pH (1% soln/water):** Not available.

**Boiling Point:** Decomposes. (130°C or 266°F)

**Melting Point:** Not available.

**Critical Temperature:** Not available.

**Specific Gravity:** 1.84 (Water = 1)

**Vapor Pressure:** Not available.

**Vapor Density:** Not available.

**Volatility:** Not available.

**Odor Threshold:** Not available.

**Water/Oil Dist. Coeff.:** Not available.

**Ionicity (in Water):** Not available.

**Dispersion Properties:** See solubility in water, methanol.

**Solubility:**  
Easily soluble in cold water. Soluble in methanol.

#### Section 10: Stability and Reactivity Data

**Stability:** The product is stable.  
**Instability Temperature:** Not available.  
**Conditions of Instability:** Not available.  
**Incompatibility with various substances:** Extremely reactive or incompatible with metals, alkalis.  
**Corrosivity:**  
Extremely corrosive in presence of steel, of aluminum, of zinc, of copper. Highly corrosive in presence of glass, of stainless steel(304), of stainless steel(316).  
**Special Remarks on Reactivity:** Decomposes on heating.  
**Special Remarks on Corrosivity:** Not available.  
**Polymerization:** No.

#### Section 11: Toxicological Information

**Routes of Entry:** Eye contact. Inhalation. Ingestion.  
**Toxicity to Animals:**  
LD50: Not available. LC50: Not available.  
**Chronic Effects on Humans:** The substance is toxic to lungs, mucous membranes.  
**Other Toxic Effects on Humans:** Extremely hazardous in case of skin contact (irritant), of ingestion, of inhalation.  
**Special Remarks on Toxicity to Animals:** Not available.  
**Special Remarks on Chronic Effects on Humans:** Not available.  
**Special Remarks on other Toxic Effects on Humans:** Not available.

#### Section 12: Ecological Information

**Ecotoxicity:** Not available.  
**BOD5 and COD:** Not available.  
**Products of Biodegradation:**  
Possibly hazardous short term degradation products are not likely. However, long term degradation products may arise.  
**Toxicity of the Products of Biodegradation:** The products of degradation are more toxic.  
**Special Remarks on the Products of Biodegradation:** Not available.

#### Section 13: Disposal Considerations

**Waste Disposal:**

#### Section 14: Transport Information

**DOT Classification:** CLASS 8: Corrosive liquid.  
**Identification:** : Fluoroboric acid : UN1775 PG: II  
**Special Provisions for Transport:** Not available.

#### Section 15: Other Regulatory Information

**Federal and State Regulations:** TSCA 8(b) inventory: Fluoboric acid  
**Other Regulations:** OSHA: Hazardous by definition of Hazard Communication Standard (29 CFR 1910.1200).  
**Other Classifications:**  
**WHMIS (Canada):**  
CLASS D-2A: Material causing other toxic effects (VERY TOXIC). CLASS E: Corrosive liquid.  
**DSCL (EEC):**  
R38- Irritating to skin. R41- Risk of serious damage to eyes.  
**HMIS (U.S.A.):**  
Health Hazard: 3  
Fire Hazard: 0  
Reactivity: 0  
Personal Protection:  
**National Fire Protection Association (U.S.A.):**  
Health: 3  
Flammability: 0  
Reactivity: 0  
Specific hazard:  
**Protective Equipment:**  
Gloves. Full suit. Vapor respirator. Be sure to use an approved/certified respirator or equivalent. Wear appropriate respirator when ventilation is inadequate. Face shield.

#### Section 16: Other Information

**References:** Not available.  
**Other Special Considerations:** Not available.  
**Created:** 10/09/2005 05:34 PM  
**Last Updated:** 05/21/2013 12:00 PM  
  
*The information above is believed to be accurate and represents the best information currently available to us. However, we make no warranty of merchantability or any other warranty, express or implied, with respect to such information, and we assume no liability resulting from its use. Users should make their own investigations to determine the suitability of the information for their particular purposes. In no event shall ScienceLab.com be liable for any claims, losses, or damages of any third party or for lost profits or any special, indirect, incidental, consequential or exemplary damages, howsoever arising, even if ScienceLab.com has been advised of the possibility of such damages.*

A-2. *HBF<sub>4</sub> unit cost*

Per 1 kilogram of 3% HBF<sub>4</sub>:

	(g)	Unit cost	Cost
H <sub>2</sub> O	786.75	\$ 0.01	\$ 7.87
NH <sub>4</sub> HF <sub>2</sub>	42.75	\$ 0.07	\$ 2.96
H <sub>3</sub> BO <sub>3</sub>	23.17	\$ 0.07	\$ 1.67
HCl	147.33	\$ 0.01	\$ 2.18
Total	<b>1000.00</b>		<b>\$ 14.67</b>